RIF1 AND NUCLEOPORINS PROMOTE THE CHROMATIN ASSOCIATION OF ORC

By

Logan Ray Richards

Dissertation

Submitted to the Faculty of the

Graduate School of Vanderbilt University

in partial fulfillment of the requirements

for the degree of

DOCTOR IN PHILOSOPHY

In

Biological Sciences

May 12, 2023

Nashville, Tennessee

Approved

Dr. Jared Nordman

Dr. Katherine Friedman

Dr. James Dewar

Dr. Andrea Page-McCaw

Dr. Lars Plate

To Robin, Stacy, and Suzie

This work is dedicated to my aunt, Robin, who has been a constant source of support, love, and encouragement during the challenges of graduate school and life. I am truly grateful for having you in my life. This work is also dedicated to Stacy and Suzie, who have always encouraged me to achieve more than I thought possible. I would not be where I am today without you three. From the bottom of my heart, thank you.

ACKNOWLEDGEMENTS

I'm grateful for my thesis advisor and mentor, Dr. Jared Nordman. Much of the work presented in this thesis was the result of me chasing data and following up on interesting observations. In fact, the entire Nucleoporin-ORC story in Chapter III was the direct result of us sitting together and simply asking, "What's going on there?", the answer resulting in my first, first-author publication. I am extremely grateful to have had the freedom to pursue projects and follow up on findings that I found interesting. I'm also thankful for his mentorship through the years. When I first came to graduate school, I had little experience performing the wide range of techniques necessary to complete my research, and I am grateful for Dr. Nordman taking the time to train me in these techniques himself (and for his patience while I got them working in my hands). Furthermore, I am grateful for his mentorship in other necessary skills to promote my success as a graduate student, most notably writing. While I was drafting my F31, we went through several intense rounds of editing, and I am grateful for him taking the time to do that, as it led to me being awarded the grant on my first application attempt. Lastly, I am grateful for him promoting my professional development outside the lab and enabling me to pursue my own career interests, supporting me along the way.

I'm incredibly grateful for the support of my thesis committee members: Dr. Katherine Friedman, Dr. James Dewar, Dr. Lars Plate, and Dr. Andrea Page-McCaw. My second rotation as a graduate student was in Dr. Dewar's lab, and I am grateful for the training I received during that rotation as well as the feedback on my graduate work over the course of my PhD. I'm thankful for Dr. Friedman serving as the chair of my committee and co-sponsor on my F31 grant, and for her taking the time to review drafts of various manuscripts and grant applications through the years. I'm also thankful for her questions and feedback on my work, which helped foster me thinking more like a scientist. I'm thankful for Dr. Lars Plate, who was my instructor for the Biological Sciences seminar course, where he helped myself and others get geared up for their qualifying exam. I am also grateful for Dr. Plate's feedback and advice regarding mass spectrometry, which was a cornerstone of my project. I'd like to thank Dr. Page-McCaw for her help in all things Drosophila, and for asking questions and providing feedback on my work. I'd like to also thank Dr. Tony Capra, who helped me learn how to code and perform bioinformatic analysis during my third rotation, and Dr. Mary-Lauren Benton for her help performing some of the analysis for the work in Chapter III. Lastly, thank you to Dr. Hayes McDonald for all his help with mass spectrometry through the years.

Through the years, I've had the pleasure of working with several outstanding graduate students in the Nordman Lab: Alex Munden, Souradip Das (both now doctors!), Reyhaneh Tirgar, and Dongsheng Han. All of you contributed to my success as a graduate student and thank you all. Alex, thank you for training me in bioinformatics when I was just starting out and tolerating all of questions as I was getting a grasp on how to analyze sequencing data. Thank you also for being my dear friend and helping me through all the struggles of life and graduate school. I sincerely hope you succeed in your postdoctoral lab and onward. Dip, thank you for reminding me to have fun in graduate school, working with me on the Rif1 project, and co-writing a review together. I am incredibly happy that you were able to break into the field of consulting, and I hope it is a good fit for you. Rey, thank you for supporting me through the years, offering feedback on my project, and always finding a way to make me laugh. Dongsheng, thank you for all your help in fly genetics and with my project. I wouldn't have had the success in graduate school without you all, and I am grateful to have worked alongside you all.

This work was also supported by excellent research assistants through the years: Saumya Patel, Marti Ramos, and Scott Churcher. Saumya, thank you for making the anti-Rif1 antibody, which was critically important to this project. I am also extremely grateful for your help with the embryo collections we had to do for the Rif1 project, which would have been much more difficult without your help. Marti, thank you for making the anti-Elys and anti-ORC2 antibodies. These antibodies were essential for me to finish the Nup-ORC project and publish in a timely manner, and I am grateful for your work in making these antibodies. Scott, thank you for your support in the overall maintenance of the lab and keeping everything running smoothly. I'd also like to thank Dr. Christopher Lord, who did several key experiments for the Nup-ORC paper and helped me finish the paper much faster than I could have on my own. Also, thank you Chris for being a good friend and co-worker as well as a source of career advice. Even though you were in the lab for only six months, I really enjoyed our time working together.

I wouldn't be where I am today without Stacy Scheetz and Suzie Clevenger. When I was in high school, my situation in life led me to believe that attending college was beyond my reach. Stacy convinced me that I could aspire to so much more in life and pushed me to apply and ultimately attend Purdue University. She, along with Karen Schlosser, moved heaven and earth to ensure I had the means of attending Purdue University. Without her and the resounding support of the Marshall County Community Foundation, there is a good chance I would have never left Plymouth, Indiana, and certainly would not have nurtured my love of biology and chemistry. Thank

you so much for your love and support through the years. Karen, I hope you are in a better place, and you will be sincerely missed. Suzie, thank you for your behind-the-scenes help when I needed it most. I am still thankful for the clothes and food you provided my brother and me all those years ago. I am incredibly lucky to have both you and Stacy in my life cheering me on along the way. The world needs more counselors and teachers like you Stacy and Suzie, and I owe so much to you both.

Robin, thank you for being my mentor and advocate through the years and for all the love and support. You are one of the few people I had growing up that I could consistently rely on. I am so glad that we have grown closer while I've attended graduate school and it's been truly amazing to watch Valorie and Claire grow up through the years. We both come from similar backgrounds, and I often find myself looking to you to remind myself what's possible for my own life, despite the cards I was dealt. Thank you for taking me on all sorts of adventures and all the memories we've made together.

TABLE OF CONTENTS

LIST OF TABLES

LIST OF FIGURES

LIST OF ABBREVIATIONS

ɣH2Av	Phosphorylated histone H2A variant
APH	Aphidicolin
ATAC-Seq	Assay for transposase-accessible chromatin with high-throughput sequencing
Cdc6	Cell division cycle 6
Cdc45	Cell division cycle 45
Cdt1	Chromatin licensing and DNA replication factor 1
ChIP-seq	Chromatin immunoprecipitation with high-throughput sequencing
CUT&RUN	Cleavage under targets and release under nuclease
DAPI	4′,6-diamidino-2-phenylindole
DDK	Dbf4 dependent kinase
Dpb11	DNA polymerase B associated protein 11
DSB	Double-strand break
dsRNA	Double-stranded RNA
EdU	5-Ethynyl-2’-deoxyuridine
Elys	Embryonic large molecule derived from yolk sac
EtoL	Early-to-Late
GFP	Green fluorescent protein
GINS	Go (5) - ichi (1) - ni (2) - san (3)
GP210	Glycoprotein 210
HP1	Heterochromatin protein 1
IDR	Intrinsically disordered region
IP	Immunoprecipitation
IP-MS	Immunoprecipitation coupled with mass spectrometry
LAD	Lamin associated domain

LLPS	Liquid-liquid phase separation
LtoE	Late-to-Early
MCM	Mini-chromosome maintenance
MGS	Meier-Gorlin Syndrome
MS	Mass spectrometry
MZT	Maternal-to-zygotic transition
NDC1	Nuclear division cycle protein 1
NPC	Nuclear pore complex
Nup	Nucleoporin
ORC	Origin recognition complex
Pol ε	Polymerase epsilon
POM121	Pore membrane protein 121
PP1	Protein phosphatase 1
RAD	Rif1 associated domain
Rae1	Ribonucleic acid export 1
Rap1	Repressor/activator protein 1
RPA	Replication protein A
Rif1	Rap1 interaction factor 1
RNAi	RNA interference
RT	Replication timing
Seh1	Sec13 homologue 1
Sld2	Synthetic lethal death 2
Sld3	Synthetic lethal death
TAD	Topologically associated domain
TPR	Translocated promoter region

CHAPTER I

INTRODUCTION

DNA Replication Initiation

DNA replication is a highly coordinated process

Successful DNA replication depends on the accurate duplication of billions of bases every cell division cycle. DNA replication is largely regulated at the initiation phase, which includes the loading and subsequent activation of replicative helicases. First, the origin recognition complex (ORC) binds to cis-acting sites throughout the genome where DNA replication will initiate, known as origins of replication (Leonard and Méchali, 2013) (Fig. 1.1). ORC, together with Cdc6 and Cdt1, facilitates loading of MCM2-7 double hexamers at replication origins in a process known as 'helicase loading' (Bell and Labib, 2016; Leonard and Méchali, 2013) (Fig, 1.1). MCM2-7 is the replicative helicase but is loaded in an inactive state in late M and G1 phases of the cell cycle, thus marking all potential initiation sites (Diffley, 2004). In S phase, loaded MCMs must be activated through phosphorylation of the N-terminal regions of MCM2,4 and 6 by Dfb4 dependent kinase (DDK) (Bell and Dutta, 2003; Sheu and Stillman, 2006) (Fig. 1.1). Once activated, S phase cyclin dependent kinase (S-CDK) is required for the recruitment of additional initiation factors and assembly of the replisome (Douglas et al., 2018; Fragkos et al., 2015; Moyer et al., 2006; Remus and Diffley, 2009; Siddiqui et al., 2013) (Fig. 1.1).

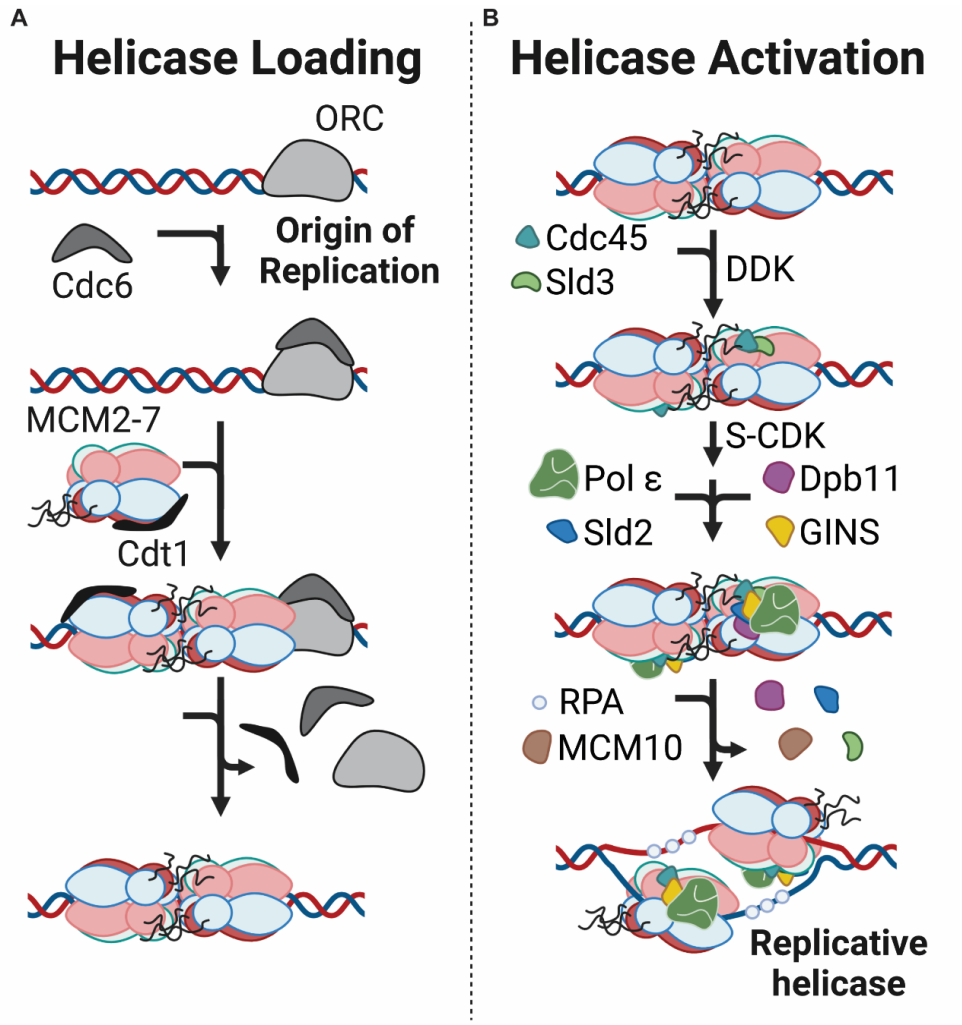

Figure 1.1. ***Summary of DNA replication initiation.*** Replication initiation occurs in two key steps: (A) helicase loading and (B) helicase activation. (A) During G1 phase of the cell cycle, ORC binds to DNA and marks sites of DNA replication initiation, termed origins of replication. ORC together with Cdc6 and Cdt1, loads MCM2-7 onto origins. Helicases are then activated throughout S phase, which is driven by DDK and S-CDK. The action of these kinases allows for the recruitment of Cdc45, Sld3, Pol ε, Sld2, Dpb11, and the GINS complex onto the assembling replisome. MCM10 promotes the activation of the helicase, and RPA coats single stranded DNA as the replisome unwinds double-stranded DNA. Many of the initiation factors dissociate from the assembling replisome after their function is performed. The remaining constitute the replicative helicase: Cdc45, the GINS complex, and MCM2-7. Adapted from Bell and Labib, 2016 and made by Logan Richards.

DNA replication initiation and disease

Given that DNA replication is a fundamental biological process, mutations in any components necessary for the accurate duplication of the genome would be harmful to an organism. This is indeed the case as there are both inherited disorders and acquired diseases directly resulting from dysfunctions in the initiation of DNA replication (Jackson et al., 2014). For example, increased cancer risk and overall reduced growth during development are frequent phenotypes of mutations in proteins involved in DNA replication initiation, specifically in humans (Jackson et al., 2014). Furthermore, there are several specific developmental abnormalities associated with these mutations including premature aging, absence of the patella (knee cap), and skin rashes (Jackson et al., 2014). Through the investigation of these diseases and the causative mutations, the important roles of certain DNA replication factors have become better understood; however, much remains to be uncovered as to why certain mutations lead to these very distinct phenotypes.

Meier-Gorlin syndrome: a replication initiation associated disorder with distinct phenotypes

Meier-Gorlin syndrome (MGS) is one such developmental disorder with distinct phenotypes arising if mutations occur in the DNA replication initiation machinery. It is an autosomal recessive disorder characterized by absent patella (knee caps) and small ears (Fig. 1.2B). Microcephaly is present in individuals with MGS, but intellect is normal (Bicknell et al., 2011; Jackson et al., 2014). Growth in individuals with MGS is also reduced before birth and postnatally, but the reduction in height varies widely depending on which replication factor is mutated (Bicknell et al., 2011). To date, five separate genes have been implicated in MGS: *ORC1*, *ORC4*, *ORC6*, *Cdt1*, and *Cdc6* (Fig. 1.2B) (Bicknell et al., 2011). Specifically, mutations that result in MGS are typically heterozygous missense mutations; however, in extreme cases, patients can be compound heterozygous, inheriting different missense mutations in the same gene from both parents. For

example, the original patient described by Robert Gorlin, whom the condition is named for, was characterized as having a guanine to adenine substitution in *ORC1*. This patient also had a two base pair deletion coupled with a one base pair insertion in *ORC1*. These combined mutations result in both a substitution from arginine to glutamine and a frameshift within the protein (Bicknell et al., 2011), likely causing loss-of-function of ORC1, but the molecular consequences of these mutations are not well characterized. All five of these genes implicated in MGS play critical roles in assembling the replisome in the earliest stages of DNA replication initiation and are responsible for causing the observed developmental defects (Bell and Labib, 2016; Bicknell et al., 2011).

Of the five causative genes in MGS, *ORC1* has the most phenotypic variation, with height being reduced by up 9.6 standard deviations from the average height and with an accompanying reduction in head circumference of up to 9.8 standard deviations (Bicknell et al., 2011). Several neurological impairments are observed in individuals with severe microcephaly as a result from severe reduction in growth (Bicknell et al., 2011). Other genes in MGS (*ORC4*, *ORC6*, *Cdt1*, and *Cdc6*) may contribute to height reduction; however, these individuals are within the lower range of normal height, with no observable reduction in cognitive abilities (Bicknell et al., 2011; Jackson et al., 2014). In contrast, the phenotypes that are consistent for all individuals with MGS are microtia (small ears) and small or missing patella (Fig. 1.2B), making these the best predictors for mutations in proteins involved in DNA replication initiation (Bicknell et al., 2011; Jackson et al., 2014).

If DNA replication initiation was impaired, cell and tissue growth are likely to be reduced. Indeed, this is true for the reduction of height in MGS; however, an overall reduction in cell proliferation does not explain the selective lack of growth in the ears and patella. These specific tissues may be sensitized to defects in replication initiation and cell proliferation. Alternatively, replication initiation factors could have unique roles in the development of these tissues, a possibility that

remains to be uncovered. Either explanation indicates a critical role of DNA replication initiation during development that is worthy of future study.

Helicase mutations

Mutations in the MCM subunits of the replicative helicase have also been observed, but the phenotypes are unexpected considering the functions that these subunits perform. The exception to this is the Chaos3 mutation in *MCM4*. The Chaos3 *MCM4* mutant is indeed associated with genomic instability in mice, which would be expected for a key factor of DNA replication. Interestingly, growth defects are not observed (Jackson et al., 2014; Shima et al., 2007). In contrast, a rare splice mutation in humans that results in a truncated MCM4 in humans has been observed (Gineau et al., 2012; Hughes et al., 2012). However, the observed phenotypes are not consistent with the expected phenotypes such as growth defects or cancer arising from genomic instability. Rather, individuals expressing truncated MCM4 display defects in the adrenal gland and natural killer cell deficiency (Gineau et al., 2012; Hughes et al., 2012). The reason for these cell types to be sensitized to defects in MCM4 is not understood. Mutations in *MCM4* appear to have different consequences in mice versus humans, with the mouse Chaos3 mutation in *MCM4* causing predisposition to cancer and the human truncation mutant causing defects in distinct cell types. This again suggests that the proteins involved in DNA replication initiation may perform additional uncharacterized functions in humans.

The regulation of DNA replication initiation is critical to promoting genome stability

The number of origins of replication across the genome far exceeds the number of origins activated through the duration of S phase (Cayrou et al., 2011). Specifically, helicases are loaded but held inactivate, serving as dormant origins (Doksani et al., 2009; Ge et al., 2007; Ibarra et al.,

2008). Typically, ~10% of origins are utilized while the rest remain dormant; however, activation of these dormant origins is required under the presence of replication stress (Demczuk et al., 2012; Dijkwel et al., 2002). Replication stress resulting from extracellular or intracellular sources may cause replication forks to stall, collapse, and ultimately result in genotoxic, double-stranded breaks in the genome (Zeman and Cimprich, 2013). Therefore, the activation of additional replication forks is essential to compensate for those encountering stress. The precise mechanism as to how dormant origins are activated in response to replication stress is not well characterized; however, previous work indicates the key checkpoint kinase ATR (Ataxia telangiectasia and Rad3 related) may promote the activation of helicases at dormant origins by phosphorylating loaded MCMs (Cortez et al., 2004). If ORC or helicase loading is severely impaired, a checkpoint is activated, delaying entry into S phase to prevent DNA replication from commencing. This checkpoint can be defective in cancer, causing cells to enter mitosis with under-replicated DNA (Boyer et al., 2016). Alternatively, cancer cells may fail to activate dormant origins, increasing sensitivity to replication stress, as well as increasing the likelihood that collapsed forks will result in DNA damage (Boyer et al., 2016) (Fig. 1.2A, see reduced origin usage). Interestingly, cells isolated from individuals with MGS exhibit delayed S phase entry, indicating this checkpoint is active (Stiff et al., 2013). Further study of the mechanism of dormant origin firing is essential to understanding how genome instability arises in cancer, and cells from MGS patients could provide key information as to how cells compensate for decreased replication initiation.

In addition to reduced origin usage, cancer cells may exhibit uncoordinated origin firing in response to the activation of oncogenes, which also results in replication stress and genome instability (Boyer et al., 2016) (Fig. 1.2A, uncoordinated origin firing). For example, cellular Myc (c-Myc) overexpression results in de-regulated origin activation (Dominguez-Sola et al., 2007). C-Myc binds near origins of replication and is proposed to play a potential role in origin activation

(Dominguez-Sola et al., 2007). Excessive origin activation directly results in genomic instability (Bester et al., 2011) (later discussed, see Fig. 1.5) and c-myc is often overexpressed in cancer, again linking DNA replication initiation to genome stability (Dominguez-Sola et al., 2007).

It is important to note that there are several cellular mechanisms in place to ensure that a given origin only activates once per cell cycle at the appropriate time during the cell cycle, to prevent partial re-replication of genomic regions (Boyer et al., 2016; Truong and Wu, 2011) (Fig. 1.2A, see re-replication). Re-replication is a phenomenon observed in cancer cells, suggesting that the cellular mechanisms responsible for preventing re-replication are compromised (Hook et al., 2007). Many replication initiation factors have been observed as being overexpressed in cancer cells, likely causing de-regulated origin activation and re-replication to occur (Boyer et al., 2016; Hook et al., 2007). For example, Cdt1 overexpression in normal mammalian cells does not cause re-replication, but does in cancer cell lines (Vaziri et al., 2003). The initiation of DNA replication is a tightly regulated process and key to promote the stability of the genome. Failure to activate the appropriate number origins can result in reduced origin usage, irregular origin activation, or re-replication at certain origins.

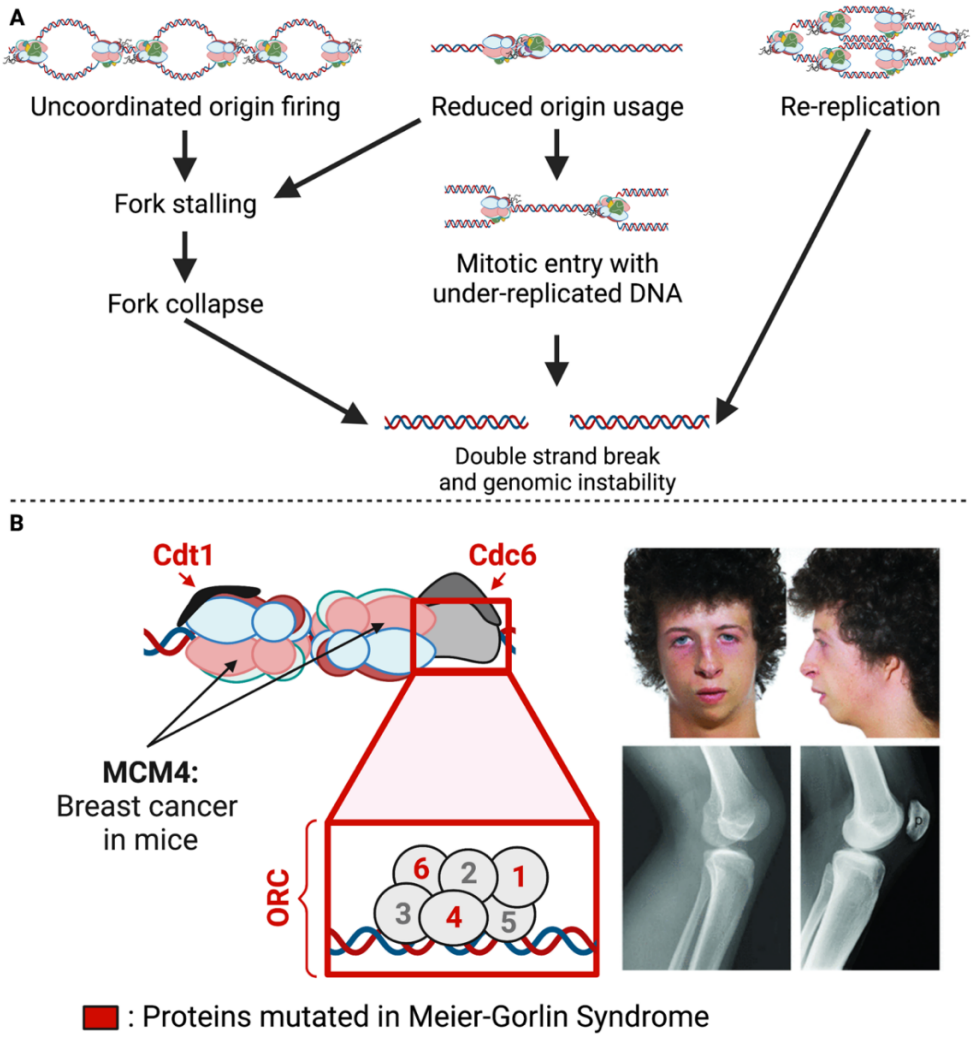

Figure 1.2. ***Defects in replication initiation and their impact on human health.*** (A) Proper regulation of replication initiation is critical to maintaining genome stability. Uncoordinated origin firing resulting from the overexpression of key cell cycle factors leads to fork stalling, collapse, and ultimately genomic instability. Reduced origin usage can also arise from the deregulation of replication initiation, reducing the number of active origins, and resulting in mitotic entry with under-replicated DNA. Deregulation of initiation factors Cdt1 and Cdc6 can result in the re-firing of origins, causing re-replication and subsequent genomic instability. (B) Mutated replication initiation proteins linked to Meier-Grolin Syndrome (MGS). Replication initiation complex is shown (top left) with proteins implicated in MGS highlighted in red (Cdt1, Cdc6, ORC1, ORC4, and ORC6). MCM4 has also been linked to breast cancer in mice. Top right panel shows patient with MGS with reduction in size of the external ear. Bottom right is a lateral X ray of a patient with MGS (left) and control subject (right), highlighting the absence of the patella (p), or kneecap, in the MGS patient. Adapted from Bicknell et al., 2011, Boyer et al., 2016, and Jackson et al., 2014, and made by Logan Richards.

The origin recognition complex determines where to start DNA replication

ORC was initially characterized in *S. cerevisiae* as a factor that bound to ARSs, or autonomously replicating sequences (Bell and Stillman, 1992), which are genomic sites where DNA replication starts along the yeast genome (Brewer and Fangman, 1987; Huberman et al., 1987). Much work has gone into determining where ORC binds and how ORC subunits differ across species. The presence of ORC appears to be nearly evolutionarily conserved across eukaryotes (Bell, 2002). While the individual subunits show evolutionary divergence, the core replication initiation function of ORC, specifically binding to the genome to mark sites where DNA replication will start, is also conserved (Fig. 1.3, canonical role) (Bell, 2002; Chesnokov, 2007). Furthermore, the genomic binding preferences of ORC differ between species (Eaton et al., 2010, 2011; Miotto et al., 2016; Remus et al., 2004; Vashee et al., 2003; Wyrick et al., 2001; Xu et al., 2006). Determining what factors contribute to where ORC binds is still an area of active research.

Although ORC genomic binding in *S. cerevisiae* is sequence specific (Eaton et al., 2010; Wyrick et al., 2001; Xu et al., 2006), the genomic binding in metazoans is not specific to any sequence with no known binding motifs identified (Eaton et al., 2010, 2011; Miotto et al., 2016; Remus et al., 2004; Vashee et al., 2003). Studies investigating the determinants of ORC genomic binding have faced challenges as origin usage and selection changes over the course of development programs (Eaton et al., 2011; Hua et al., 2018; Sher et al., 2012). In the early embryonic stages of Drosophila and Xenopus for instance, an increased proportion of origins are activated (Blumenthal et al., 1974; Coverley and Laskey, 1994), and ORC binding sites appear to lack any specificity (Coverley and Laskey, 1994). Trends in ORC binding are only apparent later in development (Hyrien et al., 1995; Sasaki et al., 1999), with ORC having a strong preference for binding to intergenic regions near promoters (Brewer, 1994; Eaton et al., 2011; Gilbert, 2001; MacAlpine et al., 2004; Wyrick et al., 2001). This suggests that transcription may influence ORC

binding across the genome. This is confounded by the fact that chromatin structure near a promoter directly affects transcriptional activity, and factors that activate or repress transcription at a certain site are often chromatin remodelers (Cairns, 2009). This work highlights that accessible chromatin is a critical requirement of ORC binding.

There is also a propensity for ORC to bind within genomic regions that have acetylated histones (Aggarwal and Calvi, 2004). Acetylated histones are associated with regions of active transcription (Roh et al., 2005), again linking ORC binding to accessible and transcriptionally active genomic regions. Interestingly, assembled transcription complex can establish a site as an origin on a plasmid in the absence of transcription in Xenopus extracts (Danis et al., 2004). Importantly, histones surrounding the loaded transcription complex are acetylated, indicating that chromatin structure changes caused by transcription machinery promote the binding of ORC and contribute to origin selection (Danis et al., 2004). The common theme that continues to emerge is that ORC binds to open chromatin; however, given that origin usage is flexible during development, this suggests that ORC genomic binding and origin activation are a dynamically regulated process. Considering the regulation of origin activation is imperative to maintaining genomic stability, investigating the drivers of ORC genomic binding and origin activation is critical to understanding the mechanisms that allow for the accurate and faithful duplication of the genome.

Other ORC functions

In addition to the conserved role of ORC in DNA replication, several ORC subunits have been associated with other biological functions (Chesnokov, 2007), some of which seem to be contrary to the previously described binding preferences of ORC. One such function is the role of ORC in the maintenance of heterochromatin in both Drosophila and Xenopus (Pak et al., 1997; Shareef

et al., 2001) and has been directly linked to gene silencing and transcriptional repression in budding yeast (Shore, 2001). In budding yeast, genetic screens revealed that strains defective in the transcriptional silencing of the HMR and HML mating loci had mutations in ORC genes (Ehrenhofer-Murray et al., 1995; Foss et al., 1993; Micklem et al., 1993). In Drosophila, ORC2 co-localizes with heterochromatin protein 1 (HP1) on DNA (Fig. 1.3G) and mutations in Drosophila ORC cause incorrect localization of HP1 (Pak et al., 1997), indicating that ORC plays a role in the proper localization of HP1 onto chromatin. Given that HP1 contributes to gene repression by driving formation of heterochromatin (Zeng et al., 2010), this suggests that ORC may also play roles in the formation of heterochromatin, which contrasts with preference of ORC to bind to transcriptionally active promoter regions when initiating DNA replication.

More recent work has also implicated ORC3 and ORC5 in mRNA export, as there is evidence of an interaction between these ORC subunits and the TREX-2 export complex in Drosophila (Kopytova et al., 2016). In this study, ORC was also found to be associated with messenger ribonucleoprotein, RNA-bound protein complexes involved in the preparation of RNA for export (Kopytova et al., 2016). Upon further investigation, the authors observed an accumulation of mRNA in the nucleus if ORC3 or ORC5 is depleted, showing that ORC3 and ORC5 are needed for proper RNA export (Kopytova et al., 2016) (Fig. 1.3E). Furthermore, purified recombinant human ORC has a stronger binding affinity for RNA and single-stranded DNA, compared to double-stranded DNA (Hoshina et al., 2013), suggesting that ORC may bind to RNA in other species as well. The exact biochemical mechanism and whether ORC regulates the export of specific RNAs or bulk RNAs remains unknown, but the possibility ORC may impact RNA export is an important consideration while studying ORC.

Lastly, ORC6 is associated with cytokinesis (Chesnokov et al., 2003) and ORC3 is associated with neurogenesis (Pinto et al., 1999; Rohrbough et al., 1999). However, the roles these ORC

subunits play in these functions are not well understood. In Drosophila cells, ORC6 is in excess relative to other ORC subunits and the localization of ORC6 is not restricted to the nucleus, as is the case with other ORC subunits (Chesnokov et al., 2001) (Fig. 1.3B). Specifically, ORC6 localizes to kinetochores and to the cell periphery in human cells during mitosis, and ORC6 is found at the midzone between the joined cells in anaphase (Prasanth et al., 2002). Furthermore, depletion of ORC6 in Drosophila causes failures in mitosis resulting in multinucleated cells (Prasanth et al., 2002). Whether ORC6 performs this role independently of the ORC complex or if DNA replication is linked to cytokinesis is unknown. Like ORC6, ORC3 can be found outside the nucleus, localizing to neuromuscular junctions in Drosophila, and is required for the proper development of these junctions (Pinto et al., 1999; Rohrbough et al., 1999). Interestingly, ORC3 in Drosophila was first characterized as a "memory" gene as olfactory memory is reduced in ORC3 mutants (Rohrbough et al., 1999). Mutations in ORC3 also cause defects in cell proliferation and in the development of the central nervous system in Drosophila (Pinto et al., 1999; Rohrbough et al., 1999) (Fig. 1.3D). The highly diverse roles of different ORC subunits indicate there may be crosstalk between DNA replication and other key biological processes, which further emphasize the importance of DNA replication initiation to other fields of study.

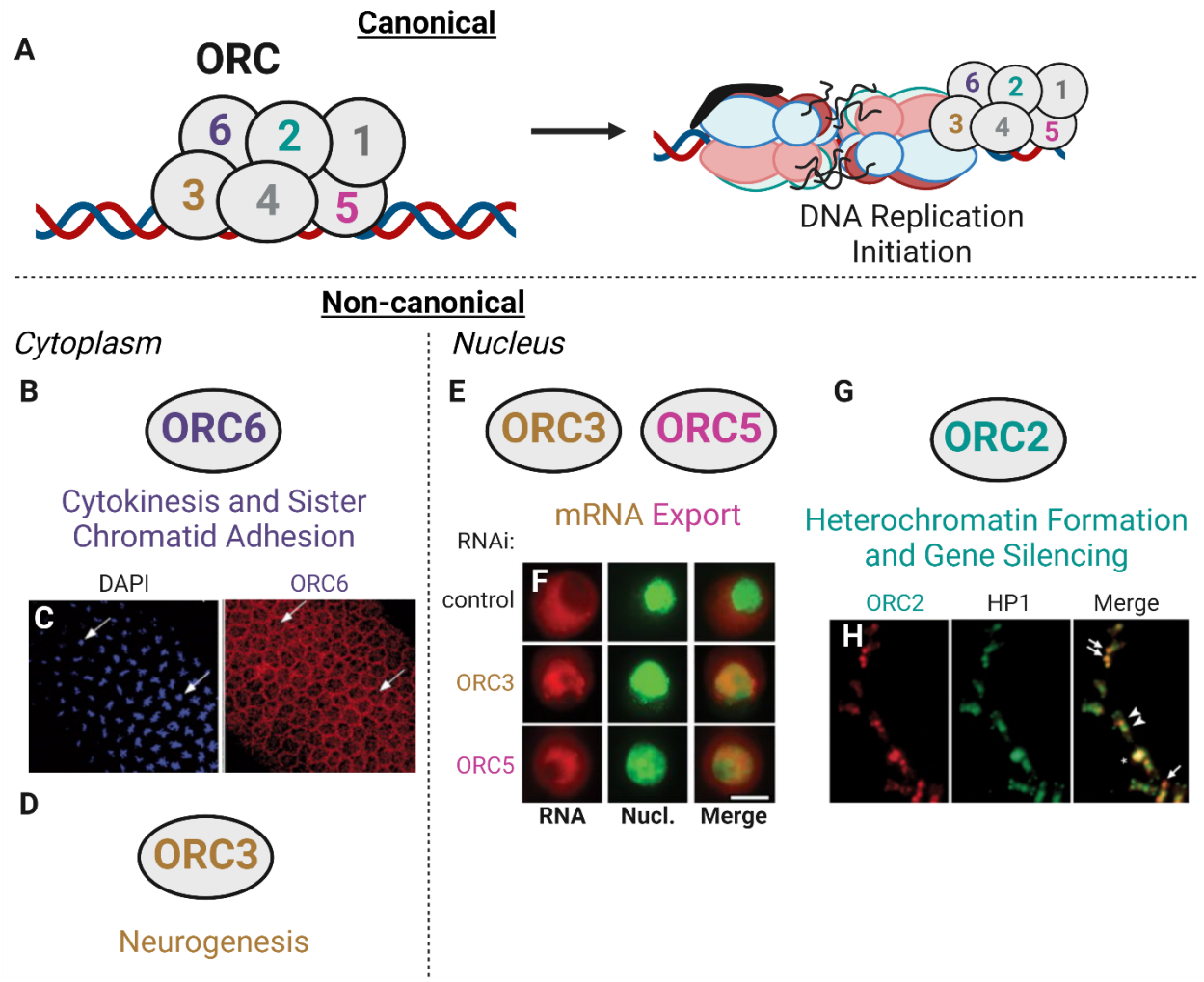

Fig. 1.3. ***The functions of ORC in*** **Drosophila melanogaster.** The functions of ORC can be separated in its into canonical functions in replication initiation (A) or its non-canonical functions (B-G). The non-canonical functions of ORC subunits both occur in the cytoplasm (B-D) and nucleus (E-H). (B) ORC6 is linked to cytokinesis and sister chromatid adhesion. (C) Localization of ORC6 in early embryos after cellularization. Arrows indicate the same cells within the Drosophila embryo. Note ORC6 in the cleavage furrow in between nuclei. (D) ORC3 has a role in neurogenesis in the early Drosophila embryo. (E) ORC3 and ORC5 are implicated in mRNA export. (F) FISH visualizing mRNA distribution in Drosophila S2 cells after RNAi against negative control (GFP), ORC3, or ORC5. RNA (red), Nucl. (nucleus) (green). Note the lack of RNA in the cytoplasm in the ORC3 or ORC5 RNAi-treated cells relative to the control. (G) ORC2 has roles in heterochromatin formation and gene silencing. (H) Immunofluorescence of ORC2 (red) and HP1 (green) on Drosophila cell mitotic spreads. Note the colocalization of ORC2 and HP1 in yellow. Arrows indicate regions of strong co-localization and arrowheads indicate regions of partial colocalization. Adapted from Chesnokov, 2007 and Kopytova et al., 2016. Made by Logan Richards.

The regulation of ORC activity

Given ORC plays a central role in DNA replication initiation, ORC is an ideal target to regulate origin activation to ensure proper DNA replication occurs. As such, there are regulatory mechanisms that ensure assembly of the replisome stops at certain point in the cell cycle to prevent re-replication; however, the regulation of ORC activity differs across species (DePamphilis, 2005) (Fig. 1.4). In budding yeast, there appear to be fewer redundant mechanisms for regulating the activity of ORC. For example, ORC protein levels through the cell cycle are constant in budding yeast (DePamphilis, 2005) whereas ORC1 protein levels are controlled by the E2F transcription factor in Drosophila and humans (Asano and Wharton, 1999; Ohtani et al., 1996). Furthermore, ORC1 in Drosophila embryos is selectively ubiquitinated by the anaphase promoting complex (APC) and degraded near the end of mitosis (Araki et al., 2003). ORC1 in humans is also ubiquitinated, but by a different complex, and is selectively degraded (DePamphilis, 2005; Méndez et al., 2002) (Fig. 1.4B-C). ORC1 is required for a functional ORC that is capable of loading helicases onto chromatin (DePamphilis, 2005), therefore selectively degrading ORC1 is an effective method of regulating ORC activity through the cell cycle.

The activities of ORC are also regulated by CDK-mediated phosphorylation. In budding yeast, ORC remains bound to chromatin throughout the cell cycle (Liang and Stillman, 1997), but phosphorylation inhibits ATPase activity and prevents helicase loading after G1 phase (Nguyen et al., 2001). Presumably, ORC must also be dephosphorylated upon entering a new cell cycle, and it is unclear if dephosphorylation occurs as a consequence of reduced CDK activity and passive dephosphorylation or if this is also an actively regulated process. Recent work has demonstrated that CDK-mediated phosphorylation of replication factors, specifically Sld2 and Sld3, are dephosphorylated by PP2A in budding yeast (Jenkinson et al., 2023). Phosphorylation of Sld2 and Sld3 is a critical part of helicase activation, and promotes the association of Sld2 and

Sld3 onto the assembling replisome; however, Sld2 and Sld3 are not components of the fully assembled and active replisome (Bell and Labib, 2016; Zegerman and Diffley, 2006). Interestingly, Sld2 and Sld3 are low abundance and limit the rate of replisome assembly (Mantiero et al., 2011). Dephosphorylation of Sld2 and Sld3 is believed to allow for the recycling of these factors at other origins of replication (Jenkinson et al., 2023). This work highlights that the dephosphorylation of replication initiation factors is an actively regulated and important process. Whether other replication factors are similarly dephosphorylated in a regulated manner remains unclear.

Akin to yeast, ORC is thought to remain bound to chromatin throughout the cell cycle in Drosophila, with the activity of ORC being controlled by selective ORC1 degradation at the end of mitosis (DePamphilis, 2005) (Fig. 1.4B). However, other studies have found that ORC1 and ORC2 are targeted for phosphorylation by CDK. This phosphorylation reduces the ability of ORC to bind to DNA and inhibits the ATPase activity of ORC (Remus et al., 2005), both of which are necessary for ORC to load helicase (Li and Stillman, 2012). Furthermore, CDK phosphorylation also inhibits the ATP-dependent DNA binding of Drosophila ORC *in vitro* (Remus et al., 2005), suggesting that ORC may be regulated by a different mechanism compared to budding yeast. More work is needed to understand the dynamics of ORC chromatin binding in Drosophila cells and the timing of phosphorylation by CDK, as the complete mechanism that directs ORC activity in Drosophila remains unclear.

The regulation of ORC activity in mammals is much more complicated. In humans, the association of ORC as a complete complex may be confined to strictly G1 phase as ORC1 is selectively degraded at the G1 to S phase transition (Araki et al., 2003), but ORC1 levels remain stable in Chinese hamster ovary cells (Li and DePamphilis, 2002) (Fig. 1.4C). During S phase, ORC dissociates from chromatin, with the exception of ORC2 and ORC3, which form heterodimers and

remain bound to the centromere to perform functions during mitosis (Li and Stillman, 2012). The displacement of ORC off chromatin may be CDK dependent, as phosphorylation of ORC2 is sufficient to displace ORC2 from chromatin (Lee et al., 2012). Furthermore, a hyperphosphorylated form of ORC1 has been observed that exhibits selective association with CDK1, appearing during mitosis (Fig. 1.4C). This phosphorylation and association with CDK1 are proposed to inhibit the chromatin association of ORC1 as inhibition of CDK1 activity causes ORC1 to efficiently re-associate to chromatin (Li et al., 2004). Whether this additional mechanism of ORC regulation is conserved across species is unknown and investigating the regulation of ORC by phosphorylation will be critical to understanding DNA replication.

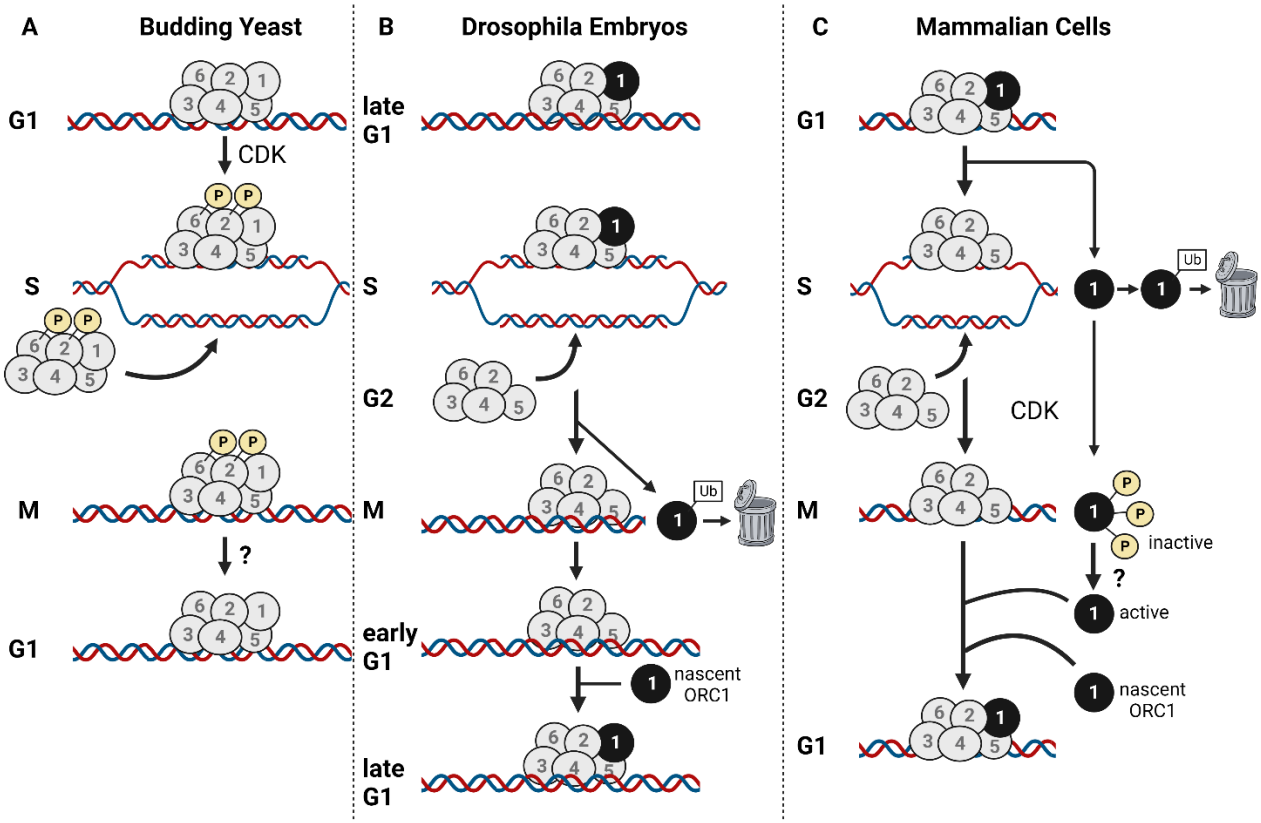

Fig. 1.4. ***Regulation of ORC activity across species.*** (A) In budding yeast, ORC (six gray circles) remains bound to DNA throughout the cell cycle. During S phase, ORC2 and ORC6 are phosphorylated by CDK to inhibit ORC activity after helicase loading to prevent re-replication. ORC2 and ORC6 are presumably dephosphorylated after mitosis to prime ORC for the next cell

cycle. (B) In Drosophila embryos, ORC subunits 2-6 remain bound to DNA throughout the cell cycle, but ORC1 (black circle) is selectively ubiquitinated and degraded during mitosis. Nascent ORC1 then reappears in late G1 to associate with ORC2-6 to enable helicase loading. (C) In S-phase Chinese hamster cells, ORC1 is ubiquitinated but not degraded, whereas in human cells, ORC1 can be ubiquitinated and selectively degraded. Presumably, new ORC complex is loaded onto DNA during S phase in an inactive state. During the S to M phase transition in hamster cells, the monoubiquitinated ORC1 is replaced with hyperphosphorylated ORC1, which is inactive. Upon entry to G1, ORC1 is presumably dephosphorylated and nascent ORC1 also reappears. ORC1 then associates with ORC2-6 to assemble active ORC capable of loading helicase. Adapted from DePamphilis, 2005, and made by Logan Richards

Replication timing[1]

Helicase Activation

Modeling and physiological studies indicate that helicase activation is the critical regulated step in DNA replication to establish replication kinetics and replication timing (RT – the time in S phase when a given DNA sequence is replicated) (Collart et al., 2013; Mantiero et al., 2011; Rhind et al., 2010). Helicase activation does not occur uniformly throughout the genome at the onset of S phase. Rather, helicase activation occurs continuously throughout S phase. Not all loaded helicases are activated during S phase. Even at a robust origin, efficiency of activation is 10% or less in mammalian cells (Demczuk et al., 2012; Dijkwel et al., 2002). When measuring RT across multiple organisms and cell types, specific patterns emerge. For example, open and active regions of chromatin often replicate early in S phase whereas condensed chromatin that is transcriptionally less active tends to replicate late in S phase (Rhind and Gilbert, 2013). RT allows thousands of independent initiation events to be orchestrated throughout S phase to ensure that the entire genome will be duplicated. The reality, however, is somewhat more random.

[1] This section was adapted from Richards et al. Genes. 2022.

Stochastic model for replication timing

While the population-level studies have established DNA replication timing is regulated at the level of genomic domains containing clusters of replication origins, a single-molecule study in human cells has revealed that initiation does not happen in a concerted manner utilizing distinct domains of frequently firing origins (Wang et al., 2021). Instead, initiation occurs stochastically within larger zones that are arbitrarily allocated. For example, even the top 5% of initiation zones are only used in 11% of the population. This suggests that RT is both heterogenous and probabilistic. This model of RT is consistent with an in-silico model of replication kinetics assuming stochastic origin firing (Gindin et al., 2014).

Replication timing has important implications in governing replication kinetics. While helicase activation appears to be the critical rate-limiting step for RT (Collart et al., 2013; Mantiero et al., 2011), the molecular underpinnings of helicase activation throughout the genome and the duration of S phase are still not fully understood. A mechanistic understanding of the factors controlling RT will be critical to understanding of replication timing kinetics and genome stability.

The biological function of replication timing

While genome-wide techniques such as Repli-seq, Timing Inferred from Genome Replication (TIGER) and optical replication mapping (ORM) have allowed for the measurement of RT with high precision and resolution across multiple organisms and cell types (Koren et al., 2021; Marchal et al., 2018; Wang et al., 2021), the biological function of RT has been more difficult to ascertain. Several key studies, however, suggest that RT has at least two key functions: maintaining genome stability by ensuring the distribution of limiting factors across replication forks

during S phase (Collart et al., 2013; Mantiero et al., 2011) (Fig. 1.5) and maintaining epigenetic information during replication (Klein et al., 2021; Zhang et al., 2002) (Fig. 1.7).

The function of replication timing in eukaryotes

In eukaryotes, the temporal order of origin firing defines the RT program. The low levels of the two CDK targets Sld3 and Sld2, their binding partner Dpb11 and the DDK subunit Dbf4 are limiting for replication initiation in budding yeast and Xenopus (Collart et al., 2013; Mantiero et al., 2011). Simultaneous overexpression of these four factors causes early firing of late origins and increases the speed of S phase (Mantiero et al., 2011). Abolishment of the RT program in this case leads to a severe growth defect and activation of the checkpoint response. This is likely due to the exhaustion of limiting replication factors such as dNTPs and establishes the importance of RT to conserve limiting pools of replication factors to prevent genome instability (Mantiero et al., 2011). Therefore, the RT program allows limiting factors such as dNTPs and histones to be distributed throughout S phase an avoids the exhaustion of these factors, which would trigger DNA damage and genome instability.

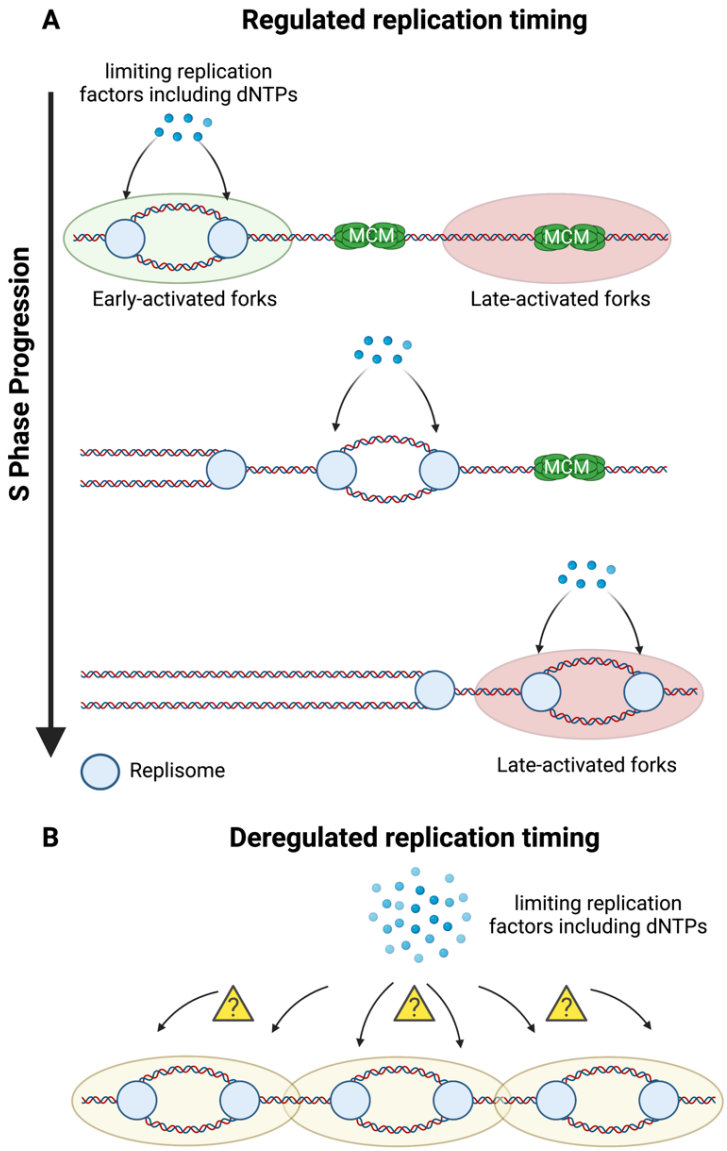

Figure 1.5. ***Replication timing maintains genome stability.*** (A) The replication timing program maintains a supply–demand equilibrium of limiting replication factors, which could be histones, replisome proteins or dNTPs. (B) In a de-regulated replication timing program, an excess of origins may become activated, resulting in the pool of limiting replication factors to be depleted and DNA damage to occur. Adapted from Richards et al., 2022a[2].

[2] Richards et al., 2022a published under open copyright.

Correlations between rates of mutation and replication timing

In addition to the genome instability caused by disruption of the RT program, the rate of mutation occurring in a genomic region is correlated with its RT in yeast, Drosophila, rodents and humans, with earlier replicating regions having a lower mutation rate than their late-replicating counterparts (Sima and Gilbert, 2014) (Fig. 1.6). The higher frequency of single nucleotide variants (SNVs) in late-replicating regions also plays a major role in acquired drug-resistance in lung cancer cells (Jia et al., 2013). In an evolutionary assessment of Human-chimpanzee substitutions and human single nucleotide polymorphism (SNP) density, the mutation rate, as reflected in recent evolutionary divergence and human nucleotide diversity, is found to be markedly increased in later-replicating regions of the human genome (Stamatoyannopoulos et al., 2009). A better understanding of the molecular underpinnings of the RT program will have substantial implications in genome stability, disease, drug-resistance, and evolutionary biology.

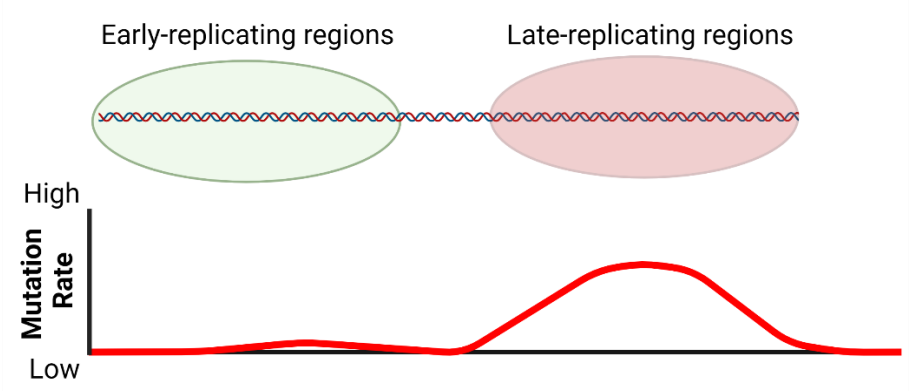

Figure 1.6. ***Late-replicating regions have a higher mutation rate than early-replicating regions.*** Green oval is representative of a region of the genome that replicates earlier in S phase whereas the red oval represents a late-replicating genomic region. A visualization of the mutation rate across these two genomic regions is shown with late-replicating genomic regions typically

having higher rates of mutation relative to early-replicating genomic regions. Adapted from Richards et al., 2022a[2].

Replication timing and the maintenance of the epigenome

RT could also be a key factor in maintaining epigenetic state (Fig. 1.7). Early work in rat cells suggested a mechanistic connection between replication timing and chromatin packaging (Zhang et al., 2002). Exogenous plasmids microinjected in nuclei during early S-phase were significantly enriched for acetylated histones, while deacetylated histones were associated with the plasmids injected in late S-phase. More recently it was shown in human cells that if RT is perturbed, the distribution of heterochromatic histone modifications is altered in human cells (Klein et al., 2021). Interestingly, there are two classes of heterochromatic regions that either affected or unaffected by perturbing the RT program. The affected domains tend to be enriched for smaller H3K9me3 peaks. In contrast, unaffected domains form much larger and broad H3K9me3 domains (Klein et al., 2021), which may somehow protect these domains from changes in RT. Additionally, the levels of active histone modifications, specifically H3K27ac and H3K4me3, are significantly depleted if RT is deregulated (Klein et al., 2021). Consistent with RT as a critical regulator of epigenetic maintenance, these changes in histone modifications coincide with S phase (Klein et al., 2021). This suggests that DNA replication is important for epigenetic modifications and that RT could play a vital role in the propagation of epigenetic information. These findings, however, were limited to human cell lines (Klein et al., 2021). It will be interesting to understand if these observations are subject to developmental regulation or if they hold true in other species. Directly coupling RT to epigenetic status represents a new and exciting function of RT, but the mechanism as to how this occurs requires further investigation.

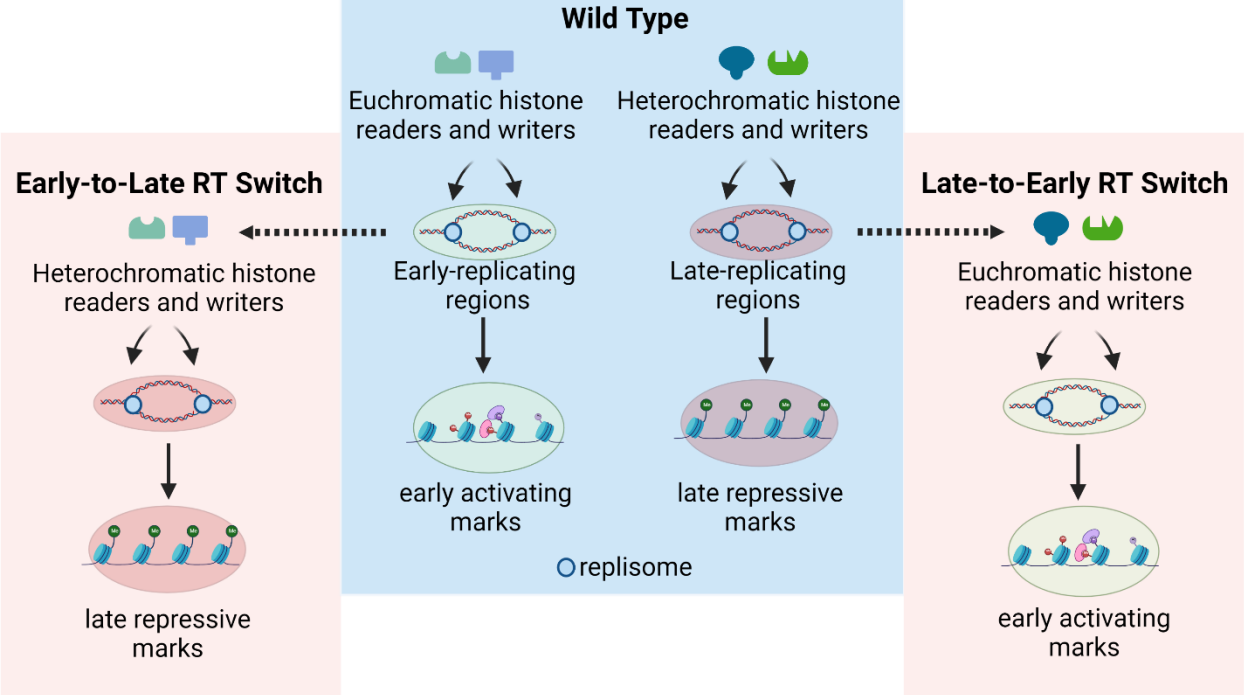

Figure 1.7. ***The replication timing program maintains the epigenetic landscape.*** In the wild type example (blue box), replication timing preserves the epigenetic landscape. This is achieved by allowing euchromatic and heterochromatic histone readers and writers to be properly recruited to replication forks within early and late-replicating regions, respectively, during S phase. The pink boxes indicate de-regulated replication timing. In this example, a region switches from early to late replicating (E to L Switch) or late to early replicating (L to E switch). Consequently, the wrong histone readers and writers are targeted to those regions. This results in the epigenetic landscape changing upon replication timing disruption. Adapted from Richards et al., 2022a[2].

Rif1 is an active regulator of replication timing[3]

Rif1 is a PP1 specificity factor that regulates replication timing across species

Because RT is closely associated with chromatin accessibly (Gilbert, 2002; Rhind and Gilbert, 2013; Schwaiger and Schübeler, 2006) and RT shows considerable cell-to-cell variability (Dileep and Gilbert, 2018; Hiratani and Takahashi, 2019), RT may simply be a passive reflection of chromatin accessibility. This is not the case; however, as the biochemical regulation of RT is

[3] This section was adapted from Richards et al. Genes. 2022.

beginning to be mechanistically understood through the discovery trans-acting factors that actively regulate RT. This indicates that, while helicase loading and activation are influenced by chromatin accessibility, the execution of the RT program is an actively controlled process. One factor that regulates RT is Rap1 interacting factor 1 (Rif1). Rif1 was initially discovered in a yeast 2-hybrid assay for proteins that interacted with Rap1, an essential regulatory protein in budding yeast (Hardy et al., 1992). The first evidence that Rif1 could regulate RT, however, arose from a study in budding yeast where *rif1Δ* cells caused genomic regions proximal to telomeres, which are normally late-replicating, to replicate earlier in S-phase (Lian et al., 2011). Later studies revealed that loss of Rif1 activity cause global changes in RT in fission yeast, fruit flies, mice and humans (Armstrong et al., 2020; Cornacchia et al., 2012; Hayano et al., 2012; Seller et al., 2018; Yamazaki et al., 2012). Therefore, determining the mechanism of Rif1's activity is critical to understanding how RT is regulated.

The mechanism of Rif1 function in RT control was initially suggested through a genetic interaction with Cdc7 (*hsk1*) in *S. pombe* (Hayano et al., 2012). Cdc7 is the catalytic subunit of DDK (Jares et al., 2000). *hsk1* null cells are inviable due to the inability to activate the replicative helicase (Takeda et al., 2001). A screen for suppressors for loss of *hsk1* revealed that deletion of *rif1* could restore growth to *hsk1* null cells (Hayano et al., 2012). This study also revealed that the origin firing throughout the genome was altered in *rif1* null cells. While this work made clear that Rif1 was a negative regulator of replication, the biochemical mechanism was still unclear.

Although Rif1 regulates RT from yeast to humans, its sequence has diverged considerably (Sreesankar et al., 2012). There are several common features present within all orthologs of Rif1. Rif1 possesses HEAT repeats, which are tandem repeats of amino acids that form alpha-helices and are important for the telomere length regulation by Rif1 in budding yeast (Fig. 1.8). Additionally, budding yeast Rif1 contains a Rap1 binding module and C-terminal domain, which

are also necessary for the yeast-specific functions of Rif1 at telomeres (Fig. 1.8). Another common feature of all Rif1 orthologs are the presence of PP1 binding motifs, the SILK and RVxF motifs (Davé et al., 2014; Hiraga et al., 2017; Mattarocci et al., 2014; Sukackaite et al., 2017) (Fig. 1.8). The proposed biochemical mechanism for Rif1-dependent control of DNA replication is based on Rif1's ability to bind Protein Phosphatase 1 (PP1) and direct PP1 activity towards specific substrates (Alver et al., 2017; Davé et al., 2014; Hiraga et al., 2017, 2014; Sukackaite et al., 2017).

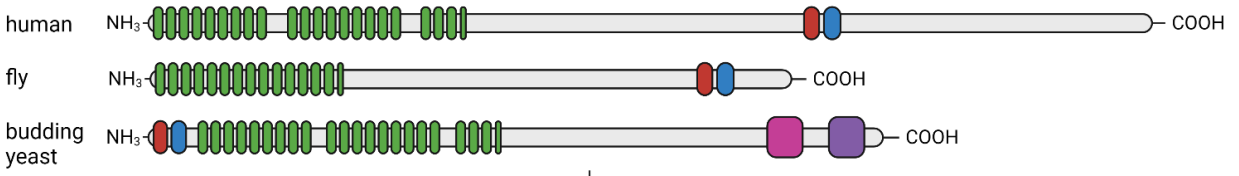

Symbol	Name	Function
	HEAT repeats	Telomere length regulation
	SILK motif	PP1 binding
	RVxF motif	PP1 binding
	Rap1 binding module	Telomere length regulation
	C-terminal domain	Telomere length regulation

Table 1.1. The domains of Rif1

Figure 1.8. ***The functional domains of Rif1 are evolutionarily conserved.*** Schematic of the protein domains and motifs present within Rif1 in humans, flies, and budding yeast with table showing domain names and functional properties below. Adapted from Mattarocci et al., 2016 and made by Logan Richards.

In the context of helicase activation, Rif1/PP1 targets MCMs to oppose DDK-mediated activation the helicase, thus preventing or delaying initiation of replication at specific start sites (Fig. 1.10B). There is a wealth of genetic data connecting Rif1 to helicase activation. For example, reducing DDK activity leads to a decrease in MCM4 phosphorylation and a loss in viability, both of which can be suppressed by deleting *Rif1* (Alver et al., 2017; Hiraga et al., 2017, 2014). Furthermore, MCM4 is hyper-phosphorylated in yeast and Xenopus if Rif1 is absent or depleted (Alver et al.,

2017; Hiraga et al., 2017, 2014). It is surprising that, while Rif1 clearly regulates MCM phosphorylation levels, there is little evidence of a direct biochemical interaction. While several studies have used an IP-mass spec approach to identify Rif1-associated proteins, the MCM complex has not been identified (Alver et al., 2017; Sukackaite et al., 2017). This could be for several reasons. For example, the association of Rif1/PP1 with MCMs could be too transient to identify by IP (although covalent cross linkers were used in these experiments). Thus, how Rif1 is targeted to, and associates with, loaded helicases is still an outstanding question.

The other potential replication initiation factors targeted by Rif1

While loss of Rif1 function suppresses a temperature sensitive (ts) allele of *Cdc7* (Hiraga et al., 2014), loss of Rif1 activity also suppresses ts alleles of *Dpb11*, *Sld3* and *Cdc45* alleles (Mattarocci et al., 2014). This observation suggests that Rif1 more broadly regulates helicase activation, perhaps beyond just controlling MCM phosphorylation levels. Both Sld3 and Cdc45 are 'readers' of MCM phosphorylation. Their recruitment to MCM hexamers is dependent on MCM phosphorylation (Deegan et al., 2016). Perhaps the increased MCM phosphorylation in the absence of Rif1 increases the efficiency of Sld3 and Cdc45 recruitment, increasing the probability of helicase activation even with limiting amounts of Sld3 and Cdc45. Loss of Rif1 activity also increases the phosphorylation level of Sld3 in G1 phase, possibly impacting the activity of Sld3 (Mattarocci et al., 2014). The suppression of *Dpb11* ts phenotype, however, is not clear. Dpb11 and Sld3 physically associate in a phospho-specific manner (Mantiero et al., 2011; Tanaka et al., 2011). This interaction, however, is dependent on CDK rather than DDK. Perhaps the increase in MCM phosphorylation that occurs upon loss of Rif1 function results in a more efficient helicase activation step. In this case, increased helicase activation could drive Dbp11-dependent replisome assembly.

In support of this model, single molecule experiments revealed that DDK phosphorylation of MCMs recruits multiple GINS and Cdc45 subunits (De Jesús-Kim et al., 2021) Furthermore, DDK is required for the efficient formation of a key intermediate complex of the replicative helicase and removing a subset of phosphorylation sites on MCM2-7 reduces the efficiency of replicative helicase formation. This model has interesting implications on RT, where Rif1 also contributes to the balance of MCM phosphorylation during helicase activation. The phosphorylation of the N-terminal tails of MCMs correlates with the efficiency of helicase activation, therefore this could provide a biochemical mechanism for Rif1-mediated delay of helicase activation and ultimate control of RT (De Jesús-Kim et al., 2021).

Rif1 in the regulation of ORC activity

In addition to Sld3, Cdc45 and Dpb11, Rif1 appears to regulate ORC1 activity (Hiraga et al., 2017) (Fig. 1.9A). An unbiased phosphoproteomic screen revealed that, in addition to MCMs, ORC1 is hyperphosphorylated upon Rif1 depletion in human cells (Hiraga et al., 2017). Additionally, the level of chromatin-bound ORC1 is reduced upon Rif1 depletion. The consequence of this is a reduction in MCM loading in G1 phase of the cell cycle. This work revealed that Rif1 protects ORC1 from phosphorylation as phosphorylation of ORC1 targets it for degradation (Hiraga et al., 2017). Rif1 appears to target ORC1 in G1 phase to promote helicase loading and targets MCMs in S phase to prevent helicase activation (Hiraga et al., 2017) (Fig. 1.9A-B). While this may contrary to the role of Rif1 in suppressing origin activation, it appears that Rif1 functions in two phases of the cell cycle to ensure enough helicases are loaded while preventing excessive helicase activation. In this regard, Rif1 is a major regulator of the overall DNA replication program.

The roles of Rif1 beyond replication timing

While Rif1 is a key regulator of RT, it has additional functions in chromatin biology that are independent of its ability to control RT. In budding yeast, Rif1 interacts with Rap1 to control telomere length (Hardy et al., 1992). Rif1's involvement in functional telomere maintenance, however, appears specific to budding yeast (Buonomo et al., 2009; Castaño et al., 2005; Kanoh and Ishikawa, 2001; Levy and Blackburn, 2004; Silverman et al., 2004; Xu and Blackburn, 2004). In mammalian cells, Rif1 is involved in DNA double-strand break (DSB) repair. In this context, Rif1 is recruited to DSBs by 53BP1 where, together with other factors, prevents end resection. This ultimately inhibits homologous recombination and promotes non-homologous end joining (NHEJ) (Chapman et al., 2013; Escribano-Díaz et al., 2013; Di Virgilio et al., 2013; Zimmermann et al., 2013). Recent work has identified several key factors and protein complexes that work with Rif1 at DSBs (Mirman et al., 2018; Noordermeer et al., 2018). Interestingly, Rif1 has a 53BP1-independent function in protecting cells from ultrafine anaphase bridges that form as a result of unresolved centromeric catenanes (Hengeveld et al., 2015). Rif1 can also be recruited to stalled replication forks in a 53BP1-independent manner (Mukherjee et al.).

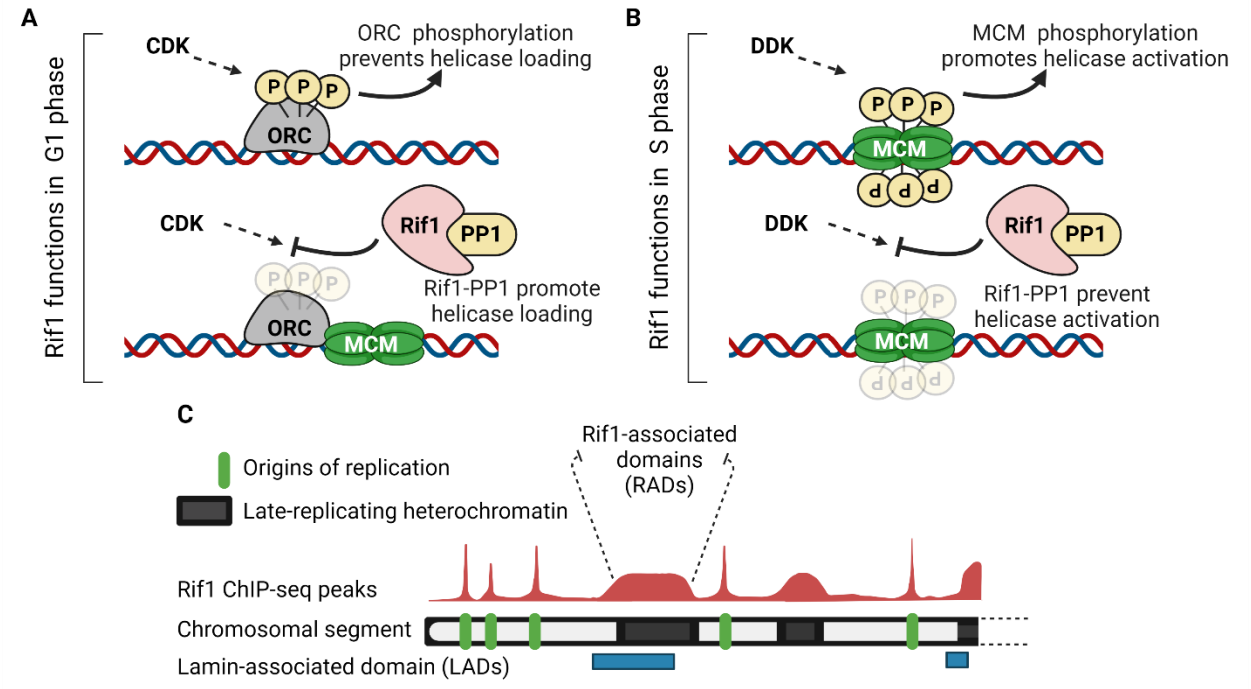

Figure 1.9. ***The functions of Rif1.*** (A) In G1 phase, Rif1 may reverse the CDK-mediated phosphorylation of ORC to promote ORC-dependent loading of MCMs. (B) In S phase, Rif1 opposes DDK-mediated MCM phosphorylation to inhibit helicase activation and origin activation in late-replicating genomic regions. (C) A representative view of Rif1 genomic binding on a chromosomal arm. Green boxes denote origins of replication, where Rif1 genomic binding has a sharp, well-defined peaks. Black boxes indicate regions of heterochromatin, where Rif1 binds to broad domains with a lower signal intensity compared to origins. The broad Rif1 binding domains also have overlap with lamin-associated domains, indicated by blue boxes. Adapted from Richards et al., 2022a[2].

Rif1 activity is regulated during development

In spite of different species-specific functions and mechanisms, Rif1 plays an important role in governing the global RT program from yeast to mammals (Armstrong et al., 2020; Cornacchia et al., 2012; Hayano et al., 2012; Klein et al., 2021; Peace et al., 2014; Yamazaki et al., 2012). The effect Rif1 has on global RT, however, varies among species and depends on developmental state. In budding yeast and fission yeast, Rif1 affects RT of 65% and 30% of the origins respectively (Hayano et al., 2012; Peace et al., 2014). In Drosophila, 8-30% of genome-wide RT depends on Rif1 depending on cell type (Armstrong et al., 2020; Das et al., 2021). In mammalian cells, Rif1-mediated control of RT can range from ~23% to ~100% depending on cell type with human embryonic stem cells (hESCs) showing the most significant dependence on Rif1 for RT (Cornacchia et al., 2012; Foti et al., 2016; Klein et al., 2021). In both Drosophila and human cells, RT is also sensitive to the dosage of Rif1 (Armstrong et al., 2020; Klein et al., 2021). While it seems that upon loss of Rif1 function, there is a predominate transition from late to early (LtoE) replication throughout the genome, often the fraction of the genome that transitions from early to late (EtoL) and LtoE are equal (Armstrong et al., 2020; Foti et al., 2016; Hayano et al., 2012; Klein et al., 2021; Peace et al., 2014). It is still unclear why such a large fraction of the genome transition from EtoL based on the Rif1's ability to prevent helicase activation. However, EtoL changes could

be driven through indirect effects of LtoE RT changes within such a large fraction of the genome (Armstrong et al., 2020). Determining the specific mechanism driving the Rif1-dependent changes in replication timing, notably the EtoL transitions, still remains a gap in knowledge to be addressed by the field.

Understanding how Rif1 activity is regulated during development and differentiation could reveal the molecular basis for how cell-type-specific RT programs are established. One powerful system to directly investigate how Rif1 activity is modulated during development is the early Drosophila embryo. The first 14 cell cycles in the Drosophila embryo are rapid and tightly coordinated (Farrell and O'Farrell, 2014). S phase in the first nine cell cycles is 3-4 minutes in length (Blumenthal et al., 1974) (Fig 1.10). Starting in cycle 9, S phase gradually slows until cell cycle 14 where S phase more dramatically slows to 50 minutes (Shermoen et al., 2010) (Fig 1.10). The slowing of S phase in cycle 14 is driven by the onset of RT and a pattern of late replication where heterochromatin is exclusively replicated (Shermoen et al., 2010). This provides a unique opportunity to study the factors and processes that drive the onset of RT. Critically, one factor that significantly contributes to the slowing of S phase in cycle 14 and the onset of late replication is Rif1 (Seller et al., 2018) (Fig. 1.10). In fact, S phase is ~60% faster in cell cycle 14 in *Rif1* mutant embryos and the characteristic pattern of late replication is lost (Seller et al., 2018). Importantly, Rif1 localization patterns anticipate the establishment of RT in cycle 14. Rif1 localizes to satellite sequences in cycle 14, but dissociates prior to their replication (Seller et al., 2018). What makes this such a powerful system is that Rif1 is present in cycles 1-13 but is held inactive. Rif1 appears to be activated prior to cycle 14 (Seller et al., 2018).

It is currently unknown what drives the switch in Rif1 activity. Rif1 contains CDK consensus sites and is heavily phosphorylated in the early embryo, raising the possibility that high levels of CDK activity in the early embryo keep Rif1 inactive (Seller et al., 2018). Consistent with this hypothesis,

expression of a Rif1 protein with all CDK sites mutated to alanine (phosphomutant) blocks replication resulting in mitotic errors (Seller et al., 2018). This suggests that phosphorylation acts as a molecular switch to control Rif1 activity. Cells are also sensitive to the level of Rif1 expression and overexpression of wild type Rif1 is detrimental to cells, which could be a caveat to this experiment (Seller et al., 2018). In human cells, Rif1-phosphorylation is also dependent on CDK1 (Moiseeva et al., 2019). In Xenopus egg extract, depletion of Rif1 or Rif1-CTD (C-terminal domain that contains PP1-binding site), results in less PP1 on chromatin and a reduced rate of MCM-phosphorylation (Ciardo et al., 2021; Moiseeva et al., 2019). This suggests that Rif1 has the potential to regulate replication in the earliest stages of vertebrate development.

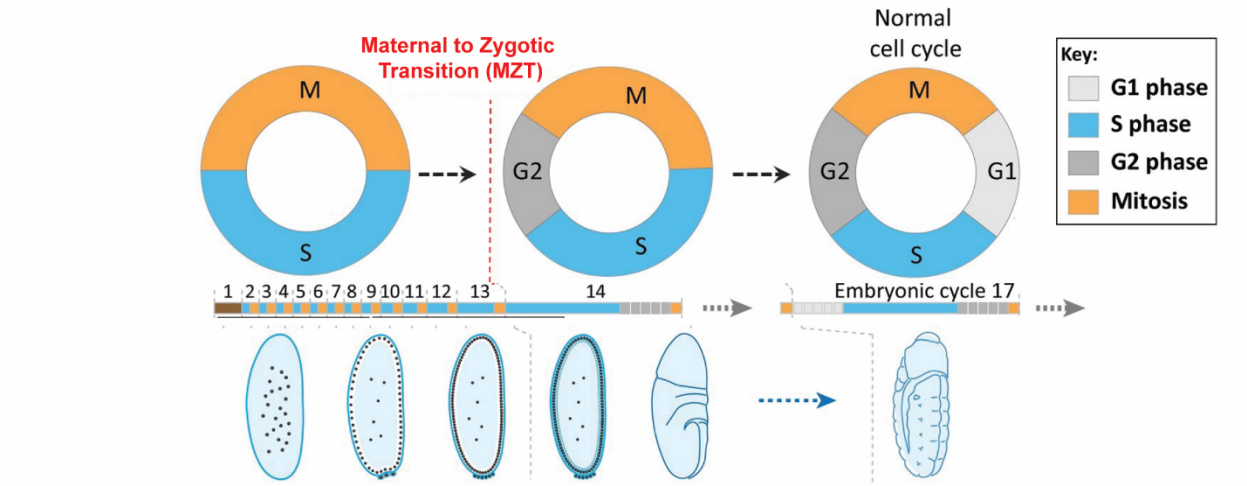

Stage of Development	Pre-MZT	Post-MZT	Late Embryogenesis
Replication Timing?	No	Yes	Yes
Length of S-Phase	3-4 minutes	~60 minutes	8 hours
Rif1 Present?	Yes	Yes	Yes

Table 1.2. The state of replication timing and the length of S phase through development

Figure 1.10. ***The onset of the replication timing program correlates with the maternal to zygotic transition.*** During the first 12 cycles, S phase proceeds quickly, replicating the entire genome in 3-4 minutes, as origins fire synchronously in the absence of replication timing and presumably Rif1 activity. At nuclear cycle 13, Rif1 is targeted to satellite sequences, delaying replication in those genomic regions and causing the extension of S phase. Importantly, Rif1 is

maternally deposited, and therefore the activity of Rif1 is predicted to be developmentally regulated. Adapted from Yuan et al., 2017 and made by Logan Richards.

Rif1 dynamically associates with chromatin through the cell cycle and development

Understanding how and where Rif1 is localized to chromatin is an important step in understanding Rif1 function. Immunofluorescence (IF) and live cell imaging studies reveal that in metazoans, Rif1 dynamically associates with chromatin during S phase (Buonomo et al., 2009b; Cornacchia et al., 2012; Seller et al., 2018; Yamazaki et al., 2012). The exact nature of Rif1 localization with respect to DNA replication is not as clear. In mouse and human cells, Rif1 localizes to chromocenters or DNaseI insoluble chromatin, which are both heterochromatic. Rif1 also colocalizes with BrdU, a marker of DNA replication, during mid S phase (Buonomo et al., 2009; Yamazaki et al., 2012). Other studies in mouse cells and Drosophila embryos, however, show that Rif1 disassociates from chromatin prior to the formation of replication foci (Cornacchia et al., 2012; Seller et al., 2018).

High-resolution localization of Rif1 has been measured using both ChIP-seq and CUT&RUN (Foti et al., 2016; Hayano et al., 2012; Hiraga et al., 2017, 2018; Kanoh et al., 2015; Klein et al., 2021). Features of Rif1 genomic binding, however, vary depending on the organism. Early work in budding yeast revealed that Rif1 binds to chromatin primarily at telomeres and is dependent on Rif1's binding partner: Rap1 (Hardy et al., 1992). Beyond budding yeast, there are seem to be two characteristics of Rif1 binding: Rif1 binds to late-replicating genomic regions (Foti et al., 2016; Klein et al., 2021) and Rif1 binding is enriched at origins of replication (Hayano et al., 2012).

The characteristics of Rif1 genomic binding sites across species

In fission yeast, Rif1 binds telomere proximal regions and late-replicating origins of replication within subtelomeric regions (Hayano et al., 2012). In G1 and early S phase cells, Rif1 also binds to both early and late-replicating origins of replication throughout the genome. Interestingly, in fission yeast, Rif1 binds to centromeres during M phase and remains bound until the completion of S phase (Hayano et al., 2012). Further work in fission yeast also revealed that Rif1 binding sites are enriched for a consensus sequence. This Rif1 consensus sequence contains G-quadruplex-like structures, and G-quadruplexes are necessary for Rif1 binding (Kanoh et al., 2015).

Consistent with Rif1's telomere-specific functions in budding yeast, Rif1 also shows strong binding to telomeres (Smith et al., 2003). Rif1's association to telomeres is dependent on Rap1, which targets Rif1 to yeast telomeres (Hardy et al., 1992; Hiraga et al., 2018). In budding yeast, however, Rif1 also binds to genomic regions independently of Rap1. Specifically, Rif1 associates with many replication origins both near and distant to telomeres (Hiraga et al., 2018), similar to fission yeast (Hayano et al., 2012). Surprisingly, Rif1 also associates with the coding regions of highly transcribed genes independently of Rap1, and the biological reason for this observation still remains unknown (Hiraga et al., 2018).

In mouse embryonic stem cells, Rif1's genomic distribution overlaps primarily with late-replicating regions and is depleted from early-replicating regions, which is consistent with the hypothesis that Rif1 is recruited to chromatin to prevent helicase activation (Alver et al., 2017; Hiraga et al., 2017, 2014). Also, Rif1 binds large genomic domains termed Rif1-associated domains or RADs. RADs show significant overlap with Lamin associated domains (LADs), which are associated with the nuclear lamina and tend to be late-replicating (Foti et al., 2016) (Fig. 1.9C). Besides the broad RADs, a smaller fraction of Rif1 forms more distinct peaks. Only a subset of these peaks, however, are associated with potential replication origins (Foti et al., 2016) (Fig. 1.9C). These

sites are often in early-replicating regions that are associated with transcription start sites and have high GC content with the possibility of forming G4 quadruplexes. Critically, while Rif1 appears to bind and regulate individual replication origins in fission yeast (Hayano et al., 2012), Rif1 appears to act more broadly at the domain level to regulate replication in mammals (Foti et al., 2016).

More recently, Rif1 binding has been profiled using CUT&RUN in human embryonic cell lines. Similar to mouse cells (Foti et al., 2016), Rif1 was enriched within late-replicating genomic regions and bound broad domains (Klein et al., 2021). Importantly, Rif1 binding occurred at genomic regions that became deregulated in their replication timing upon loss of Rif1 function (Klein et al., 2021). Rif1 seems to form broad domains within late-replicating regions across species while also binding specifically to replication origins, and the reason for this is not understood. One explanation for this is that there may be multiple populations of Rif1: Rif1 targeted to chromatin domains to promote late replication by opposing helicase activation and Rif1 targeted to replication origins and transcription start sites to perform an alternative regulatory function. Within these separate populations, Rif1 could perform different functions depending on chromatin context. The underlying factors necessary for Rif1 recruitment to chromatin is still unclear.

Rif1 and nuclear organization

RT is also highly correlated with nuclear architecture. Hi-C-based chromosome capture experiments have classified regions of self-associating genomic folding (Dixon et al., 2012; Lieberman-Aiden et al., 2009; Nora et al., 2012). These spatially organized domains are commonly called Topologically Associated Domains (TADs). TADs serve as the units for the genomic-level organization of the chromosomes that remain stable through cell divisions and diverse cell types. A TAD can be defined as a self-interacting genomic region, with two basic

features of organization: self-association and neighbor-insulation. A study of 18 human and 13 mouse cell types mapped the genomic boundaries of TADs and Replication Domains (RD; genomic regions with similar RT status) by Hi-C and discovered that they share a near 1:1 correlation (Pope et al., 2014).

While it is clear that RT is highly correlated by nuclear organization and structure, it is less clear what underlying molecular mechanisms drive these correlations. Recent work, however, has suggested that Rif1 may provide a link between nuclear organization and RT. First, Rif1 associates with Lamin, thus providing a link between Rif1-associated domains (RADs) and the nuclear periphery (Cornacchia et al., 2012; Foti et al., 2016). Second, Rif1 has a critical role in promoting 3D nuclear organization (Foti et al., 2016; Gnan et al., 2021) (Fig. 1.11).

In mouse ESCs, nuclear organization and RT are differentially sensitive to Rif1 dosage (Gnan et al., 2021). Cells hemizygous for Rif1 have normal RT but altered nuclear organization, suggesting that nuclear organization, but not RT, is sensitive to Rif1 dosage (Gnan et al., 2021). It is surprising, however, that RT is not sensitive to Rif1 dosage in mouse embryonic stem cells while RT is sensitive to Rif1 dosage in both Drosophila and human embryonic stem cells (Armstrong et al., 2020; Klein et al., 2021). One interpretation of this work is that Rif1-dependent nuclear organization is independent from Rif1's role in regulating RT. This would be consistent with 4C data in mouse cells showing that depletion of Rif1 in G1 (prior to execution of an altered RT program) causes an increase in inter-TAD interactions in G1, further arguing that Rif1 has a direct role on controlling nuclear organization independent of RT (Foti et al., 2016).

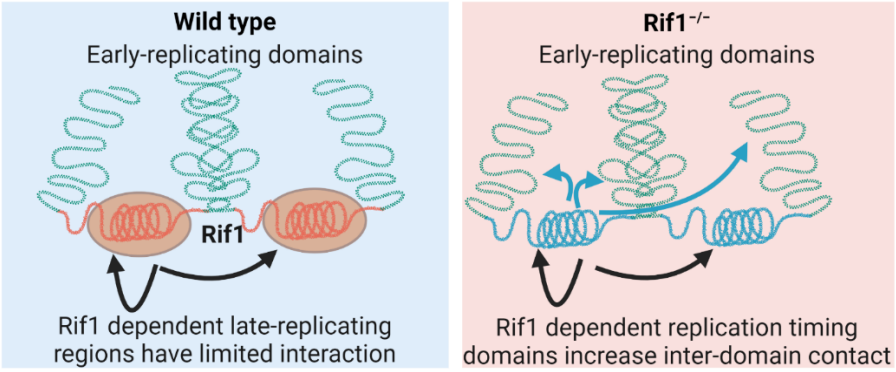

Figure 1.11. *Rif1 mediates nuclear organization*. In cells that are wild type for *Rif1* (blue box), early and late replicating domains are separated from each other (green and red DNA respectively). The late replicating domains, which are coated with Rif1, have limited physical interactions. In cells that are mutant for *Rif1*, there is an increase in physical interactions between genomic domains that depend on Rif1 to maintain their replication timing. Adapted from Foti et al., 2016 and Richards et al., 2022a[2].

Nucleoporins: NPC subunits implicated in chromatin organization and gene expression

Nucleoporins form the gateway into the nucleus

The nuclear pore complex (NPC) is a massive assembly of proteins in the cell, with a molecular mass of approximately 50 mDa (the human 80S ribosome has a molecular weight of 4.3 mDa for comparison) and is built from multiple copies of approximately 30 different proteins, termed nucleoporins (Nups) (Strambio-De-Castillia et al., 2010). The NPC sits at the barrier between the cytoplasm and nucleus and can be subdivided into three main functional structures: the barrel-shaped central channel, the cytoplasmic filaments, and the nuclear basket structure (Strambio-De-Castillia et al., 2010) (Fig. 1.12). The core structure of the NPC is comprised of spokes that form an eight-fold symmetrical cylinder, which circle the nuclear transport channel (Strambio-De-Castillia et al., 2010) (Fig. 1.12, see inner and outer rings). The inner channel functions as a sieve to allow for the passive diffusion of small metabolites in and out of the nucleus but regulates the transport of larger macromolecules such as protein and RNA (Strambio-De-Castillia et al., 2010).

The inner channel consists of Nups containing Phe-Gly repeats and are called FG Nups (Strambio-De-Castillia et al., 2010) (Fig. 1.12, see Nuclear FG). These FG Nups serve as a molecular filter as only cargo bound to nuclear transport factors, which specifically bind to FG Nups, can pass through the channel (Strambio-De-Castillia et al., 2010). The cytoplasmic filaments facing the cytoplasm direct exported RNAs towards protein synthesis machinery and funnels incoming cargo into the NPC (Strambio-De-Castillia et al., 2010). The nuclear basket structure, facing the nuclear side, plays many roles and links the NPC to mRNA synthesis, chromatin organization, and gene expression (Strambio-De-Castillia et al., 2010). Recently, individual Nups have also been found to have NPC-independent roles in epigenetic regulation and transcription (Ibarra and Hetzer, 2015). Therefore, NPCs and the Nups they consist of may be a critical factor in the regulation of RT and DNA replication initiation, both of which are linked to chromatin organization.

For example, the nucleoporin Elys binds to chromatin in late mitosis and is required to assemble nuclear pore complexes onto chromatin prior to their insertion into the nuclear membrane (Franz et al., 2007; Galy et al., 2006; Gillespie et al., 2007; Rasala et al., 2006; Shevelyov, 2020). More recent work; however, has demonstrated that several Nups regulate both transcription and chromatin condensation (Capelson et al., 2010; Kalverda et al., 2010; Kuhn et al., 2019; Panda et al., 2014; Pascual-Garcia et al., 2014, 2017; Raices and D'Angelo, 2017; Vaquerizas et al., 2010). In Drosophila, Nup98 binds to distinct regions of the genome, co-localizes with RNA polymerase II and regulates mRNA levels (Panda et al., 2014; Pascual-Garcia et al., 2014). Furthermore, the genomic localization of Nup98 and Elys correlate with actively transcribed genes (Pascual-Garcia et al., 2017). Tethering the nucleoporins Nup62 or Sec13 is sufficient to decondense chromatin within specific regions of chromatin (Kuhn et al., 2019). Interestingly, this chromatin decondensation correlates with the recruitment of Elys and the PBAP/Brm chromatin

remodeling complex (Kuhn et al., 2019). Many Nups are not permanently anchored to the NPC, but, rather, dynamically associate with the NPC throughout the cell cycle (Rabut et al., 2004) and the interaction between Nups and chromatin can occur in the nucleoplasm (Ibarra and Hetzer, 2015). Therefore, it is likely that many Nups have chromatin-related functions independent of the NPC.

Nucleoporins regulate both chromatin organization and transcription

Chromatin is typically organized into heterochromatic, transcriptionally repressed, and late-replicating regions and euchromatic, transcriptionally active, and early-replicating regions (Gilbert, 2002). This level of organization is usually preserved across cells from the same tissue type and must be maintained through DNA replication and cellular division (Almouzni and Cedar, 2016). NPCs play an important part in the maintenance of genome organization because genomic regions near the nuclear periphery are transcriptionally repressed and heterochromatic, with the notable exception being genomic regions near NPCs (Raices and D'Angelo, 2017). NPCs represent regions of transition between transcriptionally repressed and active genomic regions, as transcriptionally active regions are often near NPCs to better expedite the export of mRNA out of the nucleus (Raices and D'Angelo, 2017). The significance of this likely lies in the mechanism of NPC assembly. During mitosis, the nuclear envelope breaks down and NPCs dissemble, but then are reassembled at the end of mitosis (Franz et al., 2007; Otsuka and Ellenberg, 2018; Shevelyov, 2020). Critically, NPC assembly begins on mitotic chromatin, and as are re-inserted into the forming nuclear envelope, they remain tethered to chromatin (Shevelyov, 2020). This may be an effective way to preserve the transcriptional activity of genomic regions across cell cycles, by specifically assembling NPCs on transcriptionally active regions to ensure their close proximity to NPCs.

Movement of genomic regions to the NPC to promote the transcription of those regions has also been observed as an actively regulated phenomenon. In budding yeast, the genes inositol 1-phosphate synthase (*INO1*) and galactokinase (*GAL1*) are not near NPCs when repressed, but then are re-located to close proximity of NPCs upon activation (Brickner and Walter, 2004; Green et al., 2012). These observations have led to the model of "gene-gating," where activation of genomic regions for transcription is coupled to the re-localization of those regions to the "gate" (the NPC in this case) (Blobel, 1985). A major complication for this model is the possibility that some regions of chromatin may be unable to translocate to NPCs due to physical constraints from being buried in the interior of the nucleus. Investigations into the transcriptional roles of nucleoporins has revealed that some nucleoporins can influence chromatin organization and gene expression independently of NPCs (Kalverda et al., 2010; Kuhn et al., 2019; Panda et al., 2014; Pascual-Garcia et al., 2017), thereby eliminating the need to translocate nucleoporin-regulated genomic regions to the NPC in some cases.

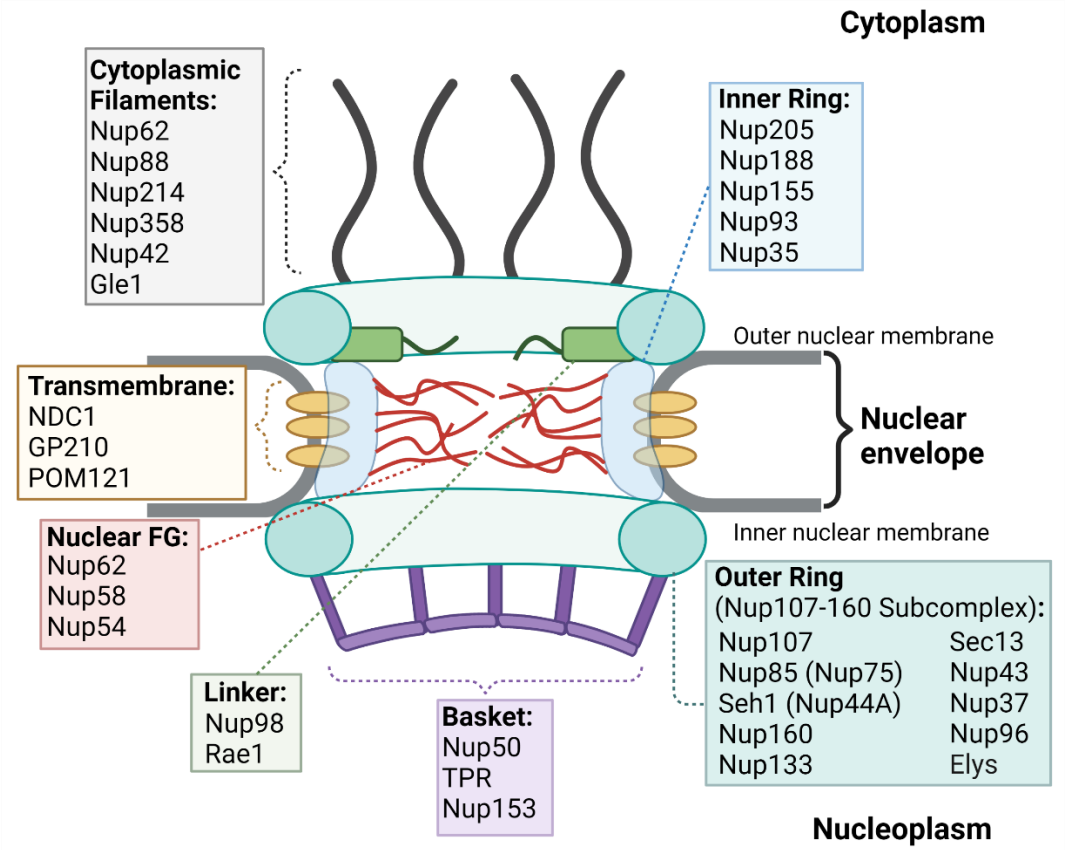

Figure 1.12. ***The nuclear pore complex***. The nuclear pore complex (NPC) is a barrel-shaped structure composed of subcomplexes forming spokes that connect the nucleoplasm and cytoplasm. The nuclear envelope is a double membrane, comprised of the outer and inner nuclear membranes, with the NPC sitting between the two membranes. The NPC is made up of several different classes of nucleoporins associating in distinct subcomplexes within the NPC. The proteins within in each subcomplex are indicated in the corresponding box. The NPC is anchored to the nuclear envelope by a transmembrane ring structure (yellow). Linker Nups (green) anchor Phe-Gly (FG) Nups. Nuclear FG Nups (red) within the core of the NPC facilitate in the trafficking of cargo across the NPC. The inner (blue) and outer (teal) rings of the NPC form stable complexes and play roles in NPC assembly. The cytoplasmic facing side of the NPC consists of cytoplasmic filaments (gray) whereas the nuclear facing side has a basket-like structure (purple). Alternative names for subcomplex and proteins are indicated in parentheses. Adapted from Strambio-De-Castillia et al., 2010 and made by Logan Richards.

The key nucleoporin Elys: linked to NPC assembly, gene expression, and DNA replication

In *Drosophila melanogaster*, Nup98, Sec13, and Nup62 localize to transcriptionally active genes (Capelson et al., 2010; Kalverda et al., 2010). Supporting the model that Nups contribute to chromatin organization, depletion of Nup98 or Sec13 in fly cell culture is sufficient to cause chromatin compaction, reduced recruitment of RNA polymerase II, and decreased mRNA synthesis at certain genes (Kuhn et al., 2019). Nup98 has been found to promote transcription by stabilizing enhancer-promoter contacts (Pascual-Garcia et al., 2017); however, the molecular mechanisms as to how Sec13 and Nup62 promote transcription remain poorly understood. Recently, the nucleoporin Elys has been implicated as a mediator of chromatin decompaction and has interactions with both Sec13 and the polybromo-containing associated proteins (PBAP) complex, a chromatin remodeling complex (Kuhn et al., 2019). Elys together with Sec13 are proposed to bind to condensed chromatin where then PBAP and the Drosophila GAGA factor (GAF) are recruited (Kuhn et al., 2019). These complexes then remodel chromatin, promoting the recruitment of RNA polymerase II and other transcription factors (TFs), and allow Nup-dependent transcription to occur (Kuhn et al., 2019) (Fig. 1.13B). Though Elys and other Nups have been implicated in gene expression, Elys is also a key nucleoporin involved in other key biological functions.

First isolated from mouse embryonic tissue, Elys was initially characterized as a transcription factor as Elys possesses an AT-hook domain that allows for DNA binding (Kimura et al., 2002). Shortly after its discovery, an ortholog of Elys, MEL-28 (materal-effect-lethal) was identified in a genetic screen in *C. elegans*, where *MEL-28* mutants failed the first mitotic division in embryogenesis (Galy et al., 2006). Extensive work revealed that Elys is the cornerstone of mitotic NPC assembly, where it is first to bind to chromatin during mitosis and promotes the recruitment of other Nup subcomplexes during NPC assembly (Shevelyov, 2020) (Fig. 1.13A). The role of

Elys in NPC assembly likely accounts for the observed failure in mitotic division, as *MEL-28* mutant embryos fail to form a functional nuclear envelop and have reduced NPC density (Galy et al., 2006).

In addition to its roles in NPC assembly and gene expression, there is a single report linking Elys to DNA replication in Xenopus (Gillespie et al., 2007). Interestingly, Elys robustly interacts with MCM subunits, Sld5 (a component of the replication fork), but not ORC2 in immunoprecipitations performed on mid S phase chromatin extract (Gillespie et al., 2007). Conversely, the interaction between Elys and replication factors was not detectable in the absence of chromatin, indicating the interaction specifically occurs on chromatin (Gillespie et al., 2007). If the AT hook domain of Elys is added to extract and an MCM3 immunoprecipitation is performed, the AT hook domain is not recovered (Gillespie et al., 2007). This result shows that the AT hook domain does not mediate the interaction between Elys and MCMs. The proposed model for the biological function of the Elys-MCM interactions pertains to the prevention of re-replication (Gillespie et al., 2007). Geminin plays an important role in the prevention of re-replication and inhibits additional helicase loading upon entry into S phase (Truong and Wu, 2011). In this model, MCMs are first loaded, followed by Elys, which then promotes NPC assembly, and allows for the import of geminin into the nucleus (Gillespie et al., 2007). Helicase loading and NPC assembly are therefore coupled to create a feedback loop, where the assembly of NPCs prevents further helicase loading (Fig. 1.13C). This work highlights another alternative function of Elys in DNA replication, and the work described hereafter (see Chapter III) will also implicate Elys in another critical biological function: the loading of ORC onto chromatin.

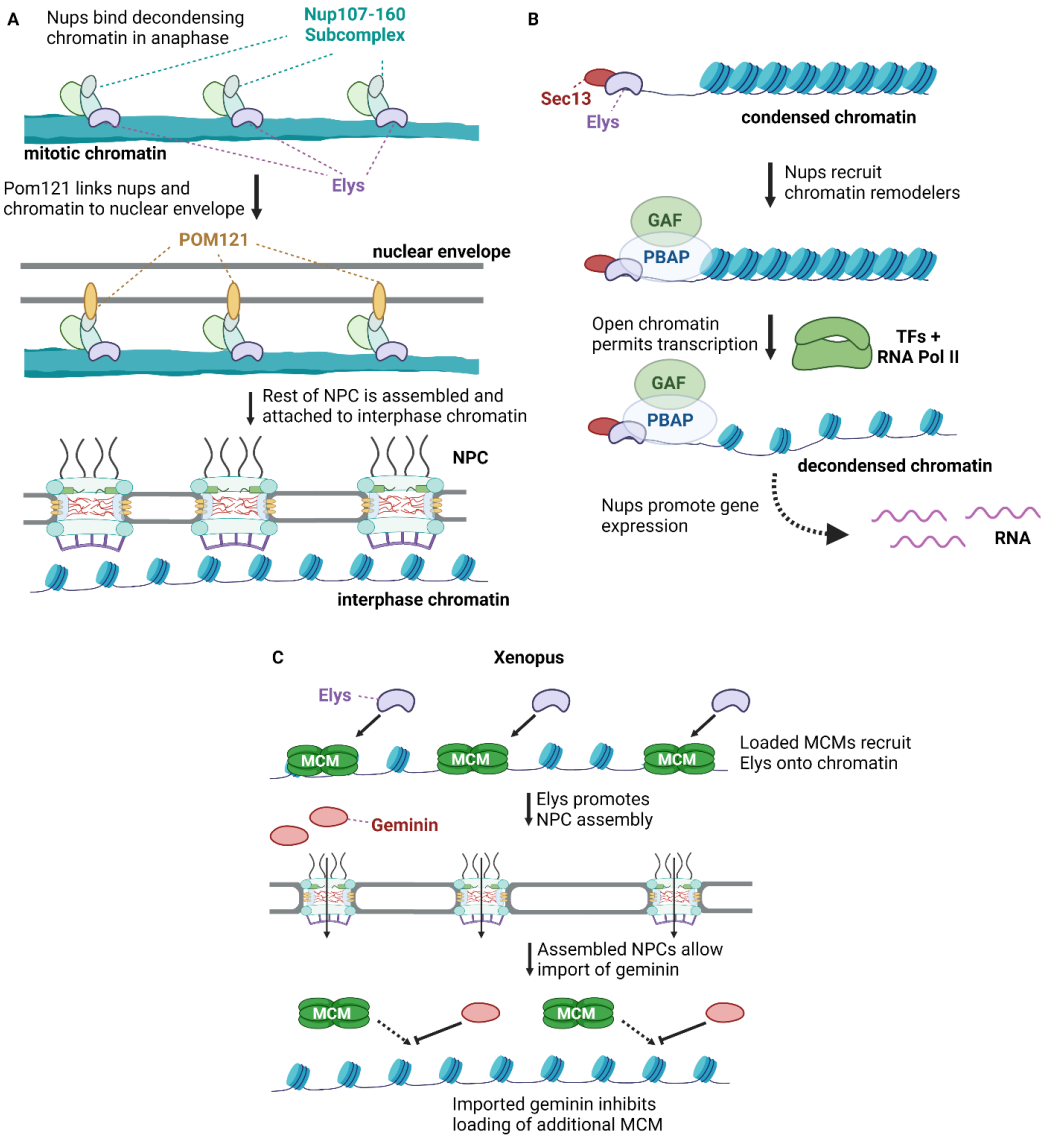

Figure 1.13. ***The diverse functions of the nucleoporin Elys.*** (A) Elys mediates NPC assembly. In anaphase, Elys binds to decondensing chromatin and subsequently recruits the Nup107-160 subcomplex. POM121 then links Elys and the Nup107-160 subcomplex to the forming nuclear envelope. After this, the rest of the NPC is assembled, the nuclear envelope is fully formed, and chromatin fully decondensed at the end of mitosis. (B) Proposed model for chromatin state and gene expression regulation by Nups. Elys and Sec13 bind to chromatin and recruit GAF and PBAP chromatin remodeling complexes, which open chromatin. This open chromatin may permit TFs (transcription factors) and RNA polymerase II to express genes targeted by Elys/Sec13. (C) In Xenopus embryos, Elys create a feedback loop to prevent re-replication. At the end of metaphase, geminin is inhibited, permitting MCMs to be loaded onto chromatin. Once loaded onto chromatin, MCMs recruit Elys, and NPCs are assembled as in (A). After the assembly of NPCs is complete, geminin is then imported, inhibiting Cdt1, preventing any further MCM loading, and creating a functional feedback loop. Adapted from Shevelyov, 2020 and Kuhn et al, 2019. Made by Logan Richards.

Thesis summary

Accurate duplication of the genome is critical to maintain genomic stability and failures in DNA replication can result in a host of diseases. DNA replication is a coordinated and tightly regulated process; however, much remains unknown regarding exactly how DNA replication is regulated. Key focal points in the regulation of DNA replication are controlling the activities of the Origin Recognition Complex (ORC) and the activation of the loaded helicase. In metazoans, it is still unclear how ORC is targeted to specific loci to initiate replication. To investigate how ORC is targeted to chromatin, we performed immunoprecipitations coupled with mass spectrometry (IP-MS) for ORC2 in Drosophila embryos and found that ORC2 associates with multiple subunits of the Nup107-160 subcomplex of the nuclear pore. We determined that nucleoporins are strongly enriched at ORC2 genomic binding sites and depleting the nucleoporin Elys reduces the chromatin association of ORC2. Depleting Elys also sensitizes cells to replication fork stalling, which could reflect a defect in establishing dormant replication origins.

To interrogate the regulation of helicase activation, which is controlled by the replication timing program, we performed IP-MS for Rif1 across Drosophila embryogenesis to determine the factors that may regulate the activity of Rif1. We discovered that Rif1 co-immunoprecipitated both with ORC and the Nup107-160 subcomplex. ChIP-seq for Rif1 revealed that Rif1 binds to similar genomic regions as ORC2, and Rif1 genomic binding sites are enriched in early-replicating regions of the genome. The chromatin association of ORC2 is dependent on Rif1, and inversely, the chromatin association of Rif1 is dependent on ORC2. In summary, this work shows that both Rif1 and nucleoporins play roles in promoting the chromatin association of ORC, implicating both Rif1 and nucleoporins in the initiation of DNA replication in Drosophila.

CHAPTER II[4]

MATERIALS AND METHODS

REAGENT or RESOURCE	SOURCE	IDENTIFIER
Antibodies		
Rabbit Anti-ORC2 Antibody	Richards et al., 2022	N/A
Rabbit Anti-Elys Antibody	Richards et al., 2022	N/A
Rabbit Anti-Rif1 Antibody #1	Munden et al., 2018	N/A
Rabbit Anti-Rif1 Antibody #2	Munden et al., 2018	N/A
HRP Rabbit Anti-Histone H3 Antibody	Abcam	Cat#: ab21054
Rabbit Anti-Histone H3 (tri methyl K27) antibody	Abcam	Cat#: ab195477
Rabbit Anti-phospho-Histone H3 (Ser10) Antibody	Sigma-Aldrich	Cat#: 06-570
Rabbit Anti-Histone H2AvD phospho137 Antibody	Rockland	Cat#: 600-401-914
Mouse Anti-Nuclear Pore Complex Proteins Antibody (mab414)	BioLegend	Cat#: 902901
Mouse Anti-H2B Antibody	Abcam	Cat#: ab52484
Rabbit IgG	Sigma-Aldrich	Cat#: I5006
Alexa Fluor 568 Goat Anti-Rabbit Antibody	ThermoFisher	Cat#: A11011
Alexa Fluor 488 Goat Anti-Mouse Antibody	ThermoFisher	Cat#: A11029
Peroxidase-AffiniPure Donkey Anti-Rabbit	Jackson ImmunoResearch	Cat# 712-035-153
Bacterial and virus strains		
Rosetta ™ 2 (DE3) Competent Cells	Novagen	Cat#: 71400
Chemicals, peptides, and recombinant proteins		
cOmplete™ Protease Inhibitor Cocktail EDTA-free	Roche	Cat#: 04693159001
Benzonase ® Nuclease	Fisher Scientific	Cat#: 70-664-3
GFP Trap ® Magnetic Agarose	Chromotek	Cat#: gtma-20
SPRIselect Beads	Beckman Coulter	Cat#: B23317
2x Laemmli Sample Buffer	Bio-Rad	Cat#: 1610737
Alexa Fluor 555 Azide	Invitrogen	Cat#: A20012
RNAse A	Sigma-Aldrich	Cat#: R4875
Proteinase K	Sigma-Aldrich	Cat#: P4850
Aphidicolin	Sigma-Aldrich	Cat#: A0781
Normal Goat Serum	Sigma-Aldrich	Cat#: G9023
Vectashield+DAPI	Vector Laboratories	Cat#: H-1000
Maxima H Minus Reverse Transcriptase	ThermoFisher Scientific	Cat#: EP0752

[4] Portions of this chapter were adapted from Richards et al. Cell Reports. 2022.

Critical commercial assays		
MagExtractor PCR & Gel Clean Up Kit	Toyobo	Cat#: NPK-601
MEGAscript ™ T7 Transcription Kit	ThermoFisher Scientific	Cat#: AM1334
4–15% Mini-PROTEAN™ TGX Stain-Free™ Protein Gels	Bio-Rad	Cat#: 4568086
DNA Clean & Concentrator-100 kit	Zymo Research	Cat# D4029
NEBNext Ultra II DNA Prep Kit for Illumina	New England BioLabs	Cat#: E7370
ATAC-Seq Kit	Active Motif	Cat#: 53150
Deposited data		
modEncode ChIP-ChIP or ChIP-seq S2 cell data	Celniker et al., 2009; Contrino et al., 2012	N/A
Drosophila S2 cell replication timing	Eaton et al., 2011	N/A
ORC2 ChIP-seq peaks in S2 cells	Eaton et al., 2011	N/A
Nucleoporin peaks in S2 cells	Gozalo et al., 2020; Pascual-Garcia et al., 2017	N/A
Raw and processed sequencing data in Chapter III	This work	N/A
Processed mass spectrometry data in Chapter III	This work	N/A
Raw and processed sequencing data in Chapter IV	Richards et al., 2022b	GSE199896
Processed mass spectrometry data in Chapter IV	Richards et al., 2022b	PXD033045
Experimental models: Cell lines		
Drosophila S2 cells	Drosophila Genomics Resource Center	Cat#: 181
Experimental models: Organisms/strains		
WT: *Oregon R* flies	N/A	N/A
ORC2-GFP flies	Gift from Shelby Blythe	endogenously tagged *ORC2*
Rif1-GFP flies	Gift from Patrick O'Farrell	endogenously tagged *Rif1*
Oligonucleotides		
Oligopaint Primers	Richards et al., 2022b	N/A
OligoPaint PCR Amplification Forward Primer: 5' GCGTTAGGGTGCTTACGTC 3'	Richards et al., 2022b	N/A
OligoPaint PCR Amplification Reverse Primer: 5' CACCTCCGTCTCTCACCT 3'	Richards et al., 2022b	N/A
Oligopaint Fluorescent Secondary Probe covalently lined to Alexa Fluor 488: AAGCACCCTAACGCTTCACGATCCAT	Richards et al., 2022b	N/A
Primers used to generate dsRNA for RNA interference (See Table 2.2)	This work and Richards et al., 2022b	N/A
Recombinant DNA		

Plasmid: pLM302 His-MBP-ORC2	Richards et al., 2022b	His-MBP-ORC2 fusion under T7 promoter
Plasmid: pLM302 His-MBP-Elys	Richards et al., 2022b	His-MBP-Elys fusion under T7 promoter
Plasmid: pET17b-Rif1 (694–1094)	Munden et al., 2018	N/A
Software and algorithms		
GraphPad Prism	Software	https://www.graphpad.com/scientific-software/prism/
FlowJo	Software	https://www.flowjo.com/
RStudio	Software	https://www.rstudio.com/
VolcaNoseR	Software	https://huygens.science.uva.nl/VolcaNoseR/
Nikon Elements	Software	https://www.microscope.healthcare.nikon.com/products/software/nis-elements
Bowtie2	Software	http://bowtie-bio.sourceforge.net/bowtie2/index.shtml
Picard	Software	https://broadinstitute.github.io/picard/
Deeptools	Software	https://deeptools.readthedocs.io/en/develop/
MACS2	Software	https://pypi.org/project/MACS2/
Bedtools	Software	https://bedtools.readthedocs.io/en/latest/index.html
UCSC Genome Browser	Software	https://genome.ucsc.edu/
Galaxy	Software	https://usegalaxy.org/

Table 2.1. ***Key resources.*** Resources, data, and software used in this body of work

Experimental model and subject details

Drosophila cells

Drosophila melanogaster S2 cells were provided by Drosophila Genomics Resource Center (DGRC stock number 181). Cells are wild type and derived from embryonic tissue. Cells were maintained following DGRC guidelines. Cells were grown at 25°C and in Schneider's medium (Gibco 21720024) supplemented with 10% heat-inactivated fetal bovine serum (ThermoFisher A3840001) and penicillin-streptomycin (ThermoFisher 15140122). Cells were passaged every 3-5 days and maintained at a concentration of $3x10^6$-$1x10^7$ cells/mL.

Fly lines

ORR flies were a gift from Terry Orr-Weaver (Whitehead Institute). ORC2-GFP flies were a gift from Shelby Blythe. Rif1-GFP flies were a gift from Patrick O'Farrell. CRISPR was used to integrate GFP at the endogenous ORC2 or Rif1 gene locus. Flies were maintained in population cages at 25°C and fed wet yeast on grape agar plates daily.

Method details

Immunoprecipitations

For Rif1-GFP, immunoprecipitations were performed on two biological replicates of both *Rif1-GFP* and *ORR* embryos. For each replicate, 1.5g of embryos aged either 0-2 hours (Pre-MZT), 2-3 hours (Post-MZT), or 18-24 hours (late stage) were collected, dechorionated, and flash frozen. For ORC2-GFP, immunoprecipitations were performed on three biological replicates of both

ORC2-GFP and *ORR* embryos aged 18-24 hours. For each replicate, 0.5g of embryos aged 18-24 hours were collected, dechorionated, and flash frozen. Frozen embryos were ground thoroughly with a mortar and pestle in liquid N2. Ground embryos were then resuspended in NP40 Lysis Buffer (50 mM Tris HCl pH 8.0, 150 mM NaCl, 1% NP40, 1 mM EDTA, 1 mM EGTA, with 2X cOmplete™ Protease Inhibitor Cocktail EDTA-free (Millipore Sigma)). The embryonic extract was treated with benzonase nuclease (Millipore #7066) at a final concentration of 30 U/ml for 30 minutes at 4°C. After benzonase treatment, the extract was centrifuged at 4,000 rcf for 5 minutes. The supernatant was then used for the immunoprecipitation.

Prior to the immunoprecipitation, GFP Trap magnetic agarose beads (Chromotek #gtma-10) were washed and equilibrated with NP40 lysis buffer. Beads were added to extract and incubated for 2 hours at 4°C. After the 2 hours, beads were isolated and washed with 4 times with NP40 lysis buffer. Beads were then resuspended in 2x Laemmli sample buffer (Biorad #1610737) and boiled at 95°C for 20 minutes to elute protein.

Mass spectrometry

Eluates in Laemmli buffer were methanol/chloroform precipitated. After precipitation, immunoprecipitated samples were separated on a 4 – 12% NuPAGE Bis-Tris gel (Invitrogen). Proteins were resolubolized in 5% SDS and prepared using S-trap (Protifi) using manufacturer's protocol. Resulting peptides were desalted via C18 solid phase extraction and autosampled onto a 200 mm by 0.1 mm (Jupiter 3 micron, 300A), self-packed analytical column coupled directly to an Q-exactive+ mass spectrometer (ThermoFisher) using a nanoelectrospray source and resolved using an aqueous to organic gradient. Both the intact masses (MS) and fragmentation patters (MS/MS) of the peptides were collected in a data dependent manner utilizing dynamic exclusion to maximize depth of proteome coverage. Resulting peptide MS/MS spectral data were

searched against the Drosophila protein database using SEQUEST (Yates et al., 1995). Identifications were filtered and collated at the protein level using Scaffold (Proteome Software).

Search results and peptide counts were refined in Scaffold using the following parameters: protein threshold false discovery rate = 5% minimum number of peptides ≥ 2, and a peptide threshold false discovery rate = 5%. Scaffold was used to perform a Fisher's Test for each individual protein identified, comparing either Rif1-GFP or ORC2-GFP to the ORR negative. For visualization purposes, p-values ≤ 0.0010 were rounded to 0.0010 in Fig. 3.1B. For Fig. 3.1C, p-values for ORC subunits were generated by a Fisher's Test using R. Fold enrichment was calculated using the raw spectrum counts for individual proteins over the negative control. For the ORC2-GFP data, volcano plots visualizing p-values and fold enrichment were made using GraphPad Prism. For the Rif1-GFP data, volcano plots visualizing p-values and fold enrichment were made using VolcaNoseR. Gene Ontology was performed using PANTHER (Mi et al., 2019) on all identified proteins in each developmental stage with a p-value greater than 0.05. Fold enrichment graphed using Graphpad prism.

Western blotting

The presence of Rif1 or ORC2 in the elute was confirmed prior to conducting mass spectrometry by SDS-PAGE followed by a Western blot for Rif1 or ORC2 using either anti-Rif1 or anti-ORC2 antibody. Briefly, samples were boiled and loaded onto a 4-15% Mini-PROTEAN TGX Stain-Free Gel (Biorad). After electrophoresis, the gel was activated and imaged using a BioRad ChemiDoc™ MP Imaging System following manufacturer recommendations. Protein was transferred to a low fluorescence PVDF membrane using a Trans-Blot Turbo Transfer System (BioRad). Membranes were blocked with 5% milk in TBST (140mM NaCl, 2.5mM KCl, 50 mM Tris HCl pH 7.4, 0.1% Tween-20). Blots were incubated with either anti-Rif1 antibody at 1:1000, anti-

ORC2 antibody at 1:1000, anti-Elys antibody at 1:250, or HRP anti-Histone H3 antibody (abcam #ab21054) at 1:1000 overnight at 4°C. After primary antibody incubation, blots were washed, incubated secondary HRP antibody (Jackson Labs 711-035-150), washed once more and imaged. For the quantification shown in Fig. 3.7, signal for either Elys or ORC2 was normalized to H3 for each depletion for three biological replicates. For Fig. 4.6, signal for Rif1 or ORC2 was normalized to total protein.

Antibody generation

Full length ORC2 tagged with Maltose Binding Protein (MBP) was expressed and purified from *E. coli*. Briefly, ORC2 was cloned into the pLM302 expression vector. The expression construct was transformed into Rosetta 2 (DE3) cells (Novagen) and cultures were induced with IPTG and His-MBP-ORC2 was purified on Ni-NTA beads (BioRad). Purified protein was injected into rabbits for serum generation and collection (Cocalico Biologicals). For affinity purification, serum was first passed over an MBP column to deplete MBP-specific antibodies and the flow through fraction was passed over a column of MBP-ORC2 and eluted. An Elys-specific antibody was generated as previously described (Pascual-Garcia et al., 2017) The C-terminal fragment of Elys, amino acids 1766-2110, was cloned into pLM302 vector, expressed in *E. coli* Rosetta cells and purified using the same techniques described above. Rif1 antibody generated as described in Munden et al., 2018.

Oligopaint fluorescent in situ hybridization (FISH)

Oligo pools were generated using the PaintSHOP application (Hershberg et al., 2021) from the Drosophila dm6 reference genome. A complete list of oligos can be found in Supplemental Table 2. Oligopaint probe production and FISH was performed largely as previously described (Nguyen

and Joyce, 2019). Oligo pools were resuspended 50 µl of ddH_20 and 1 µl was used for an initial PCR amplification along with 2.5 µl of 10 µM forward (GCGTTAGGGTGCTTACGTC) and reverse (CACCTCCGTCTCTCACCT) primers, 25 µl 2X Q5 master mix, and 19 µl ddH_20 with 30 sec 98°C denaturation, 30 sec 55°C annealing, and 30 sec 72°C extension steps repeated 34 times. The PCR product was purified using a MagExtractor PCR & Gel clean up kit (Toyobo NPK-601) according to the manufacturer's protocol and resuspended in 20 µl ddH_20. A secondary amplification was performed by mixing 1 µl of the first PCR product with 100 µl 2X Q5 master mix, 10 µl of 10 µM forward B and reverse B primers, and 79 µl ddH_20. The PCR was performed using the same program as described above, and subsequently purified as described and resuspended in 30 µl ddH_20. A Megascript T7 (ThermoFisher AM1334) reaction was performed by mixing 14 µl of the secondary PCR product with 4 µl of ATP, CTP, GTP, and UTP solutions and 4 µl reaction buffer, 2 µl RNase inhibitor, and 4 µl RT mix. The T7 reaction was incubated overnight at 37°C. A Maxima H Minus RT (ThermoFisher EP0752) reaction was setup by mixing 40 µl of the T7 reaction with 30 µl 100 uM forward B primer, 19.2 µl 100 mM dNTPs, 60 µl 5X RT buffer, 3 µl RNase inhibitor, 4 µl Maxima H Minus RT, and 143.8 µl ddH_20; this was incubated at 50°C for 3.5 hr. RNA was degraded by adding 150 µl 0.5M EDTA and 150 µl NaOH to the reaction, then heating at 95°C for 5 min. The DNA was cleaned and concentrated using a DNA Clean & Concentrator-100 kit (Zymo Research, D4029) and the DNA was resuspended in 90 µl ddH_20. The concentration ranged from 200-400 ng/µl. Pools were stored at -20°C until use.

For FISH experiments, S2 cells were concentrated and incubated in 100 µl Schnieder's Drosophila media + 10% FBS on poly-lysine-coated slides for 1-2 hours in a humid chamber underneath a strip of parafilm the size of a cover slip. The media was then aspirated and the slides were incubated in freshly-prepared fixative solution (1X PBS and 4% paraformaldehyde) after transferring to coplin jars for 10 min at RT. Slides were washed in 1X PBS then incubated in freshly-prepared 0.5% Triton X-100 for 15 min at RT. Slides were rinsed with 1X PBS then

dehydrated with successive incubations with 70%, 90%, and 100% ethanol for 2 min each at RT. Slides were then washed with 2X SSCT (2X SSC and 0.1% Tween-20) for 5 min. Next the slides were incubated with 2X SSCTF (2X SSC, 0.1% Tween-20, and 50% formamide) pre-heated to 90°C for 3 min in a new coplin jar that was also pre-heated. Slides were next incubated in 2X SSCTF at 60°C for 20 min (also pre-warmed). During this incubation, hybridization mix was prepared by vigorously mixing 300 µl formamide, 120 µl 50% dextran sulfate and 60 µl 20X SSC. 20 µl of this hybridization mix was then mixed with 4.5 µl oligo pool (at 200-300 ng/ µl) along with 0.5 µl 100 mM dNTPs, which was a sufficient quantity for one slide. Slides were dried for 5 min, then the hybridization mix + probe was added on top of the fixed cells. This was covered with a cover slip and sealed with rubber cement and dried for at least 20 min at RT. Slides were placed into a humid slide incubator and heated to 92°C for 3 min, then incubated overnight at 37°C. The next day cover slips were carefully removed and the slides were washed with 2X SSCT (pre-warmed) at 60°C for 15 min, then 2X SSCT for 10 min at RT, then 0.2X SSCT for 10 min at RT. New hybridization mix was prepared as before, and 120 µl was mixed with 29.75 µl ddH_20 and 0.25 µl 100 mM secondary fluorescent oligo probe (sequence of AAGCACCCTAACGCTTCACGATCCAT covalently linked to Alexa Fluor 488 dye), which was sufficient for 5 slides. 25 µl of this mix was then added on top of the fixed cells and sealed with a cover slip and rubber cement and the slides were incubated at RT for 1-2 hr. Cover slips were carefully removed and the slides were washed with 2X SSCT (pre-warmed) at 60°C for 15 min, then 2X SSCT for 10 min at RT, then 0.2X SSCT for 10 min at RT. 10-15 µl of Vectashield + DAPI (Vector Laboratories) was added on top of fixed cells, which were then sealed under a cover slip with nail polish.

RNA interference

Cells were diluted to 1.5x10^6 cells/mL in serum-free media. 20 µg of dsRNA generated using the T7 Transcription Kit (ThermoFisher AM1334) was incubated with cells for 45 minutes. A list of primers used to generate dsRNA can be found in Table 2.2. After 45 minutes, serum-containing media was added to the RNAi-treated cells. Cells were then incubated for 5 days at 25ºC. To confirm the depletion, 1 million cells were harvested and lysed in CSK buffer (10mM PIPES pH 7.0, 300 mM sucrose, 100 mM NaCl, 3 mM $MgCl_2$ with with 2X cOmplete Protease Inhibitor Cocktail EDTA-free (Roche)) for 8 minutes. 2X Laemmli sample buffer (BioRad) was added to lysates and samples were incubated at 95ºC for 5 mins. Depletions were confirmed by SDS-PAGE followed by western blotting for Rif1, Elys, ORC2, and Histone H3 as previously described (see *Western Blotting)*.

RNA	Forward Primer	Reverse Primer
Elys-1	5'TAATACGACTCACTATAGGGG CACGTATCTTCGCATCAGA 3'	5'TAATACGACTCACTATAGGGGACA AGGACGCTTATTGGGA 3'
Elys-2	5'TAATACGACTCACTATAGGGT GGAGCCCTACCAAAAGAC 3'	5'TAATACGACTCACTATAGGGCGC CTGGAGGAAATTTGG 3'
Nup98-96-1	5'TAATACGACTCACTATAGGGG GTGTGGCACCAAAAAGAGT 3'	TAATACGACTCACTATAGGGCACCA ATGTTTTTGGCAGTG 3'
Nup98-96-2	5'TAATACGACTCACTATAGGGG GAAGACCCAACTACCCGTT 3'	5'TAATACGACTCACTATAGGGGCC CATTGGTCAAGGTCTAA 3'
ORC2-1	5'TAATACGACTCACTATAGGGA GCGATGCTGGCAACTC 3'	5'TAATACGACTCACTATAGGGTATC CAGCATATCCTTGATGG 3'
ORC2-2	5'TAATACGACTCACTATAGGGT CGCTTGTGATGCTATCCAG 3'	5'TAATACGACTCACTATAGGGAGCA AGATCCTCACTTCGGA 3'
Nup107-1	5'TAATACGACTCACTATAGGGAT GCAGTATAGTAGGCTATTAG 3'	5'TAATACGACTCACTATAGGGCGAC GGCGGGTGTCTT 3'
Nup160-1	5'TAATACGACTCACTATAGGGG GCGGTTCATCTGGATCAA 3'	5'TAATACGACTCACTATAGGGGCTG TGGGATCGCTTTTAC 3'
Rif1	5'TAATACGACTCACTATAGGGC GGCAAAACGAACTAATGG 3'	5'TAATACGACTCACTATAGGGGTTT CTTTCGGATGGGTGTAA 3'
GFP	5'TAATACGACTCACTATAGGGAT GCCACCTACGGCAAG 3'	5'TAATACGACTCACTATAGGGGTTC TGCTGGTAGTGGTC 3'

Table 2.2. Primers used to generate dsRNA for RNA interference

CUT&RUN

CUT&RUN was performed using previously published methods (Ahmad and Spens, 2019; Skene and Henikoff, 2017; Skene et al., 2018). Briefly, 1 million S2 cells were harvested and spun down at 600 x g. Cells were washed with PBS and followed by wash buffer (20 mM HEPES pH 7.5, 150 mM NaCl, 0.1% BSA, with 2X cOmplete™ Protease Inhibitor Cocktail EDTA-free (Roche) and 0.6 mM Spermidine). Cells were attached to ConA beads in binding buffer (20 mM HEPES pH 7.9, 10 mM KCl, 1 mM CaCl2, 1 mM MnCl2) for 10 minutes. Cells were blocked and permeabilized in DBE buffer (wash buffer with 2mM EDTA and 0.05% digitonin) for 10 minutes. Cells were then incubated with 1µg of mab414 antibody (BioLegend), anti-H3K27me3 antibody (Abcam), anti-Rif1 antibody, or anti-ORC2 antibody in DBE buffer at 4°C overnight.

After primary antibody incubation, cells were washed twice in DBE buffer. pA-MNase (gift from Kami Ahmad) was diluted 1:400 in DBE buffer and added to cells. pA-MNase was allowed to bind for one hour at room temperature. Cells were then washed twice with wash buffer and suspended in cleavage buffer (wash buffer with 2 mM $CaCl_2$). DNA cleavage was carried out for 30 minutes on ice, then immediately stopped with stop buffer (170 mM NaCl, 20 mM EDTA, 4 mM EGTA). Supernatant containing the cleaved DNA was collected from the cells and treated with RNAse A and Proteinase K. SPRIselect beads (Beckman Coulter) were used to purify the fragmented DNA. To prepare this DNA for sequencing, the NEBNext Ultra II DNA Prep Kit for Illumina (New England Biolabs) was used using according to the manufacturer guidelines and then sequenced using an Illumina NovaSeq6000 for 150bp PE reads.

ChIP-seq

Rif1 or ORC2 ChIP-seq was performed as previously described (MacAlpine et al., 2010). Briefly, 20 million S2 cells for each depletion were harvested and centrifuged at 600 rcf for 5 mins. Cells were washed twice with PBS and fixed for 10 minutes with 1% PFA at room temperature. Crosslinking was quenched by adding glycine to a final concentration of 125 mM and incubating at room temperature for 5 minutes. Cells were spun down and resuspended in RIPA buffer (50 mM Tris-HCl, 140 mM NaCl, 1 mM EDTA, 1% NP-40, 0.1% Na-Deoxycholate, 0.1% SDS with 2X cOmplete™ Protease Inhibitor Cocktail EDTA-free). Cells were incubated for 1 hour at 4°C and sonicated using a Diagenode Bioruptor for 4 rounds of 10 cycles (each cycle was 30 seconds on, 30 seconds off at max power). After sonication, chromatin extract was cleared by centrifuging at 21,000 rcf for 5 mins. The remaining supernatant was used as input for the chromatin immunoprecipitation.

After preparing the chromatin extract, 1µg of anti-Rif1 antibody or anti-ORC2 antibody was added and allowed to incubate for 2 hours at 4°C. Protein A beads were washed with RIPA buffer, added to the extract and incubated for one hour at 4°C. Beads were then washed twice with RIPA buffer, twice with high-salt RIPA buffer (500mM NaCl), once more with RIPA buffer and once with TE Buffer. To elute protein, beads were incubated with elution buffer (50 mM Tris-HCl pH 8.0, 10 mM EDTA, 1% SDS) at 65°C for 15 minutes. Protein-DNA cross links were reversed by incubating at 65°C overnight. To recover DNA, samples were RNase A and Proteinase K treated, and phenol:chloroform extracted. Next, the DNA was isopropanol precipitated. Once the DNA was purified, the NEBNext Ultra II DNA Prep Kit for Illumina (New England Biolabs) was used to prepare the samples for next-generation sequencing. Barcoded libraries were sequenced using an Illumina NovaSeq for 150bp PE reads. For the Rif1 ChIP-seq, two biological replicates were

performed with two different anti-Rif1 antibodies. For the ORC2 ChIP-seq, two biological replicates were performed for the depletions and the same antibody was used in each replicate.

ATAC-seq

For the GFP, Elys, ORC2, or Nup98-96 depletions, 50,000 cells were harvested and washed with PBS. ATAC-seq was performed as described previously (Buenrostro et al., 2015) using an ATAC-seq kit (Active Motif) as described by the manufacturer. Briefly, cells were resuspended in cold lysis buffer and centrifuged at 1000xg for 10 minutes at 4°C. The cell pellet was resuspended in tagmentation buffer and the reaction was incubated at 37°C for 30 minutes. Tagmented DNA was purified and used to generate sequencing libraries following manufacturer's protocol. Libraries were sequenced with an Illumina NovaSeq6000.

Flow cytometry

To generate cell cycle profiles for RNAi-treated cells, 10 million cells were first pulsed with 20 μM EdU for 20 minutes after five days of RNAi treatment. Next, cells were washed twice with PBS and fixed overnight in ice-cold 70% ethanol. After fixation, cells were again washed with PBS and permeabilized for one hour at room temperature with PBX (PBS with 0.1% Triton X-100). Incorporated EdU was click-labeled with an Alexa Fluor 555 Azide (Invitrogen) by incubating with 4mM $CuSO_4$ and 2mg/mL sodium ascorbate in PBS for 30 minutes at room temperature. Once clicked labeled, cells were washed twice with PBX and DAPI stained overnight. For the cell cycle analysis in Fig. 3.8 and Fig. 4.13, three biological replicates were performed and the percent of cells in each phase of the cell cycle was quantified.

To quantify the amount of chromatin bound Rif1, ORC2 and Histone H2B in nuclei, 50 million cells were harvested after each depletion. The protocol was adapted from Matson et al., 2017. Cells were thoroughly washed with PBS and then lysed in cold CSK buffer supplemented with 0.5% Triton X-100 and 2X cOmplete™ EDTA-free Protease Inhibitor Cocktail for eight minutes on ice. PBS with 1% BSA was added to lysates and nuclei were pelleted by centrifugation at 2000xg for three minutes. Nuclei were then fixed with 4% PFA in PBS for 15 minutes at room temperature. After fixation, PBS with 1% BSA was added and fixed nuclei were pelleted by centrifugation at 2000xg for 7 minutes. Nuclei were washed once with PBS supplemented with 1% BSA and 0.1% NP40 (Blocking Buffer). Nuclei were incubated overnight at 4°C with either anti-Rif1, anti-ORC2 antibody, or anti Histone H2B (Abcam cat #52484) diluted 1:200 in blocking buffer. After the primary antibody incubation, nuclei were washed with blocking buffer and then incubated with anti-rabbit antibody conjugated to Alexa Fluorophore 568 (ThermoFisher) or anti-mouse antibody conjugated to Alexa Fluorphore 488 (ThermoFisher) diluted 1:500 for two hours at room temperature. Nuclei were then washed twice with blocking buffer and DAPI stained overnight.

DNA content, EdU intensity Rif1, intensity, H2B intensity, and ORC2 intensity were determined using a BD LSRII flow cytometer. Flow cytometry data was analyzed and plotted using FlowJo (BD Biosciences). For an example of gating for these experiments, see Fig. 3.8C. For quantifying the Rif1 or ORC2 intensity per nuclei for, 500 nuclei from three replicates were randomly selected and pooled for a total of 1500 nuclei for each depletion. To determine statistical significance, a one-way ANOVA was performed with a post-hoc Dunnett's test comparing each depletion to the negative control (GFP).

Immunofluorescence

Cells were first treated with RNAi for 4 days. After four days, 1-3 million cells were then treated with for 24 hours with 1.2 uM aphidicolin in PBS (Millipore Sigma cat#: A0781). This was done to be consistent with our previous depletions by still ensuring a 5-day RNAi treatment. Cells were attached to Concanavalin A coated slides for one hour at room temperature. Cells were washed with PBS and then fixed with 4% PFA for 15 minutes and permeabilized with permeabilization solution (0.5% Triton X-100) for 8 minutes. After briefly rinsing in PBS, cells were blocked for 30 minutes in TBS with 0.1% Tween-20 (TBST) supplemented with 2% Normal Goat Serum (Sigma Aldrich). Histone H2AvD phosphoS137 antibody (Rockland cat #: 600-401-914) was diluted 1:50 in TBST and incubated overnight at 4°C. Next, cells were washed three times with TBST for 5 minutes each and incubated with Alexa fluorophore 568-conjugated anti-rabbit secondary (ThermoFisher cat#: A-11011), diluted 1:200 for one hour at room temperature. Cells were washed thrice in TBST, DAPI stained and mounted with Vectashield. To determine the cell cycle impact of aphidicolin treatment, cells were RNAi treated for 4 days, and then treated with 1.2µm aphidicolin for one day for a total of a 5 days of depletion. On the fifth day, cells were pulsed with 20 μM EdU for 20 minutes, and cells were fixed and click-labeled as previously described (*see Flow Cytometry*). The percent of cells in each stage of the cell cycle was quantified for two biological replicates.

For each biological replicate, slides for each depletion were imaged at 40X with the same intensity and exposure time for each channel. To quantify the ɣH2Av signal, Nikon's NIS Elements software was used to generate regions of interests (ROIs) using DAPI to define the ROI. Mean TxRed (ɣH2Av) and DAPI intensity for each ROI was determined for 300 cells per replicate (600 cells total). To account for differences in DNA content, ɣH2Av intensity was normalized to DAPI intensity. A one-way ANOVA with a post-hoc Dunnett's test was performed for either the untreated

group or the treated group (1.2μM aphidicolin). To determine the effect of treatment within each depletion, a parametric T-test was performed.

To quantify the effects of each depletion on mitosis, immunofluorescence using an anti-phospho-histone H3 (Ser10) antibody (Sigma cat #: 06-570) was performed. Cells were RNAi-treated as previously described (see RNA interference), permeabilized for one hour with PBS supplemented with 0.1% Triton X-100 and fixed with 4% PFA for 15 mins. After fixation, cells were incubated with primary antibody diluted 1:200 overnight. Following incubation, cells were washed three times with PBS and then incubated with Alexa fluorophore 568-conjugated anti-rabbit secondary (ThermoFisher cat#: A-11011), diluted 1:200 for two hours at room temperature. Cells were again washed three times with PBS, DAPI stained, and mounted with Vectashield. Two biological replicates were performed. For each replicate, 400 cells were imaged using previously described methods and the percent of cells positive for phosphor-histone H3 staining was determined. Rif1 staining was performed using the same protocol, using anti-Rif1 antibody diluted 1:200 overnight.

Quantification and statistical analysis

Random permutation analysis

Peaks were downloaded for histone modification and transcription factor binding sites identified by ChIP-chip or ChIP-seq in Drosophila from modENCODE (Celniker et al., 2009; Contrino et al., 2012). All available ChIP-seq data in S2 cells were considered in addition to previously published ORC2 (Eaton et al., 2011) and nucleoporin peaks (Gozalo et al., 2020; Pascual-Garcia et al., 2017). For each ChIP-seq factor, the amount of base-pair overlap was calculated between the given factor and ORC2 peaks. A permutation-based technique was used to determine whether the observed amount of overlap was more or less than expected by chance. Briefly, an empirical

p-value was calculated for the observed amount of overlap by comparing to a null distribution obtained by randomly shuffling regions throughout the genome and calculating the amount of overlap in each permutation. The p-values were adjusted for multiple testing using the Bonferroni correction. In this analysis, the location of the ORC2 peaks was maintained and the locations of the histone modification or transcription factor binding peaks were shuffled. The length distribution of the shuffled peaks was matched to the original set and excluded all gap and ENCODE blacklisted regions from consideration. 1000 permutations were performed for each marker and ORC2 pair. To determine factors that were specific for ORC2 or Elys, the same analysis was performed for either Elys binding sites with either Elys alone or binding sites that contained both Elys and ORC2 peaks. The difference in Log2 Fold Enrichment was also quantified in Fig. 4.4.

Sequencing analysis

Previously published data generated by ChIP-seq in Drosophila S2 cells was retrieved for ORC2 (Eaton et al., 2011). Elys, Nup107, Nup93, (Gozalo et al., 2020), Nup98 (Pascual-Garcia et al., 2017). All other data sets were generated by this work (see *ChIP*-seq and *CUT*&RUN methods). Sequencing reads were aligned to dm6 with Bowtie2 (Langmead and Salzberg, 2012) using the pre-set --very sensitive-local. Duplicate reads were flagged after alignment with Picard: MarkDuplicates (Broad Institute) using Galaxy (Afgan et al., 2016). Coverage files were generated using Deeptools: BamCoverage (Ramírez et al., 2016) with the following options: 1X normalization, bin size = 50 bps, effective genome size = dm6. Genomic coverage was visualized using the UCSC Genome Browser (Kent et al., 2002). For peak comparisons, previously published peak files were used (Eaton et al., 2011; Gozalo et al., 2020; Pascual-Garcia et al., 2017). For Rif1, ORC2, and mab414, statistically significant peaks over an IgG negative control were called using MACS2 (Feng et al., 2012). Deeptools: plotHeatmap was used to generate the

mean ChIP-seq signal plots and heatmaps centered on ORC2 peaks as shown in Fig. 3.3, 3.4, and 4.3.

The ATAC-Seq and ORC2 ChIP-seq data in Chapter III was processed similar as above with minor differences. To generate the coverage plots for visualization, the ATAC-Seq data was normalized by CPM (counts per million) with a bin size = 50. To scale the ORC2 ChIP-seq data to the background signal, 25,000 genomic regions, each 250 base pairs long, were randomly selected. The total reads within the randomly selected regions for each depletion was determined and scaled down to the depletion with the fewest reads. The scaled coverage files were plotted in the UCSC Genome Browser. For both ORC2 ChIP-seq and ATAC-seq, the mean signal was determined using Deeptools: plotProfile for each set of peaks. To generate shuffled ORC2 peaks, ORC2 peaks were randomly distributed across the genome, and the number of peaks and the length of each peak were kept the same using BedTools: ShuffleBed.

For the plots generated in Fig. 3.11, both ChIP-seq replicates were first scaled to background as above. Replicates were then scaled again for visualization purposes by determining the maximum signal in the GFP depletion and then scaling all the data for all depletions by the same scaling factor. This was performed to account for the different number of reads and differences in signal intensity between the two replicate experiments.

Statistics

For all statistics, relevant p-values are denoted within the respective figure legends. Error bars in all graphs show the standard deviation. For the volcano plot in Fig. 3.1 and 4.1, Fold enrichment was calculated by dividing spectrum counts for GFP IP by the negative control. P-values were

calculated by performing a Fisher's Test for each individual protein. P-values less than 0.00010 were rounded for simplicity.

Black bars indicate a One-Way ANOVA with a post-hoc Dunnett's test comparing each depletion to negative control (GFP). Pink bars indicate a parametric T-test performed between each depletion comparing the untreated cells to the aphidicolin treated cells. 300 cells from two biological replicates were randomly selected for the quantification.

CHAPTER III[5]

NUCLEOPORINS FACILITATE ORC LOADING ONTO CHROMATIN[5]

Introduction

The origin recognition complex (ORC) binds to thousands of sites throughout the genome to initiate DNA replication (Leonard and Méchali, 2013). Chromatin-bound ORC, together with additional factors, performs the essential function of loading inactive MCM2-7 helicases across the genome in late M and G1 phases of the cell cycle (Fragkos et al., 2015) . The distribution of ORC-binding sites is critical to define replication start sites and to maintain genome stability, as large genomic regions devoid of replication start sites are prone to breakage upon replication stress (Cha and Kleckner, 2002; Letessier et al., 2011; Miotto et al., 2016; Newman et al., 2013). Additionally, the number and distribution of ORC-binding sites and replication start sites can change during development to accommodate cell-type-specific DNA replication programs (Eaton et al., 2011; Hua et al., 2018; Sher et al., 2012). Therefore, studying how ORC is targeted to chromatin is essential to understanding how genome stability is maintained through development.

The factors that determine where ORC binds differ across species; however, both DNA sequence and chromatin environment can be important contributors. In *S. cerevisiae*, ORC binding is largely sequence dependent and influenced by nucleosome positioning (Eaton et al., 2010; Wyrick et al., 2001; Xu et al., 2006). While there are a small number of defined initiator sequences in metazoans (Altman and Fanning, 2001; Austin et al., 1999; Lu et al., 2001), ORC binding is largely sequence independent and influenced by both chromatin state and DNA topology (Eaton et al., 2010, 2011;

[5] This chapter was adapted from Richards et al. Cell Reports. 2022. Used with permission from co-authors.

MacAlpine et al., 2010; Miotto et al., 2016; Remus et al., 2004; Vashee et al., 2003). ORC tends to localize to the transcription start sites of active genes (Eaton et al., 2011; MacAlpine et al., 2010). Hallmarks of ORC binding include open regions of chromatin, histone modifications associated with active chromatin and in Drosophila, sites of cohesion loading (Eaton et al., 2011; MacAlpine et al., 2010; Miotto et al., 2016). Furthermore, in Drosophila, specific proteins such as E2f, Rbf and a Myb-containing protein complex can help recruit ORC to a specific initiation site (Beall et al., 2002; Bosco et al., 2001; Royzman et al., 1999). In humans, ORC-associated protein (ORCA) localizes to heterochromatin and facilitates ORC loading onto chromatin (Shen et al., 2010). The number of ORC-binding sites greatly exceeds the number of replication start sites used in a given cell cycle (Cayrou et al., 2011). These excess ORC-binding sites license dormant replication origins, which have a critical role in promoting genome stability by ensuring additional replication start sites are available upon replication stress (Doksani et al., 2009; Ge et al., 2007; Ibarra et al., 2008).

Nucleoporins, or Nups, are typically associated nuclear pore complexes (NPCs) and facilitate the import and export of proteins and macromolecules across the nuclear membrane (for review, see Wente and Rout, 2010). In addition to their canonical function at NPCs, a subset of Nups bind to chromatin and regulate genome structure and function. For example, the nucleoporin Elys binds to chromatin in late mitosis and is required to assemble nuclear pore complexes onto chromatin prior to their insertion into the nuclear membrane (Franz et al., 2007; Galy et al., 2006; Gillespie et al., 2007; Rasala et al., 2006; Shevelyov, 2020). More recent work; however, has demonstrated that several Nups regulate both transcription and chromatin condensation (Capelson et al., 2010; Kalverda et al., 2010; Kuhn et al., 2019; Panda et al., 2014; Pascual-Garcia et al., 2014, 2017; Raices and D'Angelo, 2017; Vaquerizas et al., 2010). In Drosophila, Nup98 binds to distinct regions of the genome, co-localizes with RNA polymerase II and regulates mRNA levels (Panda et al., 2014; Pascual-Garcia et al., 2014). Furthermore, the genomic localization of Nup98 and

Elys correlate with actively transcribed genes (Pascual-Garcia et al., 2017). Tethering the nucleoporins Nup62 or Sec13 is sufficient to decondense chromatin within specific regions of chromatin (Kuhn et al., 2019). Interestingly, this chromatin decondensation correlates with the recruitment of Elys and the PBAP/Brm chromatin remodeling complex (Kuhn et al., 2019). Many Nups are not permanently anchored to the NPC, but, rather, dynamically associate with the NPC throughout the cell cycle (Rabut et al., 2004) and the interaction between Nups and chromatin can occur in the nucleoplasm (Ibarra and Hetzer, 2015). Therefore, it is likely that many Nups have chromatin-related functions independent of the NPC.

In this study, we show that ORC associates with members of the Nup107-160 subcomplex of the nuclear pore. We then show that Nups co-localize with ORC2-binding sites across the genome and that Nups are some of the most enriched chromatin-related factors at ORC sites. We find that depletion of Elys, but not other Nups, reduces the amount of chromatin-bound ORC2 throughout the genome. Importantly, Elys likely promotes ORC2 association independently of its role in promoting chromatin decompaction as we observe no difference in chromatin accessibility at ORC2 binding sites upon Elys depletion. Finally, we show that depletion of Elys and Nup98-96 sensitizes cells to replication fork inhibition. We propose that Elys is necessary to load the optimal level of ORC on chromatin. Reduction in ORC levels upon Elys depletion could underlie the sensitivity to replication fork stalling by jeopardizing the establishment of dormant origins. Thus, our work provides insight into how metazoan ORC is recruited to chromatin and defines a replication-associated function of Nups in Drosophila.

Results

ORC associates with nucleoporins

While a number of chromatin-associated factors are important for ORC genomic binding in metazoans, uncovering factors that facilitate ORC recruitment still remains an under-studied aspect of genome replication (Eaton et al., 2011; Shen et al., 2010). To identify factors that interact with ORC to facilitate ORC binding to chromatin or regulate ORC activity, we immunoprecipitated endogenously tagged ORC2-GFP from Drosophila embryo extracts (Fig. 3.1A). Importantly, extracts were benzonase treated to ensure ORC2-associated proteins were not indirectly bridged by DNA. We used a stringent statistical cut off to define ORC2-associated proteins (p-value of less than 0.05 and a fold enrichment greater than 2, see Chapter II). Using these parameters, we identified all six subunits of the ORC complex (Fig. 3.1C). Surprisingly, we also identified six Nups (Elys, Nup98-96, Nup75, Nup160, Nup133, and Nup107) that were statistically enriched in ORC2-GFP immunoprecipitation (Fig. 3.1B; Fig 3.2A). Interestingly, five out of the six ORC2-GFP-associated Nups are members of the Nup107-160 complex that form rings on the inner and outer faces of the nuclear pore (Beck and Hurt, 2017). Given that an antibody specific to Drosophila Elys was available, we used IP followed by Western blotting to independently validate the association between ORC2 and Elys (Fig. 3.1D).

The two most enriched Nups identified, Elys and Nup98-96, have roles beyond being structural subunits of the nuclear pore (Kuhn et al., 2019; Panda et al., 2014; Pascual-Garcia et al., 2014, 2017). In Xenopus extracts, Elys associates with the activated replicative helicase, but not ORC (Gillespie et al., 2007). Furthermore, DNA replication is severely inhibited when Elys is depleted from extracts (Gillespie et al., 2007). Given that the Xenopus extract system more closely resembles early Drosophila embryogenesis, we repeated the ORC2 IPs throughout Drosophila embryogenesis to determine if the association between ORC2 and Elys was developmentally regulated. The association between ORC and Elys; however, occurred at multiple time points through embryogenesis and mirrored protein levels (Fig. 3.2B). Taken together, we conclude that

ORC2 associates with Elys and several nucleoporins that make up the Nup107-160 subcomplex of the NPC.

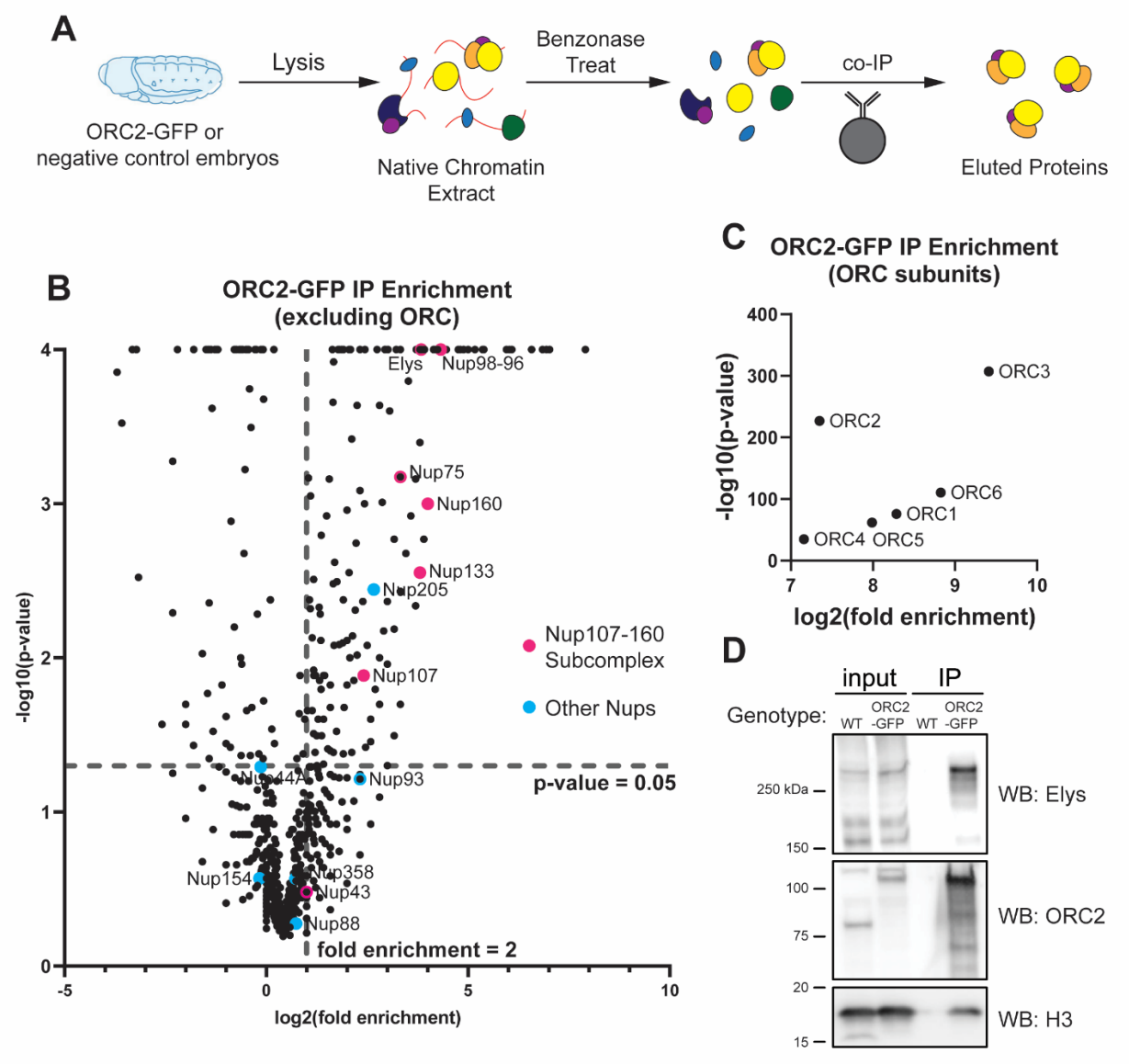

Figure 3.1. *ORC interacts with subunits of the nuclear pore complex*. (A) Schematic of extract preparation and immunoprecipitation protocol using *ORC2-GFP* or *Oregon R* (negative control) embryos. (B) Average fold enrichment and statistical significance for three biological replicates of GFP-Trap IP-mass spectrometry for *ORC2-GFP* expressing embryos relative to negative control embryos. Highlighted are all nucleoporin proteins identified by mass spectrometry. Dashed lines indicate significant level cut-offs (<0.05 for p-value and ≥2-fold enrichment). (C) Same as (B) but

with only ORC subunits. (D) Western blots using anti-ORC2, anti-Elys, or anti-Histone H3 antibody on samples derived from the IP. Contributions: Figure made by Logan Richards. Samples for IP-MS prepared by Logan Richards. MS performed at the Vanderbilt Mass Spectrometry Core and raw data analyzed by Hayes McDonald. IP-Western performed by Christopher Lord.

A

		ORC2-GFP			negative control			Comparison of abundance*
		Rep. #1	Rep. #2	Rep. #3	Rep. #1	Rep. #2	Rep. #3	(p-value)
ORC	**ORC2**	316	339	323	4	0	2	< 0.00010
	ORC1	109	80	123	2	0	0	< 0.00010
	ORC3	463	446	452	0	0	0	< 0.00010
	ORC4	58	43	42	0	0	0	< 0.00010
	ORC5	113	72	69	0	0	0	< 0.00010
	ORC6	148	151	155	0	0	0	< 0.00010
Nup107-160 Subcomplex	Elys	16	31	96	6	2	2	< 0.00010
	Nup96-98	5	6	9	0	0	0	< 0.00010
	Nup75	4	6	10	1	0	1	0.00067
	Nup160	4	5	7	0	1	0	0.0010
	Nup133	3	4	7	0	0	1	0.0028
	Nup107	6	4	6	1	1	1	0.013
	Nup44A	20	12	7	27	7	9	0.051
	Sec13	7	4	5	8	5	4	0.20
	Nup43	0	0	2	0	0	0	0.33
	Nup37	0	0	0	0	0	0	n.a.
Othr Nucleoporins	Nup205	9	3	7	0	0	0	0.0036
	Nup93	1	1	3	0	0	0	0.061
	Nup358	6	11	16	4	8	8	0.27
	Nup154	3	3	2	3	0	6	0.27
	Nup88	2	1	2	0	0	3	0.53

Table 3.1 Peptide counts for ORC2-GFP IP-MS

*Fisher's Exact Test

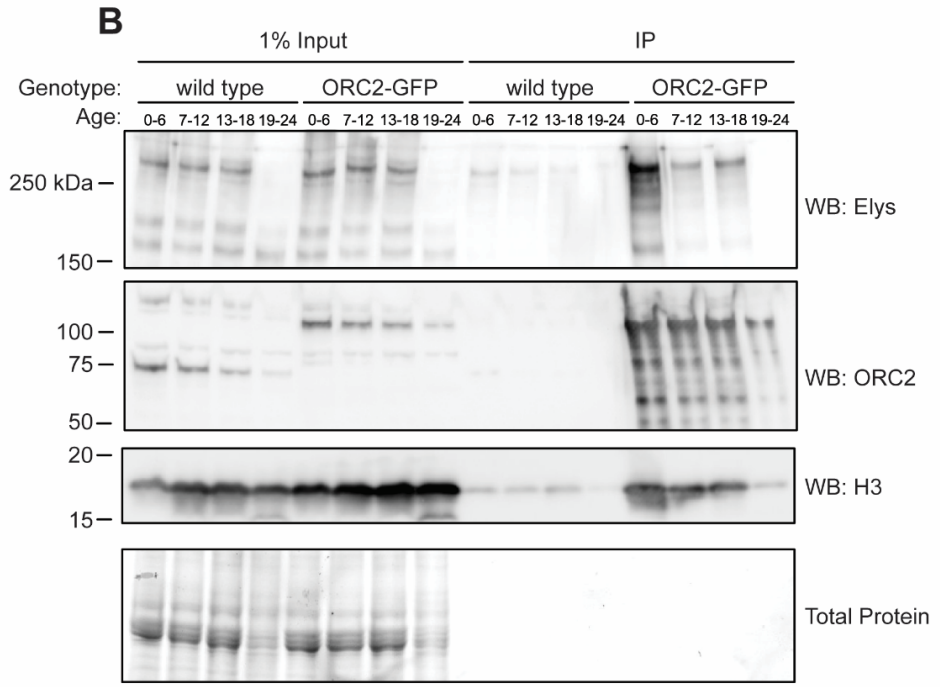

Figure 3.2. ***ORC2-GFP immunoprecipitation enriches for components of the Nup107-160 subcomplex of the nuclear pore.*** (A) Table with peptide counts for three biological replicates of anti-GFP IP mass spectrometry done in either ORC2-GFP or negative control embryos as in Figure 1. Embryos were aged 16-24 hours. P-value was calculated by performing a Fisher's Test. (B) Western blot of anti-GFP IP done in ORC2-GFP embryos throughout embryonic development. Western blots done using anti-Elys, anti-ORC2, or anti-Histone H3 antibodies. IPs were performed on embryos from indicated ages after egg laying (in hours). Total protein loaded for each sample shown in bottom box. Contributions: Samples for IP-MS prepared by Logan Richards. MS performed at the Vanderbilt Mass Spectrometry Core and raw data analyzed by Hayes McDonald. Table made by Logan Richards. IP through development (4.2B) done by Christopher Lord.

ORC binds the same genomic regions as several Nucleoporins

Individual Nups bind to distinct chromatin regions to regulate transcription, likely independent of the nuclear pore (Capelson et al., 2010; Kalverda et al., 2010; Kuhn et al., 2019; Panda et al., 2014; Pascual-Garcia et al., 2014, 2017; Raices and D'Angelo, 2017; Vaquerizas et al., 2010). Given that ORC associates with Nups, we asked if ORC and Nups co-localize on chromatin. Using previously published ChIP-seq data sets generated in Drosophila S2 cells, we visualized the genomic binding profiles of ORC2 (Eaton et al., 2011) and multiple Nups representing distinct subcomplexes of the nuclear pore (Gozalo et al., 2020; Pascual-Garcia et al., 2017). We also performed CUT&RUN using the mab414 antibody, which recognizes FG repeats found in several Nups to determine the genomic binding sites of nuclear pores more broadly (Davis and Blobel, 1986). Qualitatively, the binding profile of ORC2 shows extensive overlap with the binding profiles of Elys, Nup107, Nup98 and mab414 (Fig. 3.3A). Next, we quantified ChIP-seq signal of Nups relative to ORC2 peaks and found that Nup and mab414 ChIP-seq or CUT&RUN signal was enriched within ORC2 peaks (Fig. 3.3B). Elys followed by Nup98 showed the strongest signal across all Nups (Fig. 3.3B). Strikingly, 98% of ORC2 peaks overlap with Elys binding sites (Fig. 3.4A). These data show that ORC2 and Nups bind many of the same genomic regions.

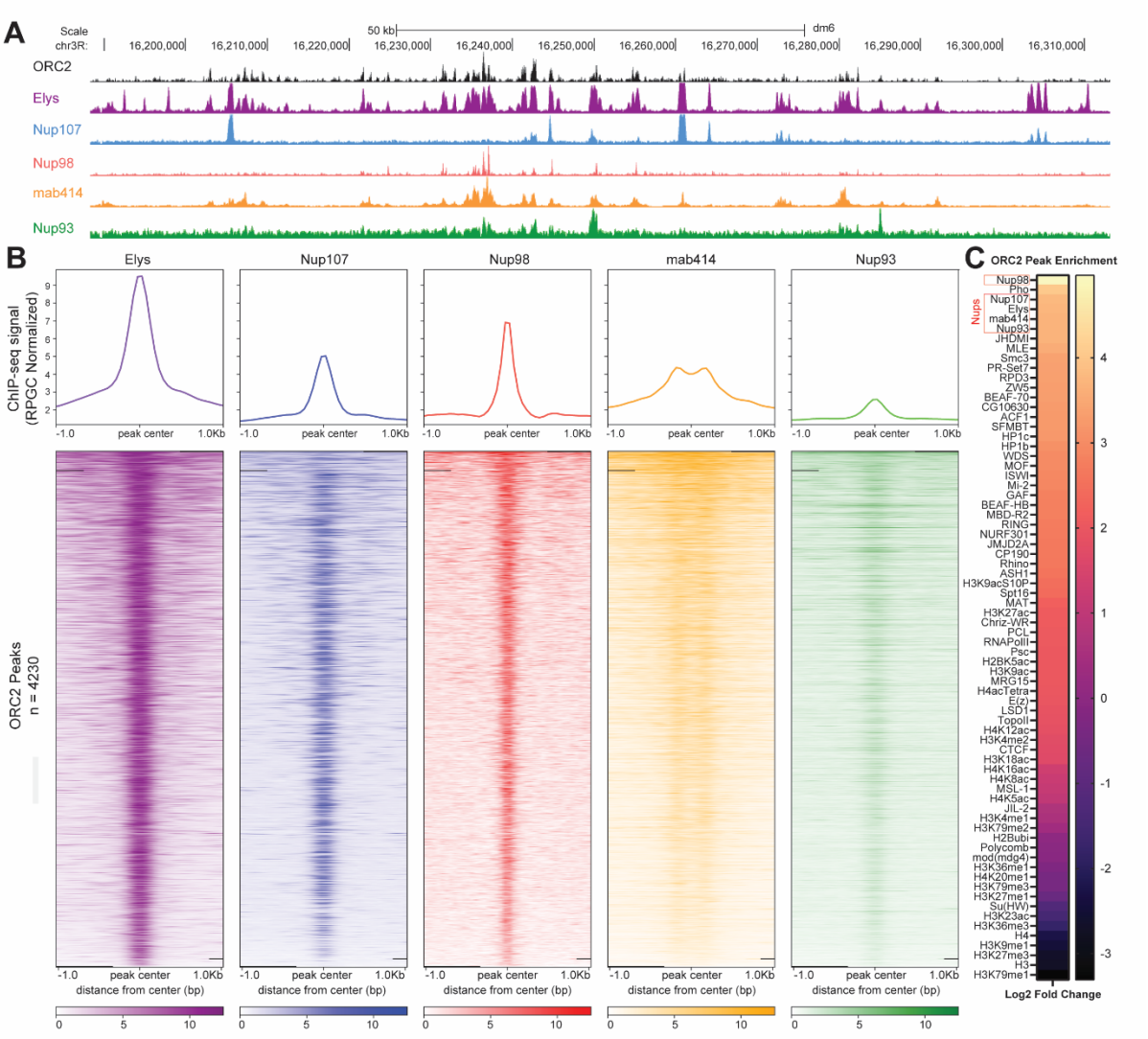

Figure 3.3. ***ORC2 binds the same genomic regions as several Nups.*** (A) Representative UCSC genome browser view of ORC2, Elys, Nup107, Nup98, mab414 and Nup93 ChIP-seq (or CUT&RUN) signal generated from previously published data. (B) Enrichment heatmap of ChIP-seq signals sorted by mean occupancy around the center of ORC2 peaks. (C) ORC2 peak enrichment heatmap for chromatin marks, transcription factors and Nup peaks from previously published data. Log2 fold enrichment for observed overlap relative to expected overlap for each comparison peak set is shown. Contributions: ORC2 and nucleoporin data previously published by Eaton et al., 2011, Gozalo et al., 2020, and Pascual-Garcia et al., 2017. Data re-analyzed and visualized in 4.3A and 4.3B by Logan Richards. Mab414 CUT&RUN performed and analyzed by Logan Richards. Data in 4.3C retrieved from the modENCODE consortium and analyzed by Mary-Lauren Benton. Heatmap prepared by Logan Richards.

Compared to all available genomic data, nucleoporins are the most enriched at ORC binding sites

While we observed extensive overlap between ORC2 and Nup binding sites, we wanted to quantitatively measure the significance of this overlap relative to other chromatin-associated factors. To this end, we evaluated the overlap between ORC2 peaks, the available Nup ChIP-seq data sets, and all available S2 cell ChIP-seq data sets available from the modENCODE consortium. For each annotation, we compared the observed overlap with the overlap observed with 1000 randomly shuffled sets of peaks (Celniker et al., 2009; Contrino et al., 2012). This allowed us to test if the degree of overlap with ORC2 peaks was greater than the expected overlap if peaks were randomly distributed along the genome (see Chapter II: *Random Permutation Analysis*). As a proof of principle, our analysis revealed several modENCODE factors that were either enriched or depleted at ORC2 binding sites consistent with previous work (Eaton et al., 2011). Strikingly, not only were Nups enriched at ORC2 binding sites, they were among the most statistically enriched factors (p-value = 0.0001, log2 fold change > 3.5 for Elys, mab414, Nup107, Nup93, Nup98) out of all 72 data sets we analyzed (Fig. 3.3C and Fig 3.4B). We also asked if there were any factors enriched at sites that contain Elys and ORC compared to sites that only contain Elys. From this analysis, we found that Polycomb-related factors are enriched at Elys and ORC2 binding sites relative to Elys only binding sites (Fig. 3.5). Taken together, we conclude that Nup binding sites show significant overlap with ORC2 binding sites genome wide.

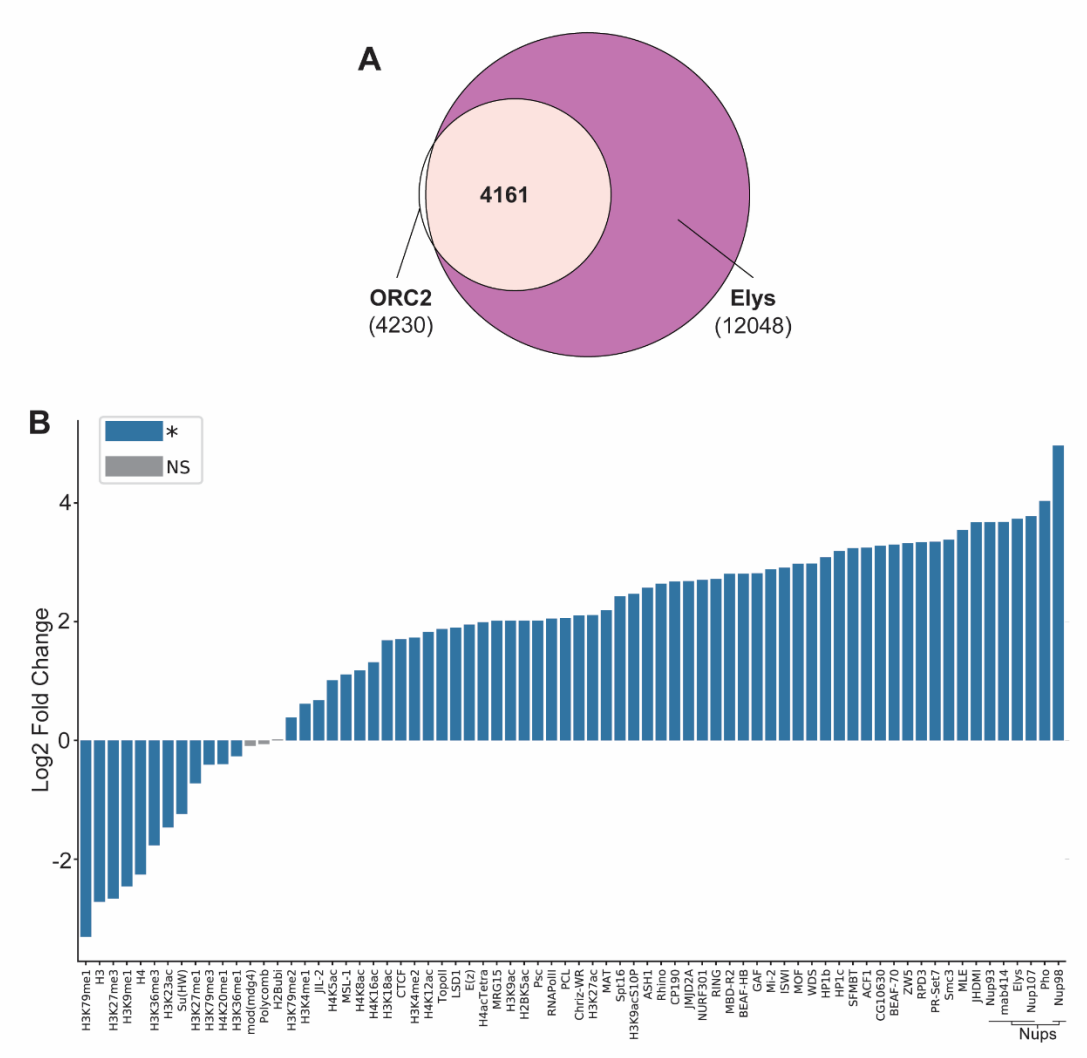

Figure 3.4. ***Nups are enriched at ORC2 binding sites.*** (A) Venn diagram visualizing peak overlap between ORC2 (white) and Elys (purple). Number in parenthesis is the total number of peaks. Bold number is the number of ORC2 peaks that overlap with Elys peaks (4161 out of 4230). (B) Bar graph visualization depicting the log2 fold enrichments for data in Fig. 2C. Blue bars denote chromatin marks, transcription factors or nucleoporins that had a statistically significance correlation (positive or negative) with ORC2 peaks. Gray bars denote those that had a nonsignificant correlation. Contributions: ORC2 and Elys peaks used in 4.4A previously published by Eaton et al., 2011 and Pascual-Garcia et al., 2017. 4.4A analysis and visualization done by Logan Richards. Data used in 4.4B is the same as 4.3C. 4.4B prepared by Mary-Lauren Benton.

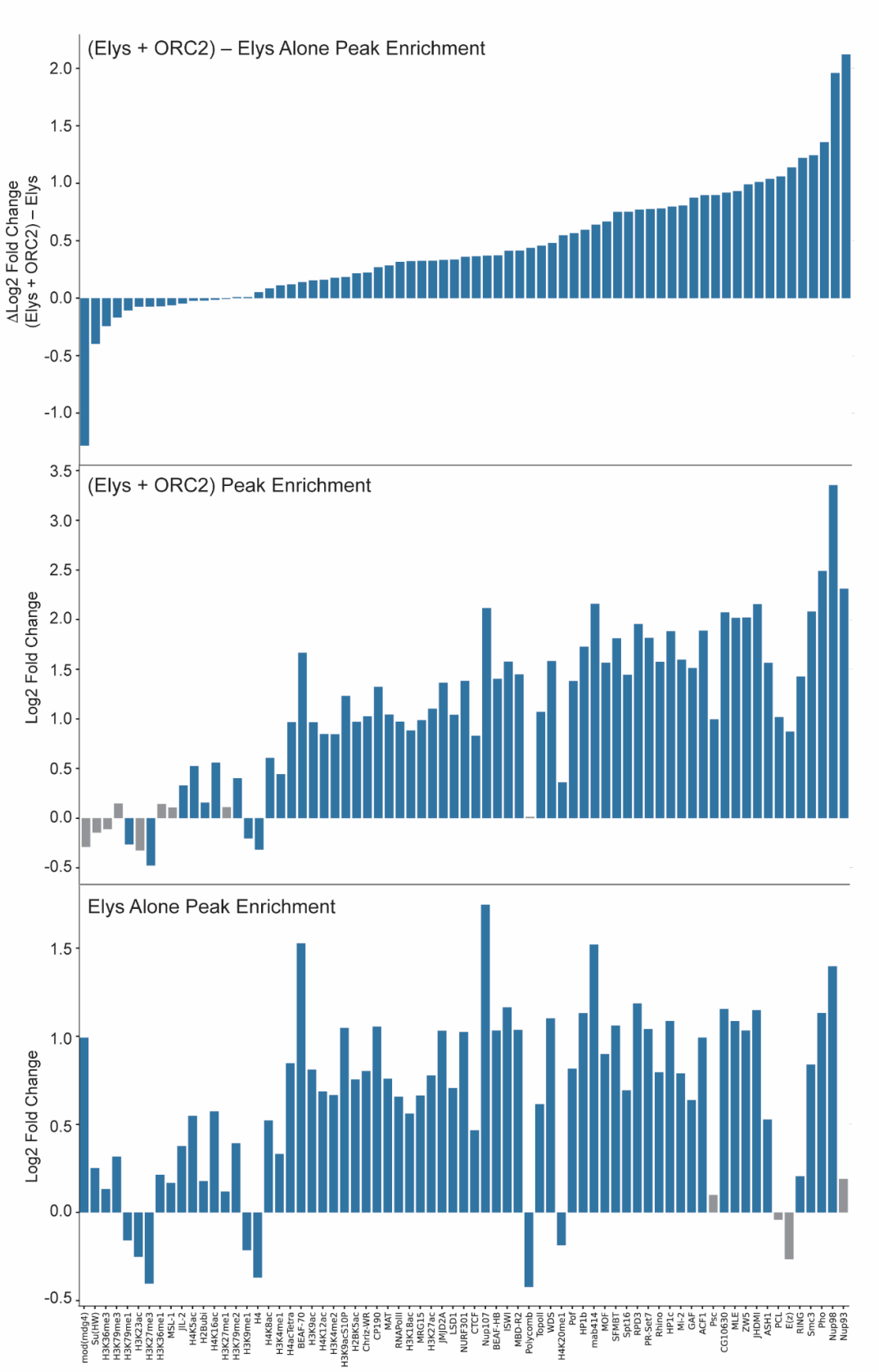
(Elys + ORC2) – Elys Alone Peak Enrichment
ΔLog2 Fold Change
(Elys + ORC2) – Elys
2.0
1.5
1.0
0.5
0.0
-0.5
-1.0
(Elys + ORC2) Peak Enrichment
Log2 Fold Change
3.5
3.0
2.5
2.0
1.5
1.0
0.5
0.0
-0.5
Elys Alone Peak Enrichment
Log2 Fold Change
1.5
1.0
0.5
0.0
-0.5
mod(mdg4)
Su(HW)
H3K36me3
H3K79me3
H3K79me1
H3K23ac
H3K27me3
H3K36me1
MSL-1
JIL-2
H4K5ac
H2Bubi
H4K16ac
H3K27me1
H3K9me2
H3K9me1
H4
H4K8ac
H3K4me1
H4acTetra
BEAF-70
H3K9ac
H4K12ac
H3K4me2
H3K9acS10P
H2BK5ac
Chriz-WR
CP190
MAT
RNAPolII
H3K18ac
HMG15
H3K27ac
JMJD2A
LSD1
NURF301
CTCF
Nup107
BEAF-HB
ISWI
MBD-R2
Polycomb
TopoII
WDS
H4K20me1
Pof
HP1b
mab414
MOF
SFMBT
Spt16
Brm3
PR-Set7
Rhino
HP1c
Mi-2
GAF
ACF1
Psc
CG10630
MLE
ZW5
JHDMI
ASH1
PCL
E(z)
RING
Smc3
Pho
Nup98
Nup93

Figure 3.5. ***Polycomb-related factors are enriched at sites where Elys and ORC2 both bind.*** Top: Bar graphs indicate difference in log2 fold enrichment (ΔLog2 Fold Change) between peaks containing both Elys and ORC2 (Elys+ORC2) and Elys only peaks for chromatin-associated factors from previously published data. Middle: Bar graph visualization depicting log2-fold enrichment for same set of factors for peaks containing both Elys and ORC2. Bottom: same as middle panel with peaks enriched for Elys but not ORC2. Blue bars: statistically enriched. Gray bars: not significant. Contributions: (Elys + ORC2 – Elys alone), (Elys + ORC2), and Elys Alone peak files prepared by Logan Richards using previously published from Eaton et al., 2011 and Pascual-Garcia et al. Analysis and visualization done by Mary-Lauren Benton.

The ORC/Nup interaction likely occurs independently of NPCs

Nups also bind chromatin when in complex with nuclear pores (Kadota et al., 2020; Kuhn and Capelson, 2019). Given this, we were curious if the ORC2 binding sites that overlap with Nup binding sites required localization to the nuclear pore, suggesting the interaction between ORC and Nups occurs at NPCs. To formally test this, we selected seven 10-kilobase regions that were positive for both Elys and ORC2 binding (ORC2 sites 1-7) and generated oligopaint probes specific to these sites (Fig. 3.6A-B). We then measured the proximity of these seven sites to the nuclear periphery. If ORC binding and colocalization with Nups requires a functional nuclear pore, we would expect these sites to be enriched at the nuclear periphery. This, however, is not the case. Just over half of the sites we tested were found in close proximity to the nuclear rim (Fig. 3.6C-D). Given that ORC2/Elys binding sites are not required to be at the nuclear periphery, this suggests that the ORC/Nup association occurs independently of the nuclear pore.

A

Site Name	Coordinates
Pos. Control	chr2L:1352742-1360992
Neg. Control	chr3R:19335000-19345000
ORC2 Site 1	chr3R:26879000-26888250
ORC2 Site 2	chr3L:14405500-14415500
ORC2 Site 3	chr3R:13644500-13654500
ORC2 Site 4	chr2L:12000000-12008000
ORC2 Site 5	chr2R:11600000-11611000
ORC2 Site 6	chrX:12727000-12742000
ORC2 Site 7	chrX:13822000-13830500

Table 3.2. Oligopaint coordinates

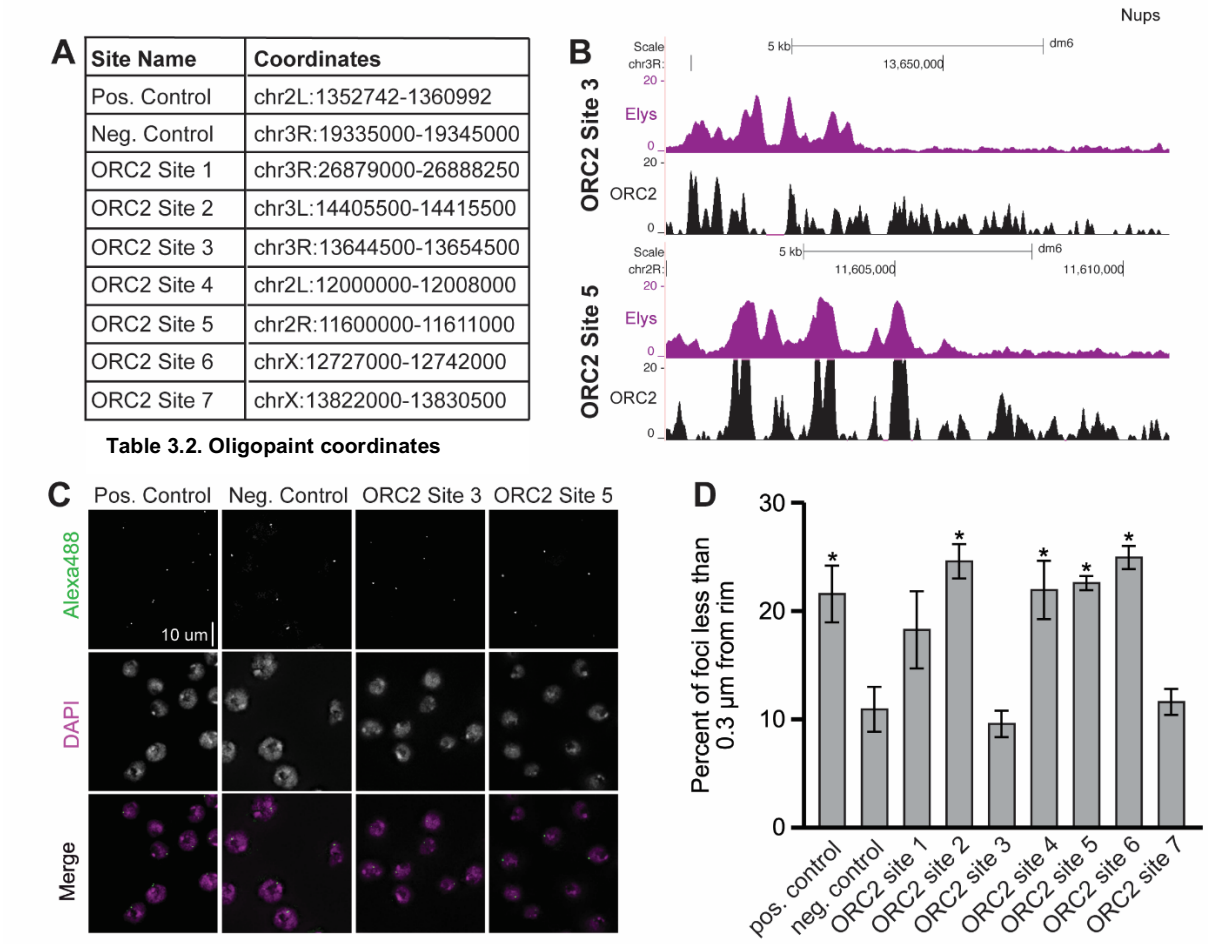

Figure 3.6. ***ORC2/Elys binding sites are not strictly at the nuclear periphery.*** (A) Table containing site names and genomic locations of oligopaint probes for Fig. 2. (B) Representative genome browser view for one biological replicate of Elys and ORC2 binding sties used for probes in oligopainting visualized in (C) (ORC2 sites 3 and 5). (C) Representative images of oligopaint performed in S2 cells for one positive (nuclear periphery associating) control site, one negative (non-nuclear periphery associating) control site and two ORC-binding sites that also Elys binding sites. (D) Quantification of the percent of oligopaint foci that were less than 0.3 µm from the nuclear rim for control sites and seven ORC2-Elys-binding sites for three biological replicates. Asterisk indicates statistical significance (p-value < 0.05) relative to the negative control. Contributions: Oligopaint sites selected by Logan Richards and Christopher Lord. 3.6A and 3.6B prepared by Logan Richards. Data for 3.6C and 3.6D generated and figure made by Christopher Lord.

ORC binding to chromatin is partially dependent on Elys

So far, we have shown that ORC physically associates with the members of the Nup107-160 subcomplex and there is a high degree of colocalization between ORC and Nups on chromatin. To determine if there is a functional relationship between ORC and Nups, we asked if the chromatin association of ORC is dependent on Nups. To this end, we depleted either GFP (negative control), ORC2, Elys and Nup98-96 using RNA interference (RNAi) in Drosophila S2 cells. Nup98-96 was selected as a control as these genes are transcribed into a single mRNA, which is translated into a larger precursor protein that is ultimately cleaved to produce Nup98 and Nup96 (Fontoura et al., 1999). Therefore, RNAi against Nup98-96 reduces the steady state protein level of both Nup98 and Nup96 (Fontoura et al., 1999). Depletions were verified by Western blotting against Elys and ORC2 (Fig. 3.7A-B).

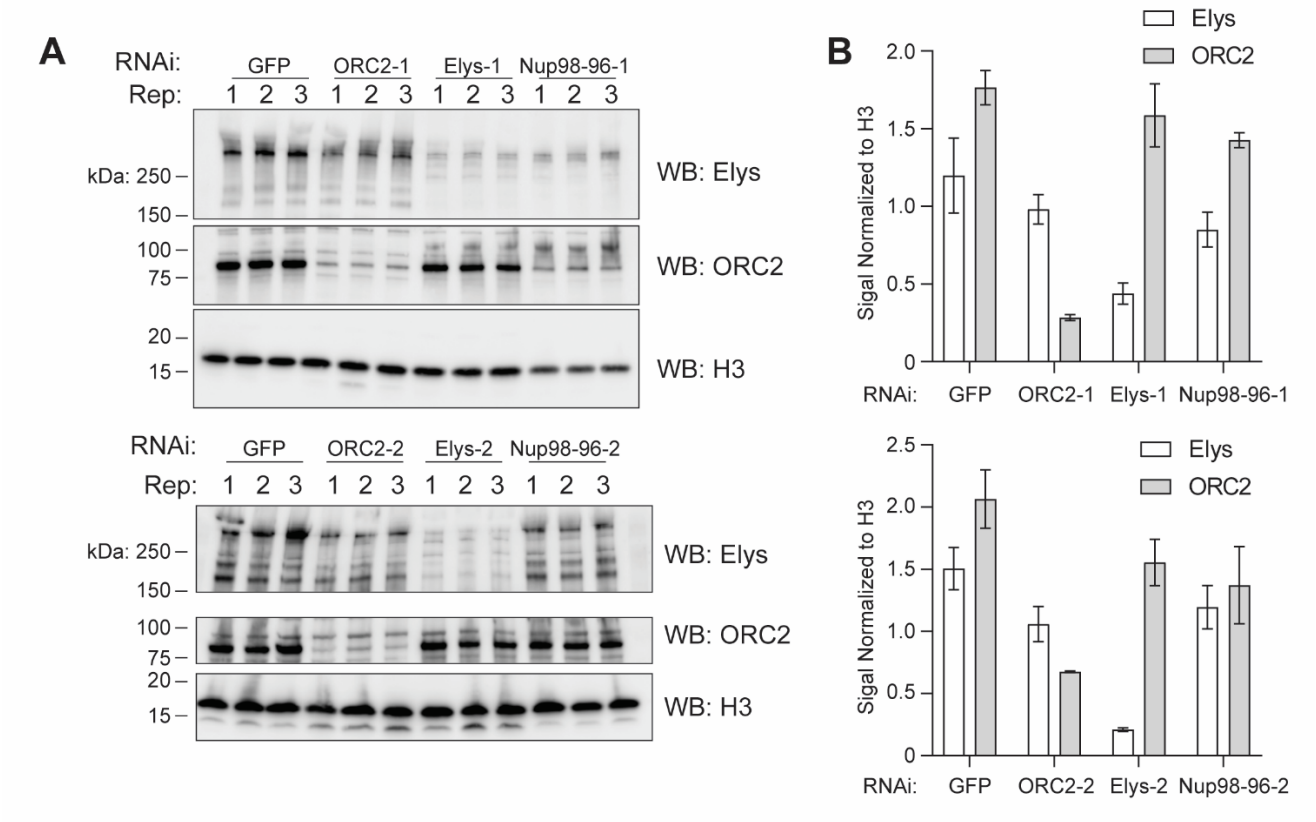

Figure 3.7. Validation of *RNA interference for GFP, ORC2, Elys, and Nup98-96.* (A) Western blots using anti-Elys, anti-ORC2 or anti-Histone H3 antibodies on samples prepared from cells treated with the indicated RNAi. Shown are three biological replicates. (B) Quantification of (A). Western blot signal for Elys (white) or ORC2 (gray) normalized to H3 for each depletion. Contributions: data and figure generated by Logan Richards.

Given that Elys binds to chromatin to promote the decondensation of chromatin (Kuhn et al., 2019), we hypothesized that Elys, and perhaps other Nups, could promote ORC binding to chromatin, as ORC preferentially associates with open and active regions of chromatin (Eaton et al., 2011; MacAlpine et al., 2010). To test this, we quantified the amount of chromatin bound ORC2 in G1 phase nuclei in GFP, ORC2, Elys or Nup98-96 depletions using quantitative flow cytometry (Matson et al., 2017) (Fig. 3.8). G1 phase nuclei were selected as any changes in ORC2 chromatin association should be most apparent in this stage, as ORC is loaded in late M and G1. In ORC2-depleted control nuclei, we observed significantly less ORC2 on chromatin as expected. Consistent with our hypothesis, we observed significantly less chromatin-associated ORC2 in G1 phase upon Elys depletion relative to control cells (Fig. 3.8A-B). Cell cycle analysis revealed that the reduction in ORC2 loading was specific to G1 (Fig. 3.9A). To ensure different cell populations were not skewing the data, we quantified only ORC2-positive nuclei and still observed reduced ORC2 chromatin association (Fig. 3.9B). Interestingly, there was no reduction in chromatin-associated ORC2 upon Nup98-96 depletion, suggesting that not all Nups contribute to ORC loading onto chromatin (Fig. 3.9C). In fact, depleting Nup107 and Nup160 (both members of the Nup107-160 subcomplex) did not affect ORC2 chromatin association, indicating that the reduction of chromatin bound ORC2 is not a generic defect of depleting Nups (Fig 3.8A-B, Fig. 3.9C).

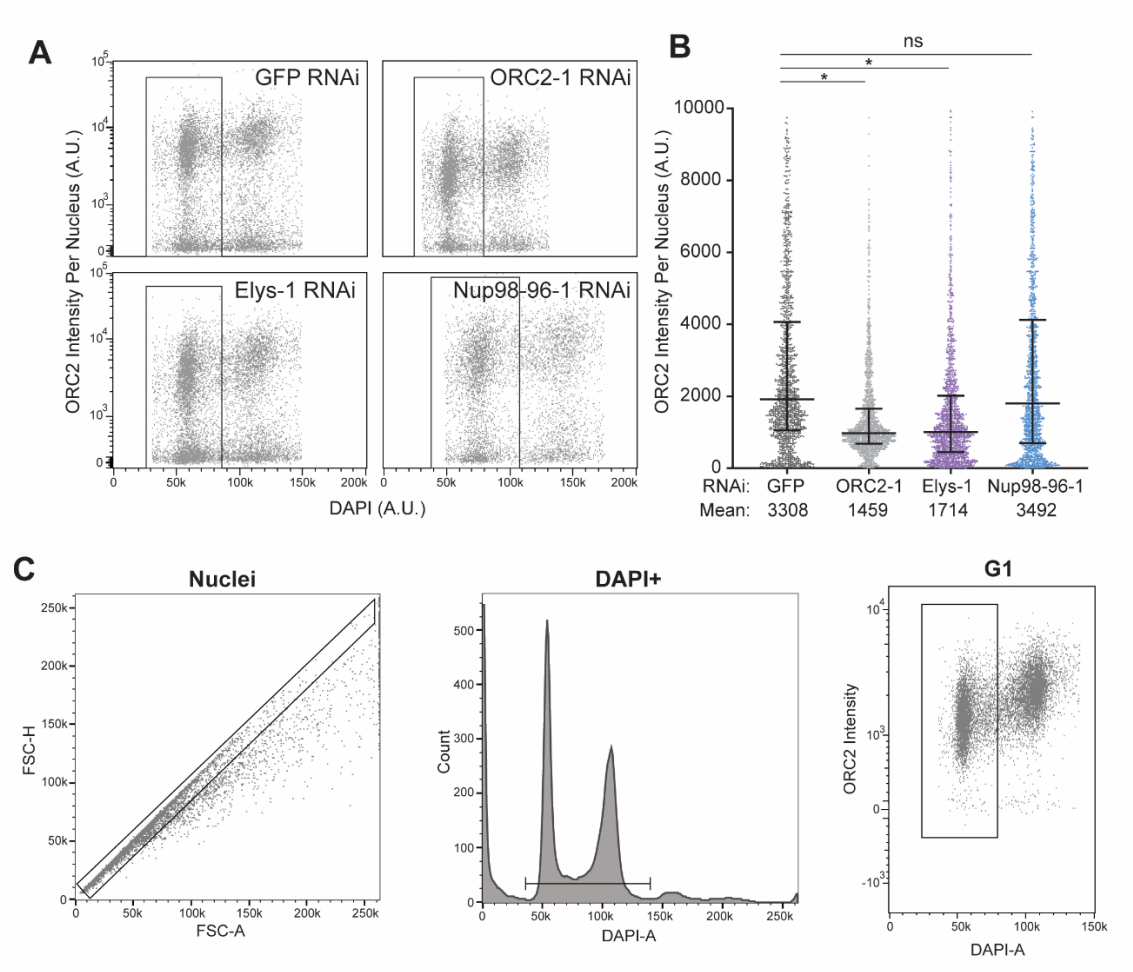

Figure 3.8. Depleting Elys, but not Nup98-96, reduces chromatin bound ORC2. (A) Horseshoe plot of nuclei with DNA content (DAPI) plotted against ORC2 intensity for each depletion from one replicate. Black box indicates G1 population of nuclei used for the quantification in (B). A.U.: arbitrary units. (B) Quantification of ORC2 intensity in 1500 randomly selected G1 nuclei from three biological replicates. Asterisk indicates $p<0.0001$ relative to the negative control determined by a one-way ANOVA with a post-hoc Dunnett's test. NS: No Significance. (C) Gating example for G1 nuclei. Single nuclei isolated in the first gate indicated by the black box. DAPI positive nuclei were selected, indicated by black line, to generate a horseshoe plot. The first DAPI peak, shown as a black box in the third panel, was used for quantification. Contributions: data and figure generated by Logan Richards.

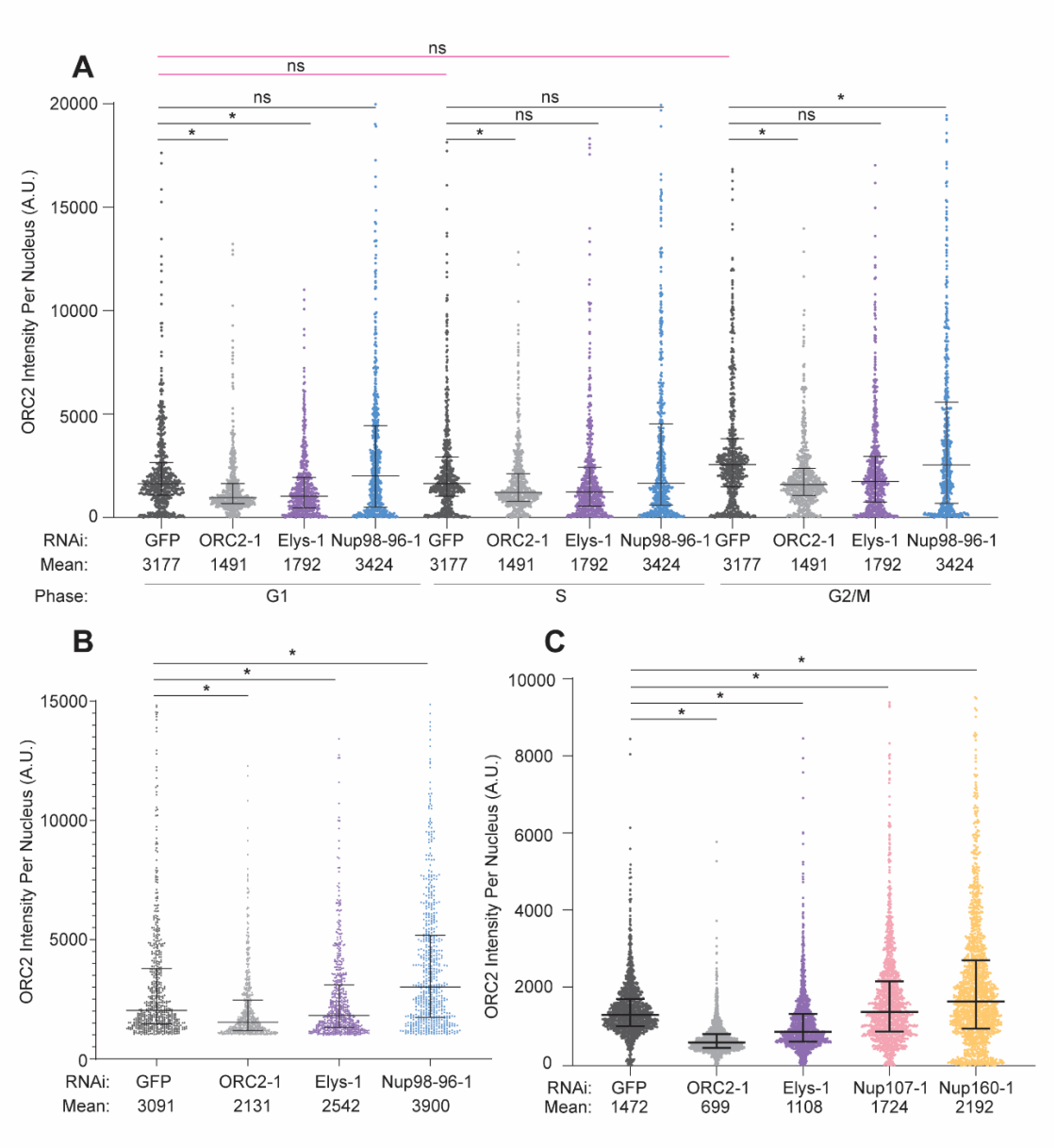

Figure 3.9. ***Not all nucleoporins contribute to ORC2 chromatin association.*** (A) ORC2 intensity quantified for each cell cycle phase. 600 nuclei from three biological replicates were pooled for the analysis. Asterisk denotes P-value of < 0.05 determined by a one-way ANOVA with a post-hoc Dunnett's test. NS: no significance. Black bars indicate comparison between GFP vs. depletion for each cell cycle phase. Pink bars indicate comparison of GFP vs. GFP for each cell cycle phase. (B) ORC2 chromatin association is reduced in Elys-depleted nuclei positive for ORC2 signal. Only nuclei with an ORC2 intensity greater than 10^3 were used to quantify the ORC2 intensity in G1 nuclei. 600 nuclei from three biological replicates for each depletion were pooled for the analysis. Asterisk denotes P-value of < 0.0001 and was determined by a one-way ANOVA with a post-hoc Dunnett's test. (C) Quantification of ORC2 intensity per nucleus using a second

set of dsRNAs against GFP, ORC2-1, Elys-1, Nup107-1, and Nup160-1. Each depletion shown contains 750 nuclei randomly selected and pooled from two biological replicates for 1500 nuclei total. Contributions: data and figure generated by Logan Richards.

As an important control, we performed the same experiment with a second set of dsRNAs against ORC2, Elys, and Nup98-96 to eliminate the possibility that our observations are due to nonspecific effects from the dsRNA (Fig. 3.10A). Additionally, we determined that induction of the RNAi machinery itself does not reduce ORC2 chromatin association (Fig. 3.10B). Finally, there was no reduction in histone H2B signal across the depletions, indicating the reduction we observe is specific to ORC2 (Fig. 3.10C-D). Taken together, we conclude that proper ORC2 chromatin association is dependent on Elys and that the reduction in ORC2 chromatin association is not a general defect caused by Nup depletion.

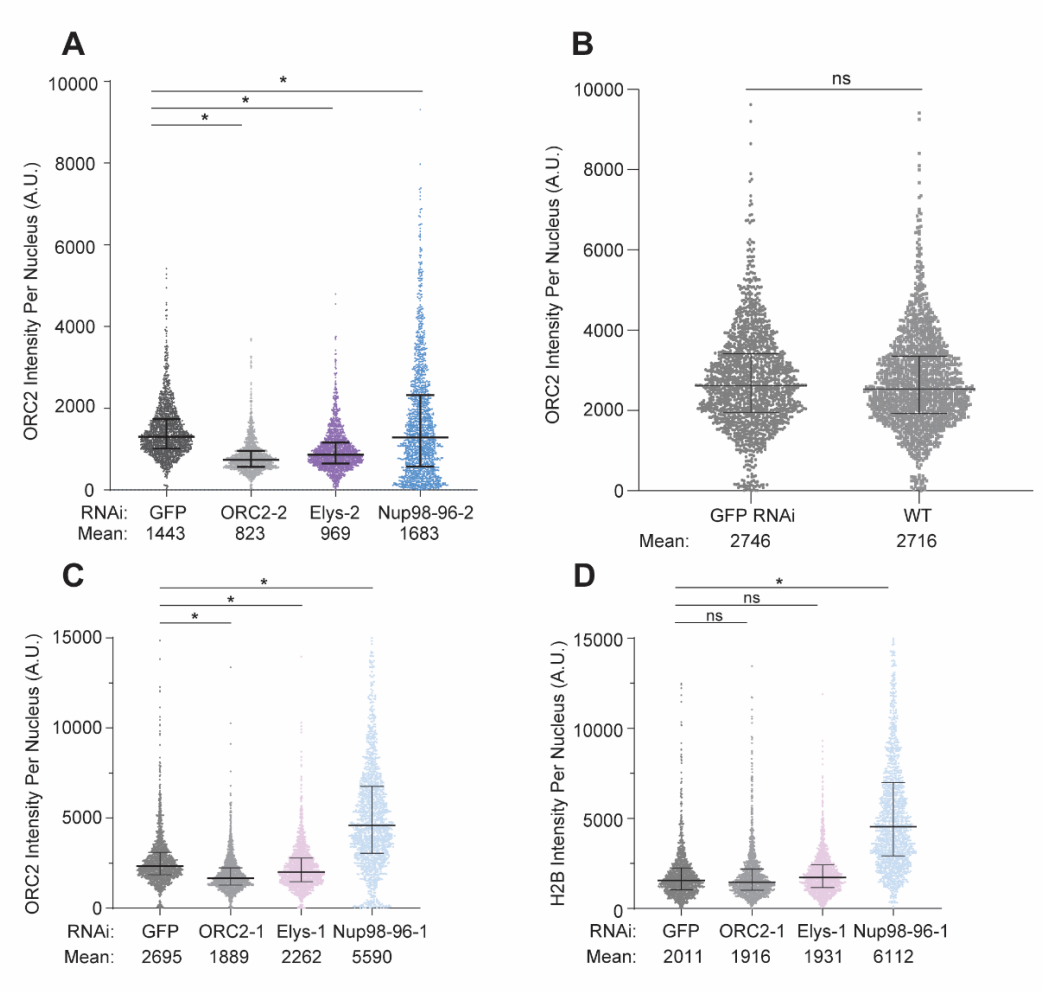

Figure 3.10. ***Depleting Elys reduces chromatin bound ORC2, but not H2B.*** (A) Quantification of ORC2 intensity per nucleus using a second set of dsRNAs against ORC2, Elys, and Nup98-96. Each depletion shown contains 1500 nuclei taken from one biological replicate. Asterisk denotes a P value of < 0.0001 and was determined by a one-way ANOVA with a post-hoc Dunnett's test. (B) Chromatin bound ORC2 levels in GFP RNAi-treated G1 nuclei compared to untreated wild type G1 nuclei. The ORC2 intensity was quantified in 1500 G1 nuclei taken from two biological replicates. NS: no significance determined by an unpaired parametric T-test. (C) 1500 randomly selected G1 nuclei across two biological replicates were used to quantify the ORC2 intensity per nucleus for each depletion. Asterisk indicates p<0.0001 relative to the negative control by One-Way ANOVA with a post-hoc Dunnett's test. (D) Same as (C) for Histone H2B intensity. Increases in H2B levels correlate with increased ploidy upon Nup98-96 depletion. Contributions: data and figure generated by Logan Richards.

The reduction in ORC chromatin association in Elys depleted cells occurs throughout the genome

Next, we asked if the reduction of chromatin-bound ORC2 upon Elys depletion occurs throughout the genome or if only specific genomic regions or ORC2 binding sites are affected. To answer this, we performed ChIP-seq using an ORC2 antibody in Drosophila S2 cells that were depleted for either GFP, ORC2, Elys, or Nup98-96. We then quantified the ChIP-seq signal intensity within previously identified ORC2 binding sites throughout the genome (Eaton et al., 2011). For our positive control, we observed less ORC2 ChIP-seq signal in the ORC2 depletion relative to the GFP negative control (Fig. 3.11). Consistent with our flow cytometry results, there was less ORC2 ChIP-seq signal in the Elys depletion, but not Nup98-96 depletion (Fig. 3.11). Furthermore, we observed a reduction in ORC2 signal throughout the genome, indicating that depletion of Elys impacts all ORC2 binding sites. To ensure the reduction in ORC2 ChIP-seq signal was specifically within ORC2 peaks, and not a general trend throughout the genome, we shuffled all ORC2 peaks across the genome and found no difference in the mean ORC2 ChIP-seq signal (Fig. 3.11B). Therefore, the reduction of signal is specific to ORC2 binding sites (Fig. 3.11B). Taken together, we conclude that depleting Elys results in less ORC2 binding throughout the genome and that Elys, but not the other Nups tested, facilitates ORC2 loading onto chromatin.

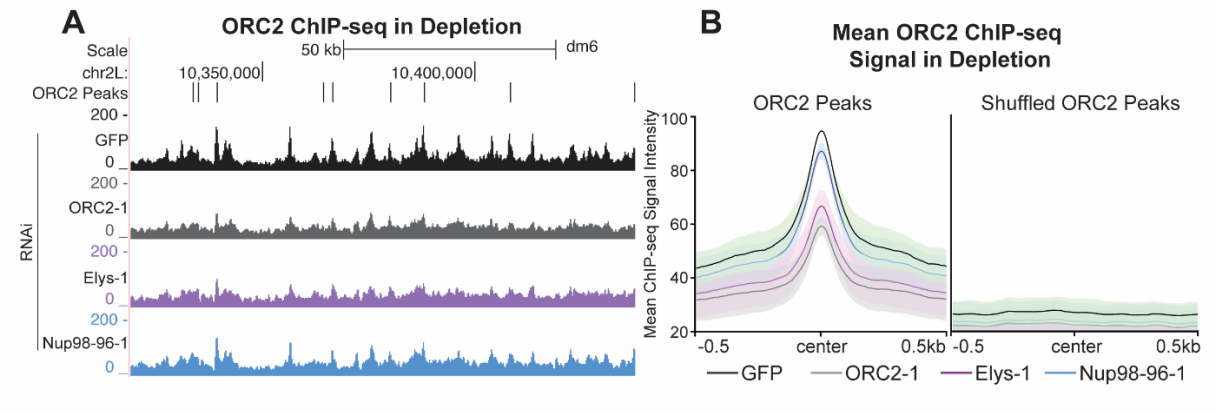

Figure 3.11. ***Elys depletion reduces chromatin bound ORC2 across the genome.*** (A) Representative UCSC genome browser view of ORC2 ChIP-seq profiles for each depletion. ORC2 binding sites (ORC2 Peaks - defined by Eaton et al., 2011) are indicated by black bars. (B) Quantification of mean ORC2 ChIP-seq signal within defined ORC2 peaks or shuffled ORC2 peaks, centered on ORC2 peaks or shuffled ORC2 peaks, respectively for two biological replicates. Contributions: data and figure generated by Logan Richards.

Depleting Elys is not sufficient to reduce chromatin accessibility by ATAC-Seq

Given that Elys is known to promote chromatin decondensation, one possibility is that Elys facilitates ORC loading indirectly by promoting chromatin accessibility, as ORC binds to open chromatin (Eaton et al., 2011; MacAlpine et al., 2010). To test this possibility, we performed ATAC-seq in RNAi-treated cells to measure chromatin accessibility within each depletion (Fig. 3.12A, 3.12C). Importantly, there was no global change in accessibility when comparing all ATAC-seq peaks throughout the genome upon Elys, ORC or Nup98-96 depletions (Fig. 3.12B, 3.12D). When comparing accessibility specifically within ORC2 binding sites, we noticed a significant reduction in accessibility upon ORC2 depletion (Fig. 3.12B, 3.12D). ORC can directly promote chromatin accessibility at ORC binding sites (Eaton et al., 2010), which could drive the reduced chromatin accessibility at ORC2 binding sites. Interestingly, depleting Elys or Nup98-96 is not sufficient to cause a significant reduction in chromatin accessibility at ORC2 binding sites (Fig.

Fig. 3.12A-D). Together, these data argue that the reduction in ORC chromatin association upon Elys depletion may not be driven by changes in chromatin accessibility.

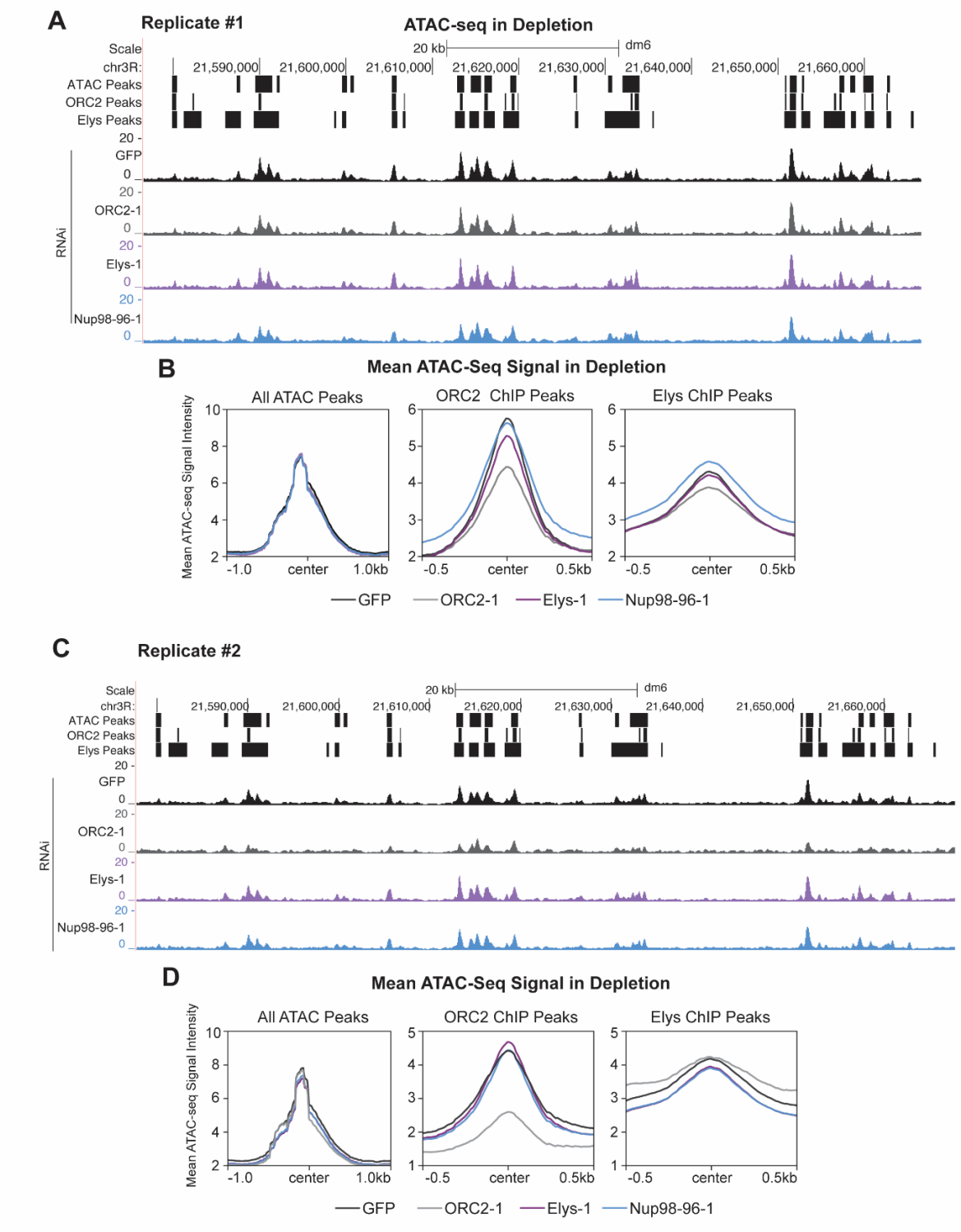

Figure 3.12*. Depleting Nups does not reduce chromatin accessibility as measured by ATAC-Seq.* (A) Representative UCSC genome browser view of ATAC-seq for each depletion for one biological replicate. ATAC-seq peaks, ORC2 ChIP-seq peaks and Elys ChIP-seq peaks are indicated by black bars. (B) Quantification of mean ATAC-seq signal for either all ATAC-seq peaks (n=12771), ORC2 ChIP-seq peaks (n=4280) or Elys ChIP-seq peaks (n=12048) centered on their respective peaks. Note the scales are different for all ATAC-seq peaks plots. (C) Representative UCSC genome browser view of ATAC-seq profiles for a second biological replicate for each depletion. (D). Quantification of (C) as performed in (B). Contributions: data and figure generated by Logan Richards.

Depleting Nup98-96, but not Elys, drastically reduces the fraction of cells in S phase

Given that ORC associates with Nups, co-localizes with Nups on chromatin, and that the association of ORC with chromatin is partially dependent on Elys, we wanted to ask if depletion of Elys and Nup98-96 affects cell cycle progression and/or genome stability. We reasoned that if ORC loading on chromatin was compromised, then we may observe a defect in S phase entry. Therefore, we pulsed cells with EdU and measured the fraction of cells in G1, S and G2/M based on their DNA content and EdU status by flow cytometry. In our ORC2 depletion that serves as a positive control, we saw a modest increase in G1 cells and reduction in S phase cells relative to the GFP negative control, consistent with a defect in S phase entry (Fig. 3.13A-B). The modest effect is expected since excess ORC is loaded onto chromatin to ensure sufficient replication start sites to complete DNA replication (Kawabata et al., 2011). Depletion of Elys, however, did not significantly alter the cell cycle profile relative to the negative control (Fig. 3.13A-B).

Given the modest effect observed with the ORC2 depletion, and the level of ORC still associated with chromatin upon Elys depletion (Fig. 3.8A-B and 3.11), this was not entirely unexpected. Depletion of Nup98-96, however, drastically reduced the fraction of cells in S phase while increasing the fraction of cells in G1 and G2/M (Fig. 3.13A-B). Depletion of Nup98-96 did not significantly affect the level of chromatin-bound ORC (Fig. 3.8A-B and 3.11). Therefore, we conclude that Nup98-96 influences cell cycle progression independently of ORC chromatin

association. Given that Elys functions at kinetochores during mitosis in mammalian cells and meiosis in *C. elegans* (Galy et al., 2006; Rasala et al., 2006), we measured the impact depletion of Elys, ORC2 or Nup98-96 has on mitotic index using immunofluorescence with an anti-phospho (Ser10) Histone H3 antibody (PH3). We found that depletion of Elys had no effect on mitotic index, suggesting that Elys may not have the same mitotic roles in Drosophila (Fig. 3.13D-E).

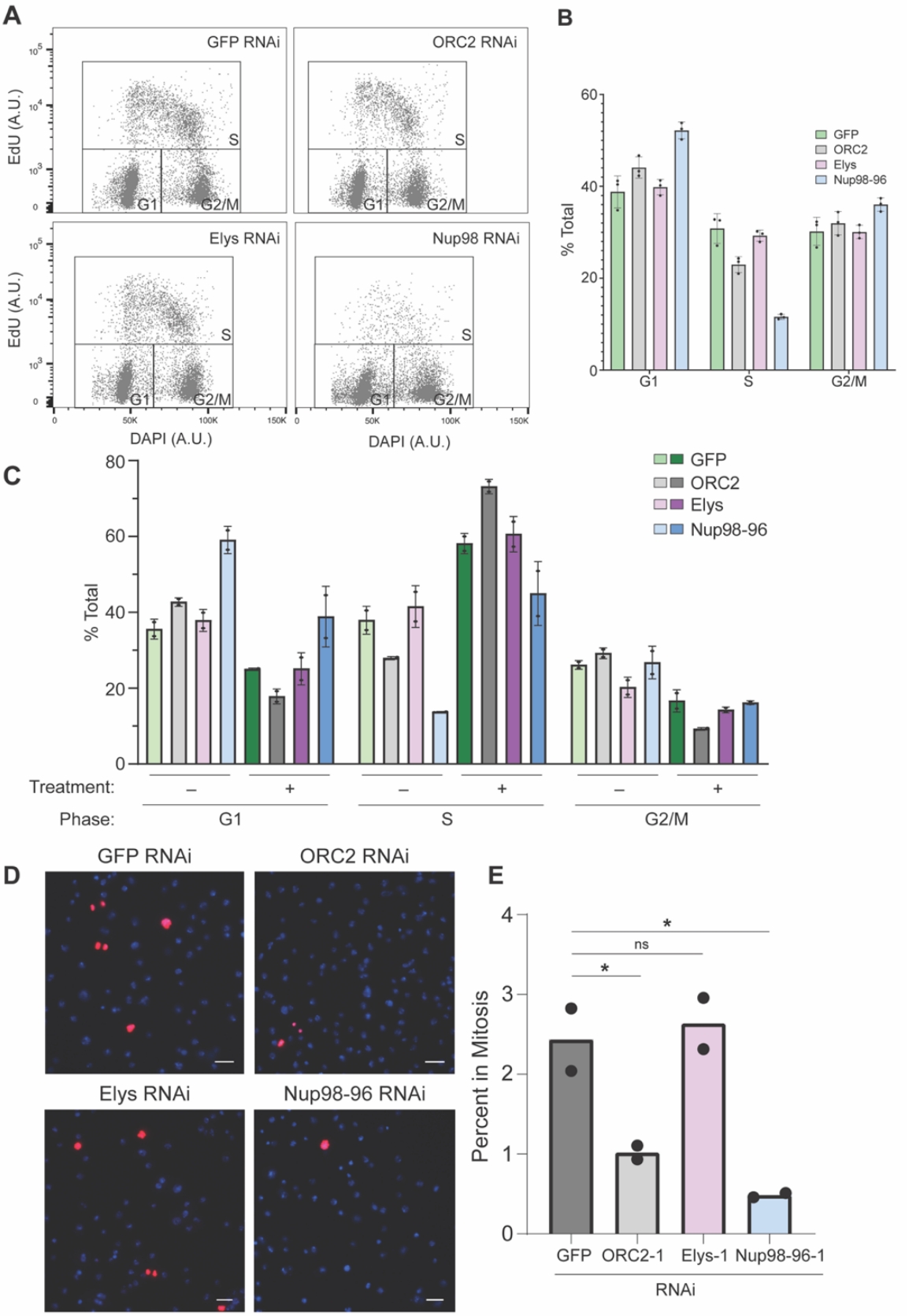
A
GFP RNAi
ORC2 RNAi
Elys RNAi
Nup98 RNAi
EdU (A.U.)
DAPI (A.U.)
S
G1
G2/M
B
% Total
GFP
ORC2
Elys
Nup98-96
C
Treatment:
Phase:
D
E
Percent in Mitosis
ns
GFP
ORC2-1
Elys-1
Nup98-96-1
RNAi

Figure 3.13. ***Nup depletions differentially affect cell cycle progression*** (A) Horseshoe plot of RNAi-treated cells. Cells were DAPI stained and EdU pulsed to determine cell cycle phase. Black boxes indicate gating used to quantify percent of cell population within each cell cycle phase. (B) Percentage of cells in each indicated phase of the cell cycle (A). Shown are three biological replicates. Error bars represent the standard error of the mean. (C) Quantification of the effects a low dose of aphidicolin has on cell cycle progression for each depletion. Percentage of cells in each indicated cell cycle phase in either untreated cells (–) or cells treated with 1.2 uM aphidicolin. Data are from two biological replicates. Error bars represent the standard error of the mean. (D) Representative images of phospho-histone H3 (PH3) immunofluorescence performed on RNAi-treated cells. Blue: DAPI. Red: PH3. Scale bar: 10 μM. (E) The percent of PH3 positive cells (percent in mitosis) from two biological replicates was quantified. Approximately 400 cells from each biological replicate were used for quantification. Asterisk denotes P-value < 0.05 determined by a one-way ANOVA followed by a post-hoc Dunnett's Test. NS: no significance. Contributions: data and figure generated by Logan Richards.

Nucleoporin depletion sensitizes cells to fork stalling

Excess replication start sites are not always essential during an unperturbed S phase, but become critical upon replication stress (Alver et al., 2014). This is largely due to the need to fire dormant replication origins to complete DNA synthesis when replication is perturbed (Doksani et al., 2009; Ge et al., 2007; Ibarra et al., 2008). Given we observe a reduction of chromatin bound ORC but no change in the percent of cells in S phase in an Elys depletion, we hypothesized that a reduction in chromatin-bound ORC could lead to a defect in dormant origin firing. While we attempted to perform DNA combing to measure inter-origin distance, we were unable to measure IdU incorporation in Drosophila S2 cells and, therefore, could only measure single CldU tracks, which is not ideal for measuring inter-origin distance (data not shown and Munden et al., 2022). If there are insufficient dormant origins upon an Elys depletion, then Elys-depleted cells should be sensitive to replication fork inhibition as there are less origins available to rescue stalled replication forks (Alver et al., 2014; Doksani et al., 2009; Ge et al., 2007; Ibarra et al., 2008). Therefore, we treated cells depleted for GFP, ORC2, Elys or Nup98-96 with a low dose of aphidicolin and measured the level of γH2Av (the Drosophila equivalent of γH2Ax in mammals) by quantitative immunofluorescence. We chose a dose of aphidicolin that did not increase the

level of DNA damage, as measured by γH2Av, in our negative control (GFP), but did cause a modest increase in the fraction of cells in S phase (Fig. 3.14A-B; Fig 3.13C). We found that depletion of Elys and Nup98-96 alone caused a modest increase in DNA damage (Fig. 3.14A-B). Upon aphidicolin treatment, however, there is a significant increase in the amount of DNA damage both relative to the negative control (Fig 3.14A, bottom panel and Fig. 3.14B, right) and relative to the untreated depletions (Fig. 3.14A-B, pink bars). From these findings, we conclude that the sensitivity to aphidicolin we observe is consistent with the possibility that dormant origin firing is reduced in an Elys depletion.

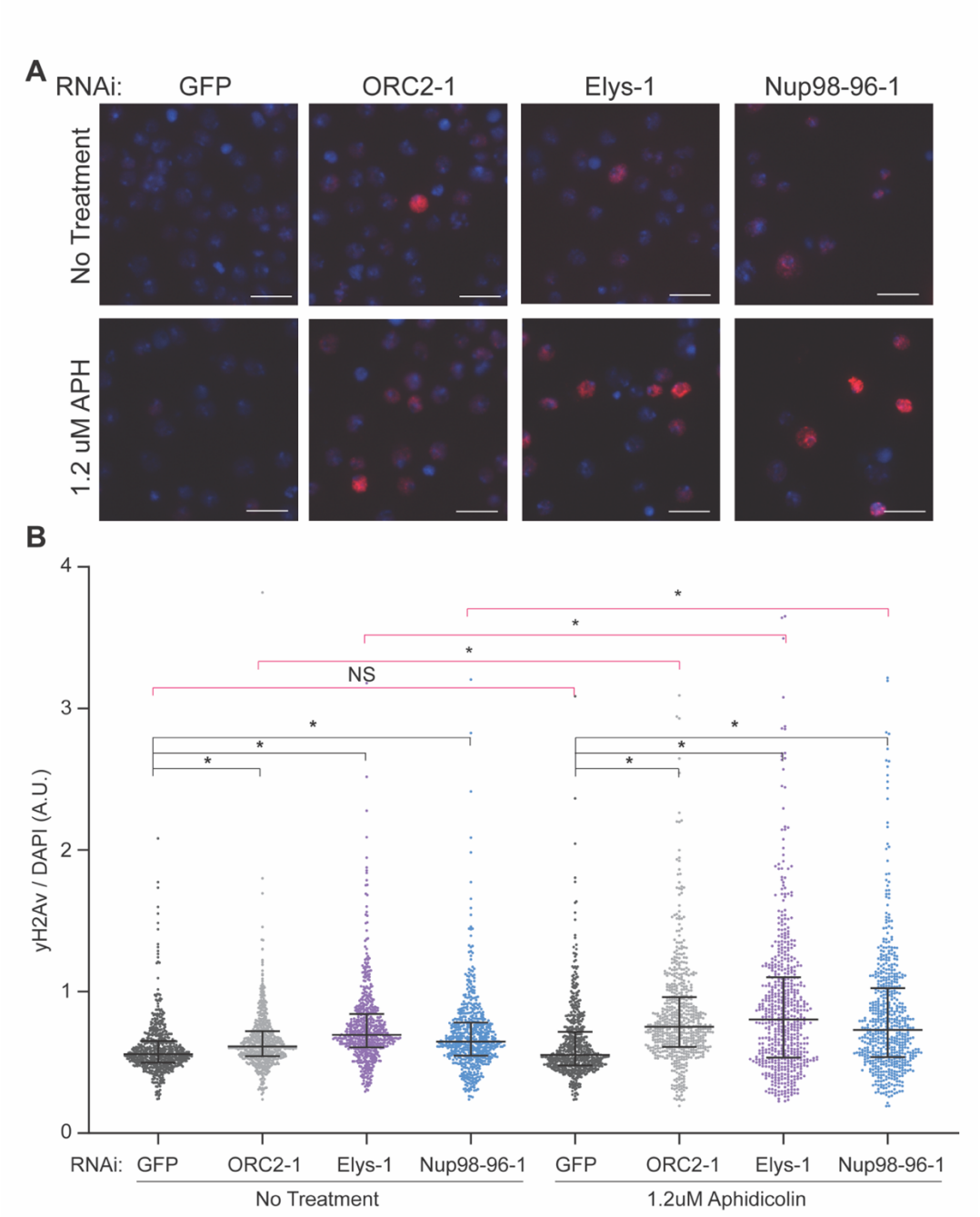

Figure 3.14. ***Nup depletion sensitizes cells to fork stalling.*** (A) Representative images of γH2Av immunofluorescence performed on RNAi-treated cells with or without aphidicolin treatment. Blue: DAPI. Red: γH2Av. Scale bar: 10 uM. (B) Quantification of (A). γH2Av and DAPI intensity for 600 total cells randomly selected from two biological replicates were quantified for each depletion with and without aphidicolin treatment. Black bars compare each depletion to negative control (GFP) and indicate a One-Way ANOVA with a post-hoc Dunnett's test. Pink bars compare untreated cells to aphidicolin treated cells (GFP untreated vs. GFP treated for example) and indicate a parametric T-test. Asterisk denotes $p < 0.0001$. NS: No Significance. Contributions: data and figure generated by Logan Richards.

Discussion

Our results show that ORC interacts with members of the Nup107-160 subcomplex of the nuclear pore, most notably the nucleoporins Elys and Nup98-96, establishing a link between replication inititation and Nups. Elys, Nup98, Nup93, Nup107 and FG-repeat-containing Nups are enriched at ORC2 binding sites and Nups are among the most significantly enriched chromatin factors at ORC2 binding sites. Strikingly, 98% of ORC sites are also Elys binding sites. Not all these sites are localized to the nuclear periphery, suggesting that the association between ORC and Nups are likely occuring off pore. Furthermore, if ORC and NPCs were present in the same protein complex, we would have expected to identify Nup subunits more broadly, rather than just a subset of Nups. Therefore our observations are most consistent with a model where Elys, and possibly other members of the Nup107-160 subcomplex, associate with ORC indpendently of the nuclear pore. This would be consistent with previously-published data where Elys and other Nups perform chromatin-related functions beyond their canonical role in the NPC.

Based on our present findings, we argue that Elys functions to load ORC onto chromatin (Fig. 3.15). Importantly depletion of other Nups, including members of the Nup107-160 subcomplex, do not reduce the amount of ORC on chromatin. This reveals two important points. First, the reduction in chromatin-associated ORC upon Elys depletion is not a generic effect of altered NPC function. Second, out of the Nups tested, the ability to promote ORC loading seems to be specific to Elys. We do not rule out the possibility, however, that other Nups could contribute to ORC loading either independently or together with Elys. Interestingly, Elys and ORC both bind to chromatin in late M phase. It is possible that Elys, or another Nup, directly or indirectly interacts with ORC late in mitosis to facilitate ORC binding on chromatin by providing a molecuar bridge between chromatin remodelling and ORC. While we did not observe a global change in chromatin

accessibilty upon Elys depletion, it is possible that Elys, together with it's known interactor PBAP, could generate a nucleosome free region that would be optimal for ORC binding. If this happens specifically in late M phase, then it would be difficult measure changes in chromatin accessibilty by ATAC-seq from an asychronous population of cells.

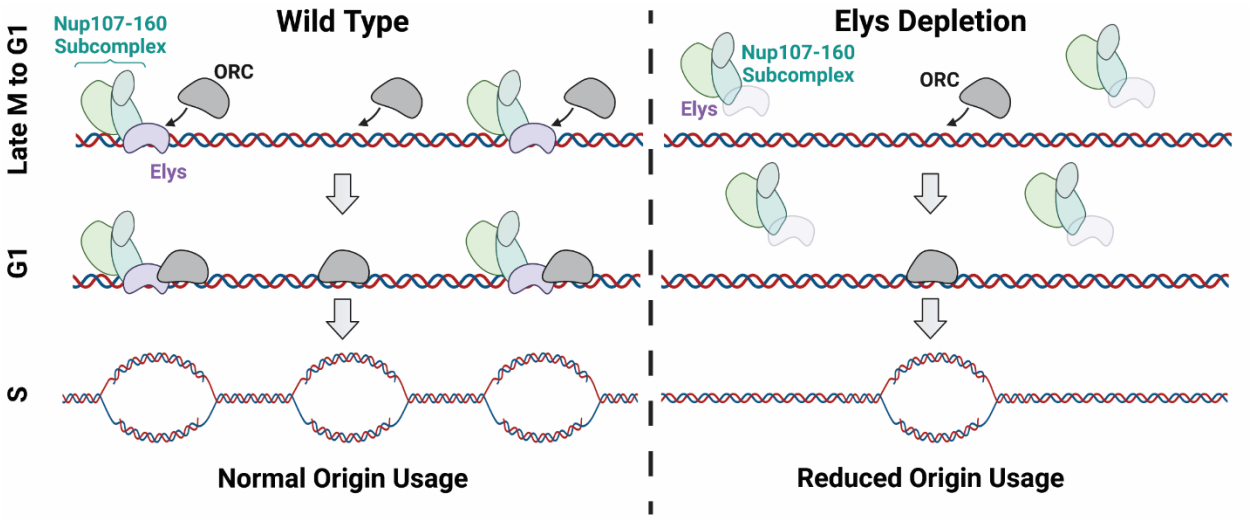

Figure 3.15. ***Nups promotes ORC loading to ensure sufficient origin usage.*** Model depicting the function of the Nup-ORC interaction. In this model, Elys binds to chromatin prior to ORC and facilitates the chromatin association of ORC. If Elys is depleted, less ORC associates with chromatin, causing the overall origin usage to be reduced and increased sensitivity to fork stalling. Contributions: figure made by Logan Richards.

Given that the number and distribution of loaded helicases is necessary to maintain genome stability, depletion of Elys could compromise genome integrity due to a defect in origin licensing. Consistent with this, depletion of Elys shows an increased sensitivity to replication fork stalling. One possible explaination is that upon Elys depletion there is insufficient ORC to promote dormant origin licensing (Fig. 3.15). Alternatively, depletion of nucleoporins could result in fork stalling through mechanisms independent of replication initiation (Kosar et al., 2021). *ORC2* mutants in Drosophila have cell cycle related phenotypes and altered replication timing (Loupart et al., 2000). Given that nuclear organization is coupled to replication timing (Smith and Aladjem, 2014),

depleting Elys may cause changes in replication timing that indirectly influence fork stalling. Interestingly, we observe a similar sensitivity to fork stalling in the Nup98-96 depletion. We predict this occurs through a different mechanism than the Elys depletion; however, as Nup98-86 depletion results in a stark reduction in cells in S phase but does not significantly change ORC levels. Nup98-96 depletion could affect helicase activation, explaining the Nup98-96 depletion phenotypes. Additionally, a failure to fire dormant replication origins would explain the increased sensitivity to fork stalling. Understanding how Nups differentially affect genome duplication and stability is an exciting area of future research.

Limitations of study

While we demonstrated that ORC and Nups associate, bind the same genomic regions, and that depleting Elys is sufficient to reduce the chromatin association of ORC2, there are several unanswered questions. First, it is not clear what the exact direct interactions are between Nups and ORC. While our data suggest that Elys would be a good candidate for subsequent interaction studies, it is unknown if Elys, or any other Nup, directly interacts with ORC or if the interaction is bridged by additional factors. Even if there is a direct interaction between Elys and ORC, it could be regulated by post-translational modifications during the cell cycle. Also, it is still unclear when Nups and ORC associate during the cell cycle. Given both Nups and ORC associate with chromatin starting late in mitosis, this interaction could be confined to a short window within the cell cycle. Our data show that depletion of Elys causes a reduction in ORC binding, which could lead to an increase in inter-origin distance. Due to technical limitations, however, we are unable to measure this directly. Lastly, the mechanism that Elys or other Nups use to promote ORC binding across the genome still remains to be determined. Understanding the molecular interactions between Nups and ORC will be critical to understanding how ORC is recruited to chromatin to ensure faithful DNA replication.

CHAPTER IV

THE CHROMATIN ASSOCIATION OF ORC IS REGULATED THROUGH AN INTERACTION WITH RIF1

Preamble

I began working on the Rif1 project in my first year in the lab. The initial results indicated that Rif1 interacts both with the Nup107-160 subcomplex of the nuclear pore and ORC. Based on this result, I split my thesis into two goals: understanding the interaction between Rif1 and ORC (Chapter IV) and determining if ORC also interacts with the Nup107-160 subcomplex (Chapter III). Though this Rif1-ORC work is still very much in progress, it created the foundation that my thesis stands on and promoted my growth as a scientist, as I adapted several important techniques for the routine use in Dr. Jared Nordman's lab.

Introduction

The faithful duplication of the genome during S phase is essential in maintaining genome stability. Proper regulation of DNA replication is a key aspect in preventing chromosomal aberrations and genetic mutations associated with cancer (Jackson et al., 2014), with the initiation of DNA replication being a focal point in regulation. To begin DNA replication, the Origin Recognition Complex (ORC) binds to sites, termed origins of replication, throughout the genome and determines where DNA replication will initiate (Leonard and Méchali, 2013). ORC, together with other replication factors, loads the MCM2-7 double hexamer in an inactive state during the end of mitosis and through G1 phase (Bell and Labib, 2016; Leonard and Méchali, 2013). To begin S phase and start DNA replication, the N-terminal regions of the loaded helicase subunits,

specifically, MCM2, 4, and 6, are phosphorylated by Dbf4-dependent kinase (DDK) (Bell and Dutta, 2003; Sheu and Stillman, 2006). Upon activation, S phase cycle dependent kinase (S-CDK) targets other replication initiation factors, which are then recruited to the assembling replisome, and DNA replication begins throughout the genome (Douglas et al., 2018; Moyer et al., 2006; Remus and Diffley, 2009; Siddiqui et al., 2013).

Importantly, the process of helicase activation driven by DDK, subsequent replisome assembly, and the initiation of DNA replication, do not occur simultaneously at the start of S phase. Rather helicases are activated throughout the duration of S phase. The timing of helicase activation is directed by the replication timing program, which is defined as the order in which chromosomal segments are replicated during S phase (Rhind and Gilbert, 2013). As DNA replication proceeds, replication factors, such as nucleotides and histones, are at risk of being rapidly depleted (Collart et al., 2013; Mantiero et al., 2011). Replication timing is thought to prevent the exhaustion of these factors by limiting the number of active replication forks during S phase. For example, the replication factors Sld2, Sld3, and Dpb11, as well as Dbf4, are limiting for replication initiation in Xenopus and budding yeast (Collart et al., 2013; Mantiero et al., 2011). If these four factors are overexpressed, origins that normally activate late in S phase activate earlier, decreasing the length of S phase. Additionally, perturbing replication timing in this manner also results in severe growth defects and activation of the checkpoint response (Collart et al., 2013; Mantiero et al., 2011), likely due to increased replication stress and genome instability arising from the depletion of nucleotides or histones. The biological phenomenon of replication timing is conserved across species as it has been observed from budding yeast to flies to humans (Rhind and Gilbert, 2013); however, much remains to be uncovered regarding how replication timing itself is regulated.

How replication timing is biochemically regulated is starting to be understood through the discovery of factors that actively regulate replication timing. One such factor is Rap1 interacting

factor 1 (Rif1) (Mattarocci et al., 2016). The first evidence that Rif1 regulates replication timing arose from initial work in budding yeast, where the genomic regions near telomeres, which replicate late in S phase, were shown to replicate earlier in *rif1*Δ cells (Lian et al., 2011). Rif1's role in regulating replication timing is not restricted to budding yeast as loss of Rif1 activity causes global changes in replication timing in fission yeast, fruit flies, mice and humans (Armstrong et al., 2020; Cornacchia et al., 2012; Hayano et al., 2012; Seller et al., 2018; Yamazaki et al., 2012). The specific mechanism for Rif1-mediated control of replication timing is based on Rif1's binding to PP1 (Mattarocci et al., 2014; Sukackaite et al., 2017). Rif1 together with PP1 is proposed to target loaded helicases within late-replicating regions of the genome, where Rif1-PP1 opposes DDK-mediated phosphorylation of MCMs to delay the initiation of DNA replication. Under this model, regions of the genome targeted by Rif1-PP1 start replication later in S phase, where Rif1 functions a regulator of replication timing. However, how Rif1 is targeted to a subpopulation of helicases to delay their activation, or how Rif1 may alternatively regulate replication timing remains unknown.

Although there is a wealth of genetic evidence connecting Rif1 to MCMs, there is data suggesting Rif1 may regulate DNA replication initiation through alternative mechanisms beyond delaying helicase activation. For example, loss of Rif1 activity suppresses temperature sensitive (ts) alleles of Dpb11, Sld3 and Cdc45 in addition to Cdc7, the catalytic subunit of DDK in budding yeast (Mattarocci et al., 2014). This observation suggests that Rif1 more broadly regulates helicase activation, perhaps beyond just controlling MCM phosphorylation levels. Loss of Rif1 activity also increases the phosphorylation level of Sld3 in G1 phase, possibly impacting the activity of Sld3 (Mattarocci et al., 2014). In addition to Sld3, Cdc45 and Dpb11, Rif1 appears to regulate ORC1 activity (Hiraga et al., 2017), where loss of Rif1 causes hyperphosphorylation of both ORC1 and MCMs in human cells (Hiraga et al., 2017). Furthermore, the level of chromatin-bound ORC1 is reduced upon Rif1 depletion (Hiraga et al., 2017). Interestingly, Rif1 has been proposed to target

ORC1 in G1 phase to promote helicase loading and target MCMs in S phase to prevent helicase activation (Hiraga et al., 2017), thereby promoting helicase loading while preventing excessive helicase activation in distinct phases of the cell cycle. The exact mechanisms of how Rif1 achieves this are still unknown and are critical to understanding how replication timing is regulated.

Here we show that Rif1 associates with all subunits of ORC and the Nup107-160 subcomplex of the nuclear pore. If Rif1 interacts with MCM2-7 to regulate the phosphorylation state of these helicase subunits, we would expect Rif1 to also interact with MCM2-7; however, we find no evidence of this interaction by our methods. We show that Rif1 co-localizes to a subset of ORC2-binding sites across the genome. We also find that Rif1 binds to regions of the genome that replicate early in S phase, suggesting that Rif1 may have functions beyond the regulation of helicase activation. We show that depletion of Rif1 reduces chromatin bound ORC2 and inversely, depletion of ORC2 reduces chromatin bound Rif1, suggestive of co-dependence between Rif1 and ORC2. We propose that Rif1 has a stable interaction with ORC and regulates the activity of ORC, but has a transient interaction with MCMs that we were unable to capture. Thus, our work our work strengthens the link between Rif1 and ORC and shows that Rif1 and ORC interact to possibly promote the chromatin association of ORC in *Drosophila melanogaster*.

Results

Rif1 associates with the Nup107-160 subcomplex and ORC

How Rif1 activity is regulated and the factors that are targeted by Rif1 to regulate the replication timing program remain unclear. Through Drosophila embryogenesis, the replication program is flexible. S phase in the early embryo occurs in 3-4 minutes and slows to approximately 50 minutes at the maternal-to-zygotic transitions (MZT) (Farrell and O'Farrell, 2014). Later in embryogenesis,

S phase is much slower, taking approximately 8 hours (Farrell and O'Farrell, 2014). This change in S phase duration occurring at the MZT correlates with the onset of the replication timing program (Shermoen et al., 2010) and activation of zygotic transcription, occurring at the maternal-to-zygotic transition (MZT). Additionally, the extension of S phase length that occurs at the MZT is dependent on Rif1 (Seller et al., 2018).

To investigate how the activity of Rif1 is regulated, as well as investigate the regulation of replication timing through development, we leveraged the Drosophila embryonic program. To this end, we immunoprecipitated endogenously tagged Rif1-GFP from Drosophila embryo extracts and used mass spectrometry to identify the protein-protein interactions of Rif1. We staged these embryos so we could determine the key interactions of Rif1 where replication timing is absent (Pre-MZT), just after the activation of replication timing and zygotic transcription (Post-MZT), and later in embryogenesis, after cells have differentiated and S phase is much slower (Late Stage). We immunoprecipitated Rif1 and Rif1's binding partner, PP1 (also referred to as PP1-87B), at all stages of development (Fig. 4.1A-B, 4.2A). Additionally, Rif1 interacts with multiple protein phosphatases besides just PP1 through Drosophila embryogenesis (Fig. 4.1A-B, 4.2A), suggesting that Rif1 may interact with other protein phosphatases to perform alternative functions beyond regulating replication timing. From these data, we conclude that the regulation of the interaction between Rif1 and PP1 is not a mode of controlling Rif1 activity and replication timing in early Drosophila embryogenesis.

A

	Pre-MZT			Post-MZT			Late Stage		
	Rif1-GFP	neg. control	P-value	Rif1-GFP	neg. control	P-value	Rif1-GFP	neg. control	P-value
Rif1	895	9	< 0.00010	906	23	< 0.00010	1026	29	< 0.00010
PP1-87B	194	4	< 0.00010	216	4	< 0.00010	319	2	< 0.00010
ORC1	0	0	1	0	0	1	29	0	< 0.00010
Elys	2	0	0.56	0	0	1	131	0	< 0.00010

Table 4.1. Summary of peptide counts for Rif1-GFP IP-MS through development *P-value determined by Fisher's Test

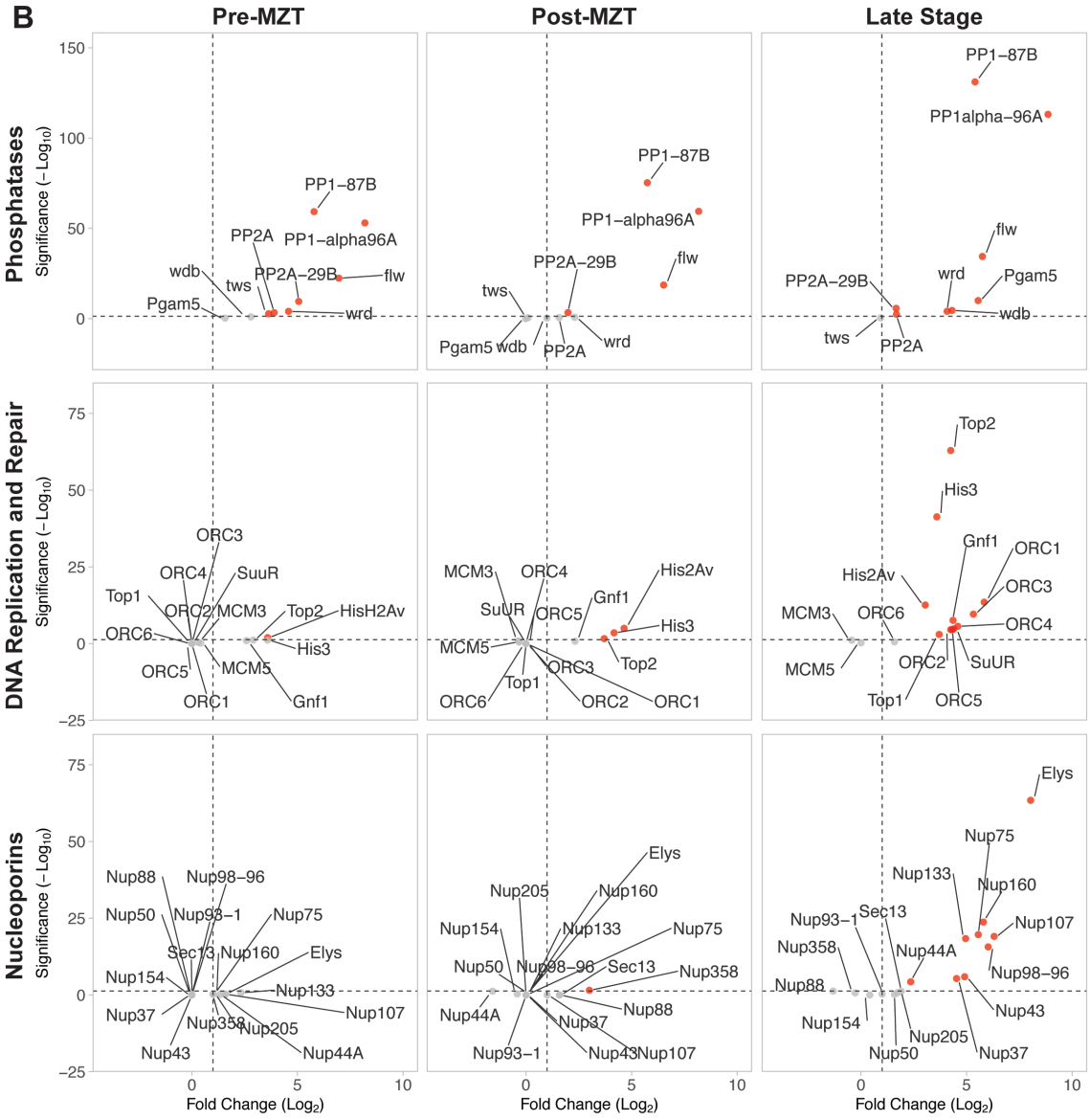

Figure 4.1. ***Rif1 interacts with all subunits of ORC and the Nup107-160 subcomplex of the nuclear pore only late in embryogenesis.*** (A) Table summarizing peptide counts of proteins identified of GFP-Trap IP-mass spectrometry for *Rif1-GFP* expressing embryos relative to neg. (negative) control embryos through embryonic development for a single biological replicate. Embryos were aged 0-2 hours for Pre-MZT, 2-3 hours for Post-MZT, and 18-24 hours for Late Embryogenesis. P-value was calculated by performing a Fisher's Test using peptide counts from 2 biological replicates. (B) Average fold enrichment and statistical significance for two biological replicates of GFP-Trap IP-mass spectrometry for *Rif1-GFP* expressing embryos relative to

negative control embryos through embryogenesis. Highlighted are phosphatases, DNA replication and repair proteins, or nucleoporin proteins identified by mass spectrometry. Proteins depicted in red are above significant level cut-offs (<0.05 for p-value and ≥2-fold enrichment), and proteins in gray are below significant level cut-offs (not statistically enriched). Contributions: immunoprecipitations, data analysis, and data visualization performed by Logan Richards. Mass spectrometry of IP samples performed by the Vanderbilt Mass Spectrometry Core Lab. Raw processing of mass spectrometry data performed by Hayes McDonald.

It is important to note that while Rif1 clearly regulates MCM phosphorylation levels (Alver et al., 2017; Hiraga et al., 2017, 2014; Mattarocci et al., 2014), there is a lack of evidence for a direct biochemical interaction. We are also unable to provide evidence for a physical interaction between Rif1 and MCMs as we do not identify any MCM subunits interacting with Rif1 by our methods. In addition to our findings, there have been several studies that have also performed immunoprecipitation coupled with mass spectrometry for Rif1 to identify Rif1-associated proteins. Similar to our results, the MCM complex was not been identified in these studies (Alver et al., 2017; Sukackaite et al., 2017). Thus, how Rif1 is targeted to, and associates with, loaded helicases remains an open question in the field.

Surprisingly, we identified all six subunits of the ORC complex and all 10 subunits of the Nup107-160 subcomplex of the nuclear pore but only in late-stage embryos (Fig. 4.1A-B, 4.2A). Furthermore, GO analysis of Rif1-associated proteins revealed enrichment of DNA replication initiation (ORC) and mRNA export from the nucleus (nucleoporins), again only in late-stage embryos (Fig. 4.2B). Rif1 has been reported to regulate the activity of ORC in human cells, by promoting MCM loading in G1 phase (Hiraga et al., 2017). As for Rif1's interaction with the Nup107-160 subcomplex, that remains an open question; however, there is a functional link between ORC and the Nup107-160 subcomplex (Richards et al., 2022b). Given Rif1's previously reported connection to ORC, we decided to pursue how Rif1 may control ORC activity and DNA replication initiation. Much of the work on Rif1 has centered on Rif1 delaying helicase activation to delay replication initiation and cause certain regions of the genome to replicate later in S phase.

Based on our initial results, we sought to investigate a possible additional function of Rif1: the regulation of ORC activity.

A

		Rif1-GFP			negative control			Comparison of abundance*		
		Pre-MZT	Post-MZT	Late Stage	Pre-MZT	Post-MZT	Late Stage	Pre vs. Pre	Post vs. Post	Late vs. Late
	Rif1	895	906	1026	9	23	29	< 0.00010	< 0.00010	< 0.00010
Phosphatases	PP1-87B	194	216	319	4	4	2	< 0.00010	< 0.00010	< 0.00010
	PP1α-96A	147	145	232	0	0	0	< 0.00010	< 0.00010	< 0.00010
	flw	63	46	81	0	0	0	< 0.00010	< 0.00010	< 0.00010
	Pgam5	2	0	24	0	0	1	0.56	1	< 0.00010
	PP2A-29B	34	36	58	1	9	18	< 0.00010	0.00044	< 0.00010
	wdb	3	1	10	0	0	0	0.10	0.53	< 0.00010
	wrd	12	3	9	0	0	0	< 0.00010	0.16	< 0.00010
ORC	ORC1	0	0	29	0	0	0	1	1	< 0.00010
	ORC3	1	0	20	0	0	0	1	1	< 0.00010
	ORC4	1	0	12	0	0	0	1	1	< 0.00010
	ORC2	0	0	10	0	0	0	1	1	< 0.00010
	ORC5	0	0	10	0	0	0	1	1	< 0.00010
	ORC6	0	0	2	0	0	0	1	1	0.27
Nup107-160 Subcomplex	Elys	2	0	131	0	0	0	0.56	1	< 0.00010
	Nup98-96	0	0	56	0	0	1	1	1	< 0.00010
	Nup75	1	0	47	0	1	1	0.56	1	< 0.00010
	Nup160	1	1	40	0	0	0	0.56	1	< 0.00010
	Nup133	3	0	47	0	0	2	0.17	1	< 0.00010
	Nup107	2	0	33	0	0	0	0.56	1	< 0.00010
	Nup44A	5	1	15	4	3	1	0.78	0.059	< 0.00010
	Sec13	1	0	12	2	0	0	0.61	1	< 0.00010
	Nup43	0	0	23	0	0	5	1	1	< 0.00010
	Nup37	1	2	8	0	1	2	1	1	0.065
Other Nucleoporins	Nup88	0	2	2	0	1	5	1	1	0.054
	Nup205	1	1	5	0	0	2	0.56	1	0.17
	Nup358	1	4	7	0	0	9	0.56	0.029	0.20
	Nup93	0	1	1	0	0	0	1	1	0.51
	Nup50	0	1	2	0	0	1	1	1	0.64
	Nup154	1	2	4	1	2	3	1	0.44	1
	CG42232	0	1	221	0	0	2	1	0.53	< 0.00010
	BRWD3	0	0	108	0	0	0	1	1	< 0.00010

Table 4.2. Peptide counts of protein complexes identified in Rif1-GFP IP-MS

*P-value determined by Fisher's Test

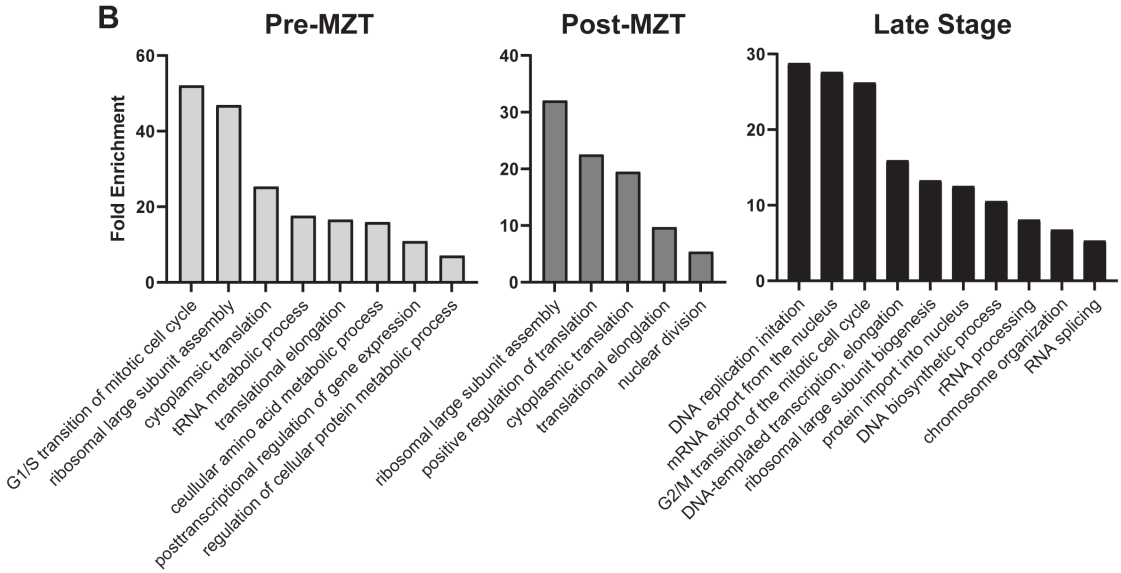

Figure 4.2. ***Rif1-GFP immunoprecipitation enriches for components of the Nup107-160 subcomplex of the nuclear pore, ORC, and phosphatases.*** (A) Table with peptide counts for a single biological replicate of anti-GFP IP mass spectrometry done in either Rif1-GFP or negative control embryos as in Figure 4.1. P-value was calculated by performing a Fisher's Test using data from two biological replicates. (B) Gene ontology analysis of statistically enriched protein in each stage of development. Note the scales are different for each graph. Contributions: same as 4.1. Gene ontology analysis performed by Logan Richards.

Rif1 binds to a subset of ORC2 genomic binding sites

ORC binds across the genome to initiate DNA replication (Bell and Labib, 2016), and Rif1 binds to distinct regions of chromatin in yeast and humans (Hiraga et al., 2018; Klein et al., 2021). We therefore asked if Rif1 and ORC localize to similar sites on chromatin by performing chromatin immunoprecipitations followed by high throughput sequencing (ChIP-seq) using a highly specific antibody for Rif1 in Drosophila S2 cells. Using previously published ChIP-seq data for a subunit of ORC, ORC2, generated in Drosophila S2 cells (Eaton et al., 2011), we visualized the genomic binding profiles of Rif1 and ORC2. The binding sites of Rif1 shows extensive overlap with the binding sites of ORC2 (Fig. 4.3A). We also performed CUT&RUN using an anti-Rif1 or anti-ORC2 antibody and observed the same results (Fig. 4.4A). Quantifying the ChIP-seq signal for Rif1 at ORC2 peaks confirmed that Rif1 ChIP-seq signal is enriched at ORC2 binding sites (Fig. 4.3C). Additionally, we observed a similar enrichment when we quantified ORC2 ChIP-seq signal at Rif1 peaks (Fig. 4.3D). These finding were consistent when we performed CUT&RUN for Rif1 and ORC2 (Fig. 4.4C-D) Furthermore, we found that 48% of ORC2 ChIP-seq peaks are found within Rif1 ChIP-seq peaks (Fig. 4.3B), and 54% of ORC2 CUT&RUN peaks are found within Rif1 CUT&RUN peaks (Fig. 4.4B), again indicating that Rif1 and ORC2 bind to similar genomic regions. Importantly, we found a strong Pearson correlation between ChIP-seq and CUT&RUN Rif1 replicates, showing we were able to consistently identify Rif1 peaks through ChIP-seq or CUT&RUN. We also compared Rif1 peaks identified by these separate methods, and we found a

weaker correlation between Rif1 ChIP-seq and Rif1 CUT&RUN peaks, indicating these methods themselves produce somewhat different Rif1 binding profiles (Fig. 4.5B). From these data generated from these two distinct methods, we conclude that Rif1 and ORC2 co-localize across the genome.

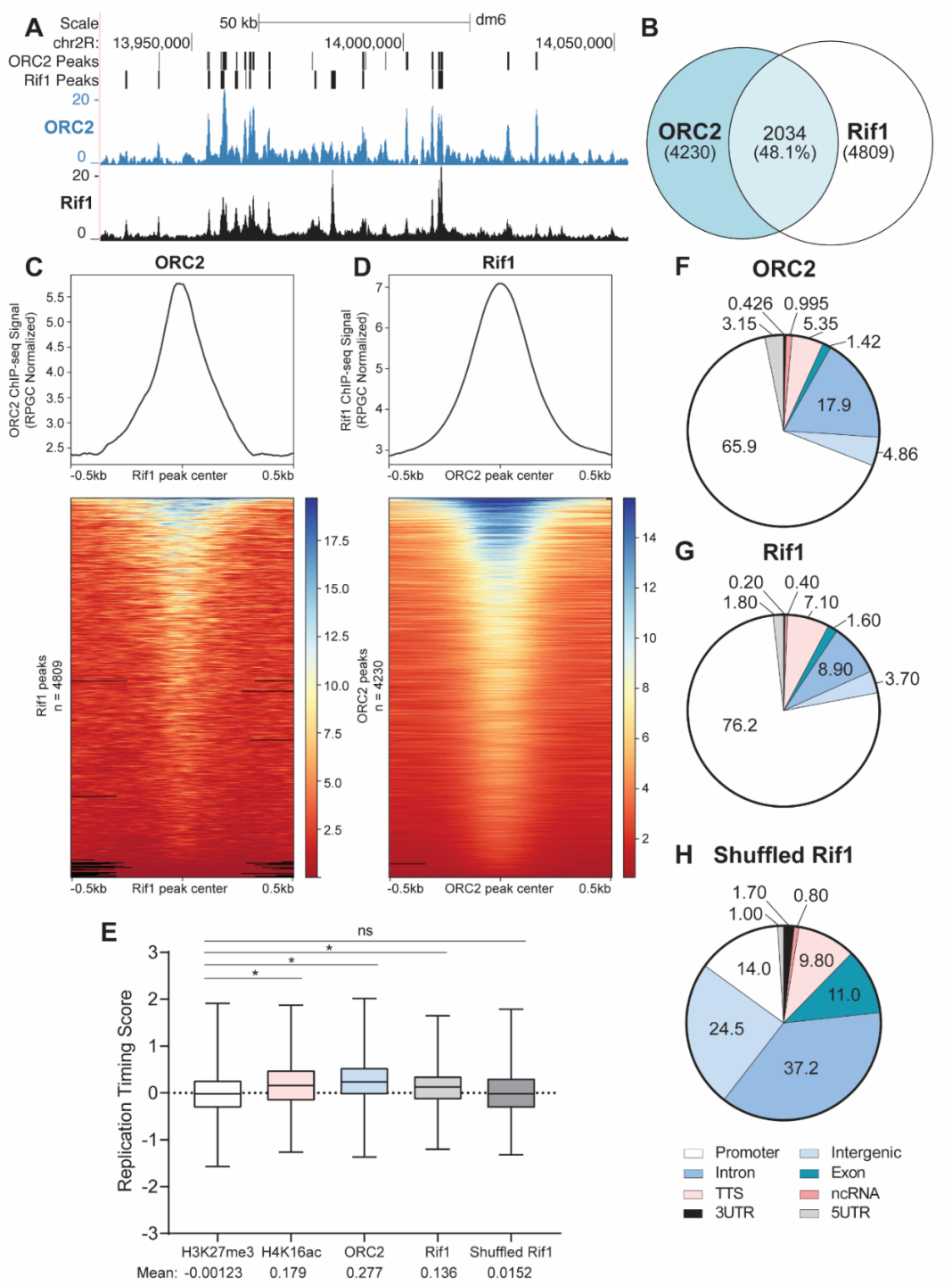

Figure 4.3. ***Rif1 and ORC2 bind similar genomic regions.*** (A) Representative UCSC genome browser view of Rif1 and ORC2 ChIP-seq signal. ORC2 ChIP-seq signal and peaks generated from previously published data (Eaton et al., 2011). (B) Venn diagram visualizing peak overlap between ORC2 (blue) and Rif1 (white). Number in parenthesis is the total number of peaks. Number in intersection is the number of ORC2 peaks that overlapped with Rif1 peaks (2034 out of 4230). (C-D) Enrichment heatmap of ORC2 (C) or Rif1 (D) ChIP-seq signals sorted by mean occupancy around the center of Rif1 (C) or ORC2 (D) peaks. (E) 2000 randomly selected replication timing scores found within H3K27me3, H416ac, ORC2, Rif1, or Shuffled Rif1 ChIP-seq peaks. Box plots show medians and interquartile range. Asterisk denotes statistical significance determined by One-Way ANOVA with post-hoc Dunnett's Test. NS: no significance. (F-H) Gene ontology analysis for either ORC2 (F), Rif1 (G), or shuffled Rif1 (H) peaks. Numbers in pie chart correspond to the percent of peaks found in each genomic classification. Contributions: Rif1-ChIP seq, data analysis, and visualization done by Logan Richards. H3K27me3 and H4K16ac ChIP-seq peaks generated by the modENCODE consortium and analyzed by Logan Richards. ORC2 ChIP-seq and Drosophila S2 cell replication timing data previously published by Eaton et al., 2011 and analyzed by Logan Richards.

To further investigate the characteristics of Rif1 genomic binding sites and their similarities to the binding sites of ORC2, we performed motif analysis of Rif1 ChIP-seq or CUT&RUN peaks, which revealed that the sequence motifs found were similar to sequence motifs that transcription factors bind to at promoters in the Drosophila genome (Fig. 4.5A). We also performed an annotation of Rif1 peaks, ORC2 peaks, or shuffled Rif1 peaks, which served as our control to determine the annotation of a randomized set of peaks for both ChIP-seq and CUT&RUN. As expected, the ORC2 peaks are enriched at promoter regions of the genome, consistent with previously published data (Eaton et al., 2011) (Fig 4.3F-H, Fig. 4.4F-H). Rif1 peaks show a stark enrichment at promoter regions, with 76% of ChIP-seq Rif1 peaks and 53% of CUT&RUN Rif1 peaks, falling within promoters. We therefore conclude that Rif1 binding sites have promoter characteristics similar to ORC2.

Rif1 binding sites are in early-replicating regions of the genome

Rif1 is expected to localize to heterochromatin to delay helicase activation within those regions (Alver et al., 2017; Hiraga et al., 2017, 2014), therefore, Rif1 binding sites should predominantly localize to late-replicating regions of the genome. To see if this is the case, we determined the replication timing scores in H3K27me3 (heterochromatic), H416ac (euchromatic), ORC2, Rif1, or shuffled Rif1 ChIP-seq peaks, serving as our negative control. By this quantification, positive values correlate to genomic regions replicating in the first half of S phase, with higher values replicating earlier. Inversely, negative values indicate genomic regions that replicate in the second half of S phase, with more negative values replicating later. We found that Rif1 peaks had a replication timing score similar to H416ac, found at euchromatic early-replicating regions of the genome (Allis and Jenuwein, 2016; Rhind and Gilbert, 2013), and was significantly higher than to H3K27me3, associated with late-replicating heterochromatin (Allis and Jenuwein, 2016; Rhind and Gilbert, 2013) (Fig 4.3E). Rif1 CUT&RUN peaks were also found within earlier replicating regions of the genome, with a positive replication timing score (Fig. 4.4E). These observations are consistent with our previous data, as promoter regions tend to fall within early-replicating euchromatic regions of the genome (Allis and Jenuwein, 2016; Hiratani et al., 2009; Rhind and Gilbert, 2013). Previous work has demonstrated that Rif1 associates with the coding regions of highly transcribed regions, which tend to replicate early in S phase, in budding yeast (Hiraga et al., 2018), but Rif1 primarily associates with late-replicating regions in mouse embryonic stem cells (Alver et al., 2017; Hiraga et al., 2017, 2014). Drosophila Rif1 may also have a distinct genomic binding profile, and with our present data, we conclude that Rif1 binds to primarily promoters and early-replicating regions of the genome. We; however, do not discount the possibility that we were unable to capture Rif1 associating with heterochromatic regions by ChIP-seq or CUT&RUN.

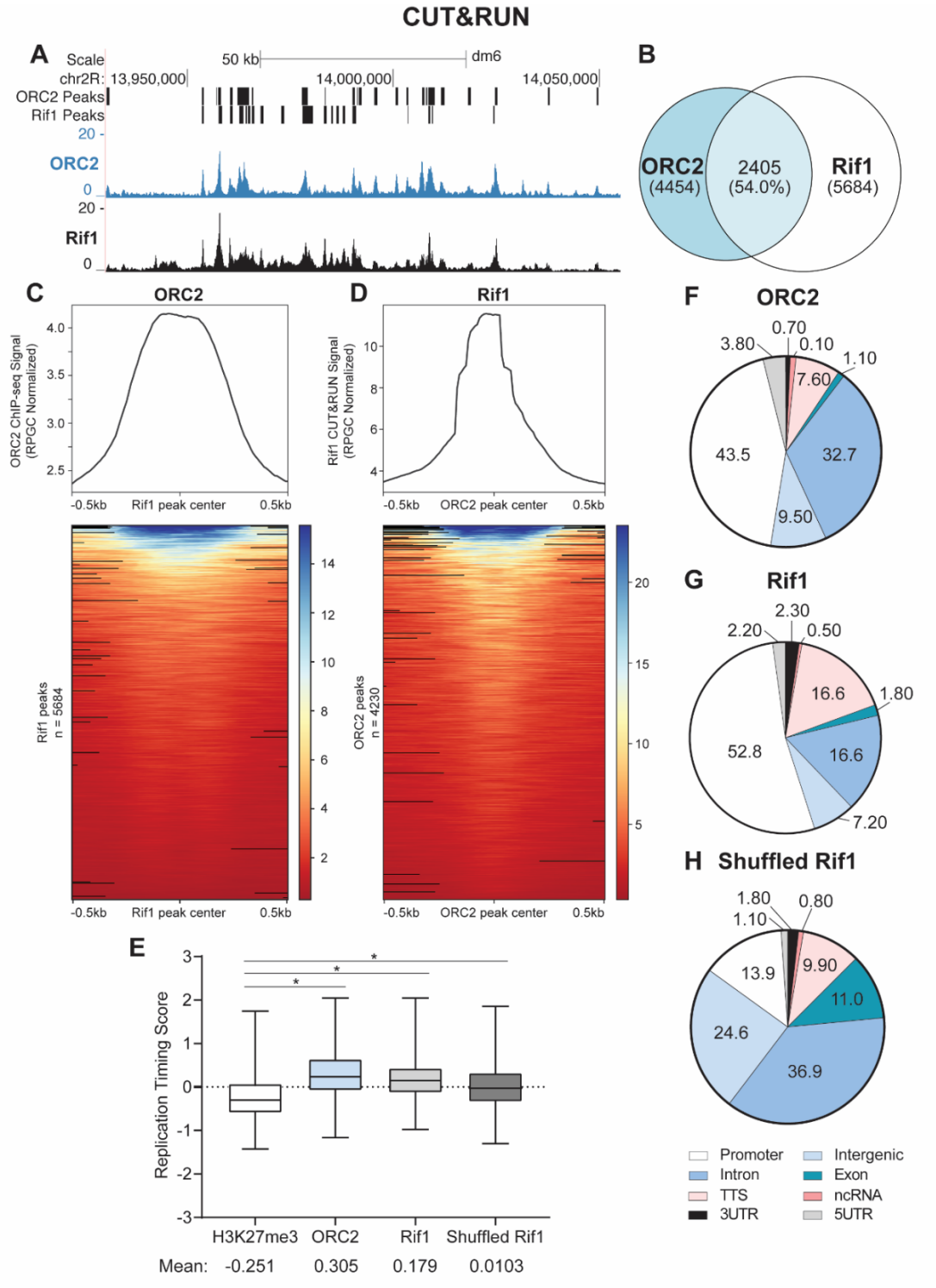

Figure 4.4. ***Rif1 and ORC2 bind similar genomic regions also by CUT&RUN.*** (A) Representative UCSC genome browser view of Rif1 and ORC2 CUT&RUN signal. (B) Venn diagram visualizing CUT&RUN peak overlap between ORC2 (blue) and Rif1 (white). Number in parenthesis is the total number of peaks. Number in intersection is the number of ORC2 peaks

that overlapped with Rif1 peaks (2405 out of 4454). (C-D) Enrichment heatmap of ORC2 (C) or Rif1 (D) CUT&RUN signals sorted by mean occupancy around the center of Rif1 (C) or ORC2 (D) peaks. (E) Replication timing scores (Eaton et al., 2011) in H3K27me3, ORC2, Rif1, or Shuffled Rif1 CUT&RUN peaks. 2000 randomly selected regions were used for quantification. Asterisk denotes statistical significance determined by One-Way ANOVA with post-hoc Dunnett's Test. Box plot shows median and interquartile range. (F-H) Gene ontology analysis for either ORC2 (F), Rif1 (G), or shuffled Rif1 (H) CUT&RUN peaks. Numbers in pie chart correspond to the percent of peaks found in each genomic classification. All data shown was generated using Drosophila S2 cells. Contributions: Rif1, ORC2, H3K27me3 CUT&RUN, data analysis, and visualization done by Logan Richards. Protocol provided by Kami Ahmad. Drosophila S2 cell replication timing data previously published by Eaton et al., 2011 and analyzed by Logan Richards.

A

Motif	Name	P-value	% of Peaks with Motif	% of Background with Motif
	Unknown 1 (NR/Ini-like)	1e-339	15.43	2.47
	M1BP(Zf)/S2R+-M1BP-ChIP-seq (GSE49842)	1e-309	15.06	2.61
	E-box	1e-247	14.33	3.00
	Unknown 2	1e-225	19.63	5.98
	DREF	1e-191	11.75	2.58
	Unknown 3	1e-113	6.67	1.38
	Unknown 4	1e-70	7.78	2.68
	Unknown 5	1e-64	16.76	8.98
	Unknown 6	1e-26	25.97	19.59
	Trl(Zf)/S2-GAGAfactor-ChIP-Seq(GSE40645)	1e-9	16.97	13.76

Table 4.3. Sequence motifs in Rif1 genomic binding sites

B

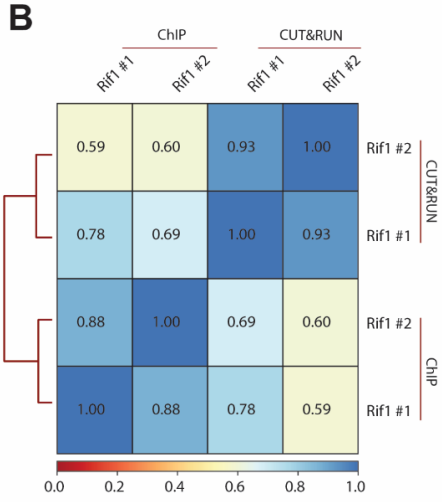

Figure 4.5. ***Rif1 peaks have promoter motifs.*** (A) Motif analysis of Rif1 ChIP-seq peaks. P-values below 1e-10 are considered significant in this analysis. Percent of Rif1 peaks vs. percent of random peaks (background) containing each motif is also shown. (B) Pearson correlation between ChIP or CUT&RUN biological replicates. Number shown is correlation value. Contributions: data analyzed and visualized by Logan Richards.

Rif1 may contribute to cell cycle progression

To investigate the functional relationship between Rif1 and ORC in Drosophila, we set out to reduce steady state protein levels of Rif1 or ORC2 by performing RNA interference in Drosophila S2 cells. After, we validating our RNAi treatments by western blot (Fig. 4.6), we determined the

effects of depleting ORC2 or Rif1 on the cell cycle. We found that there is an increase in cells in early S phase and a reduction of cells in late S phase in Rif1 depleted cells (Fig. 4.7A, 4.7C). Additionally, the fraction of cells in G1 was reduced while the fraction of cells in G2/M was increased in Rif1 depleted cells (Fig. 4.7B). Taken together, we conclude that in the Rif1-depleted cells, progression through S phase is perturbed, consistent with the model that Rif1 is the key regulator in replication timing, and Rif1 may contribute to cell cycle progression.

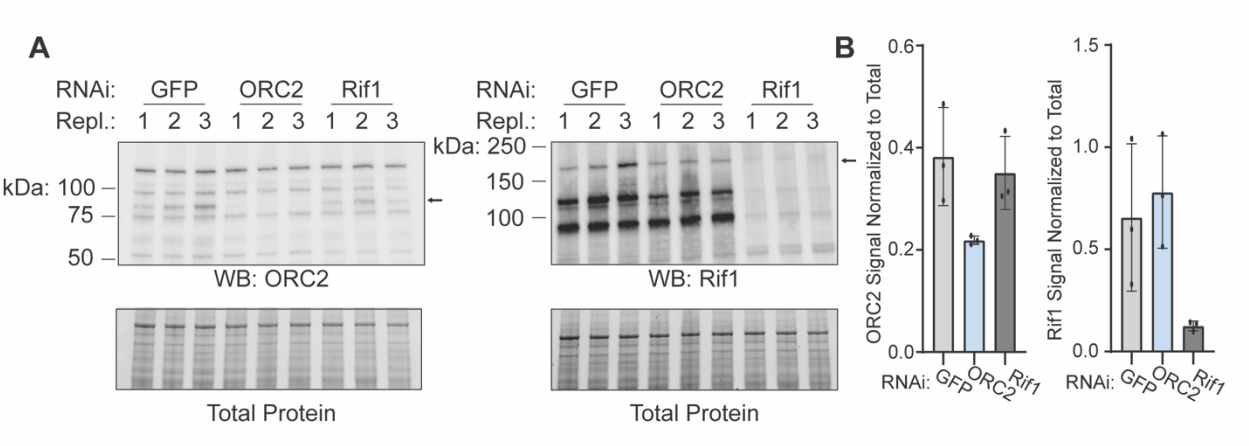

Figure 4.6. ***Validation of RNA interference against Rif1 and ORC2.*** (A) (Left) Western blot using anti-ORC2 antibody on samples prepared from cells treated with the indicated RNAi. Arrow indicates ORC2 band. (Right) Western blot using anti-Rif1 antibody on same samples as anti-ORC2 Western blot. Protein gel showing total protein present in each sample. Arrows denotes ORC2 or Rif1 band. (B) Quantification of (A). For both graphs, western blot signal for GFP (light gray), ORC2 (blue), or Rif1 (dark gray) is normalized to total protein for each depletion. Error bars denote standard deviation. Contributions: data and figure generated by Logan Richards.

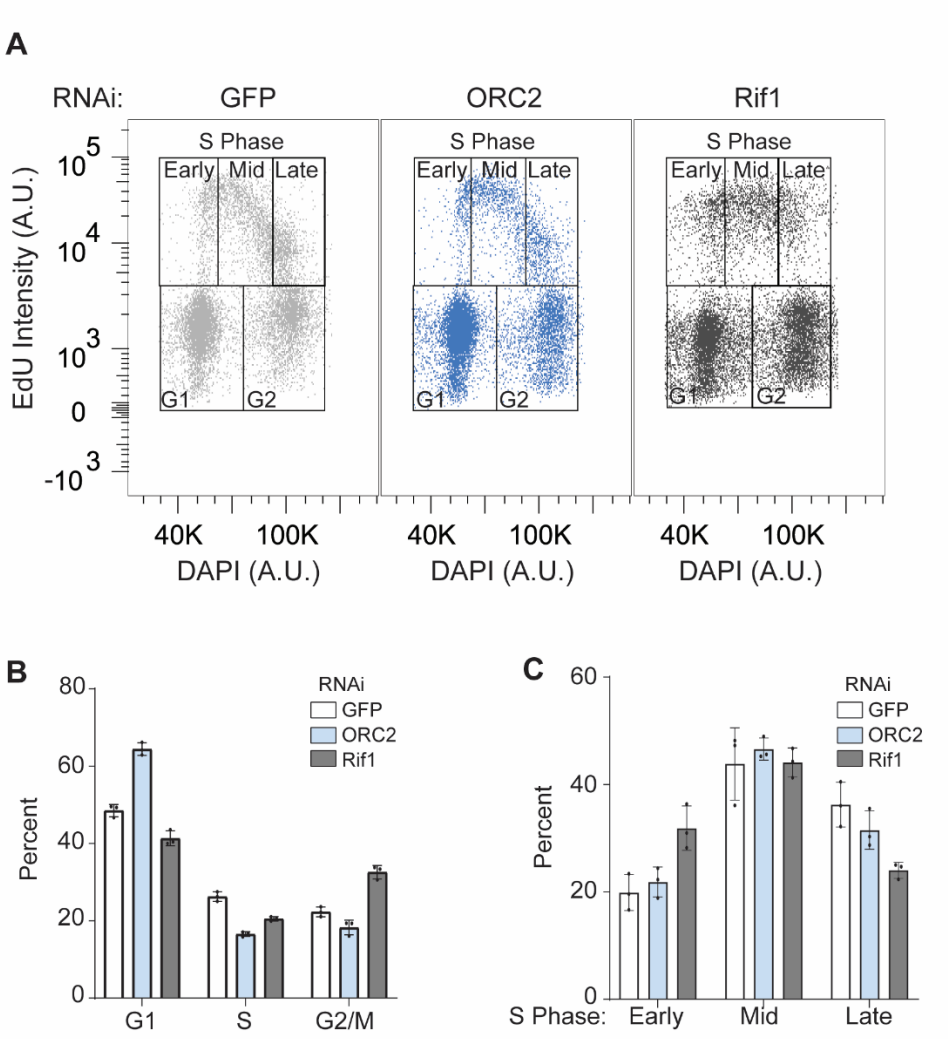

Figure 4.7. ***Depleting Rif1 perturbs progression through S phase.*** (A) Horseshoe plot with DNA content (DAPI) plotted against EdU intensity for each depletion for one biological replicate. Black boxes indicate cell populations selected for quantification in (B) and (C). S phase was divided into three bins, early, mid, and late. (B) Quantification of fraction of cells in each cell cycle phase relative to the total number of cells for three biological replicates for each depletion. (C) Quantification of the fraction of cells in each S phase bin relative to total number of cells in S phase for three biological replicates for each depletion. Contributions: data and figure generated by Logan Richards.

Rif1 and ORC2 are dependent on each other for chromatin association

Dephosphorylation of replication factors has recently been observed as an actively regulated process critical for proper helicase activation in budding yeast (Jenkinson et al., 2023). Specifically, Sld2 and Sld3 are phosphorylated during helicase activation but do not associate in the completed replisome (Jenkinson et al., 2023). During helicase activation occurring through S phase, Sld2 and Sld3 are proposed to be recycled via dephosphorylation so they may be used for helicase activation at other origins. Considering that the DNA binding of ORC in Drosophila is inhibited by phosphorylation (Remus et al., 2005) and this recent work, we hypothesized that Rif1-PP1 may regulate the DNA binding of ORC by reversing CDK-mediated phosphorylation in an actively regulated manner. To begin to investigate this, we quantified the chromatin associated ORC2 in ORC2, Rif1 or GFP depleted cells, focusing on the G1 population. G1 was selected, because this is the cell cycle phase where ORC is loaded onto chromatin, therefore any changes should be most apparent in this cell cycle stage. Relative to the GFP negative control, there is less chromatin associated ORC2 in the ORC2 depletion, as expected. Interestingly, there is also less chromatin associated ORC2 in the Rif1 depletion in both G1 and G2/M. (Fig. 4.9A-B). Importantly, we also performed FACS analysis for H2B as a control in cells treated with ORC2, Rif1, or GFP RNAi, and we observed no changed in chromatin associated H2B as expected (Fig. 4.8). From these results, we conclude that depleting Rif1 is sufficient to reduce chromatin associated ORC2.

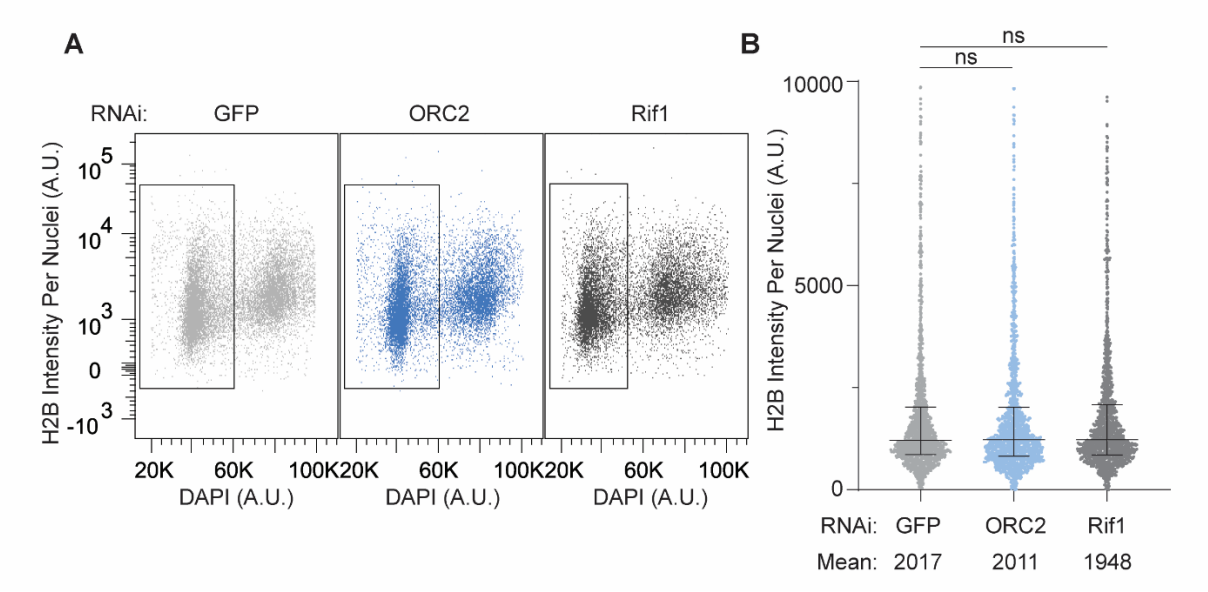

Figure 4.8. ***H2B chromatin association is not reduced in Rif1 or ORC2 depletions.*** (A) Horseshoe plot with DNA content (DAPI) plotted against H2B intensity for each depletion for one biological replicate. Black box indicates G1 population of nuclei used for the quantification in (B). A.U.: arbitrary units. (B) Quantification of H2B intensity in 1500 randomly selected G1 nuclei from three biological replicates. Shown is the median and interquartile range. NS: no statistical significance determined by One-Way ANOVA with post-hoc Dunnett's Test. Contributions: data and figure generated by Logan Richards.

If Rif1 and ORC physically interact as suggested by our IP-MS results, the chromatin association of Rif1 may also depend on ORC. In this manner, Rif1-PP1 could potentially promote the chromatin association of ORC thereby promoting the chromatin association of Rif1 itself. To begin to test this, we performed the inverse experiment where we depleted ORC2 and quantified the amount of chromatin bound Rif1. The reduction in chromatin bound Rif1 we observe, although statistically significant, was not as drastic as the reduction of ORC2 in the Rif1 depletion (Fig 4.9C-D), within the G1 population of nuclei. Specifically, the Rif1 and ORC2 depletion had similar reductions in chromatin bound ORC2, in contrast to the reduction in Rif1 in the same depletions (Fig. 4.9B, 4.9D). The dependence of Rif1 on ORC2 is more obvious by immunofluorescence using an anti-Rif1 antibody in GFP, ORC2, or Rif1 depleted cells, as we see a clear decrease in nuclear Rif1 in the ORC depletion (Fig 4.9E). While performing these experiments, we observed

that the Rif1 signal appeared to be reduced more in the G2/M rather than G1 population of nuclei, using DAPI signal to determine the cell cycle phase. Interestingly, quantification of the Rif1 signal in the G2/M population confirmed this (Fig 4.9D). This pattern of signal reduction in G2/M is specific to Rif1, as the ORC2 signal is reduced in similar magnitudes across in both G1 and G2/M (Fig. 4.9C). This suggests that Rif1 is sensitized to loss of ORC2 preferentially in G2/M, indicating a function of the Rif1-ORC interaction within this cell cycle phase. From these data, we conclude that Rif1 and ORC2 are partially co-dependent on each other for chromatin association, with ORC2 binding diminished in the absence of Rif1 in both G1 and G2/M and Rif1 binding more diminished only in G2/M.

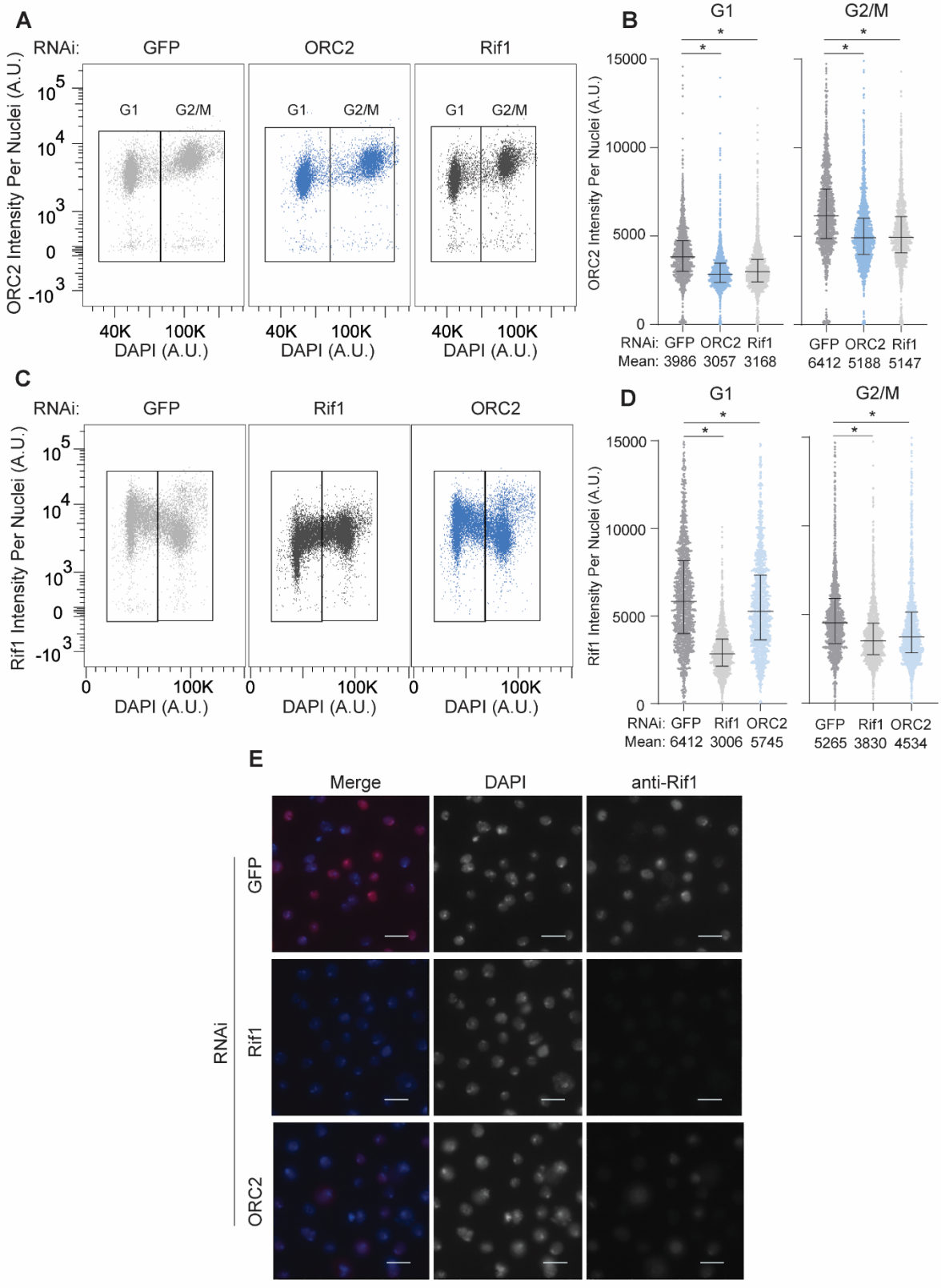
A
RNAi:
GFP
ORC2
Rif1
G1
G2/M
ORC2 Intensity Per Nuclei (A.U.)
DAPI (A.U.)
B
G1
G2/M
ORC2 Intensity Per Nuclei (A.U.)
RNAi: GFP ORC2 Rif1
Mean: 3986 3057 3168
GFP ORC2 Rif1
6412 5188 5147
C
RNAi:
GFP
Rif1
ORC2
Rif1 Intensity Per Nuclei (A.U.)
DAPI (A.U.)
D
G1
G2/M
Rif1 Intensity Per Nuclei (A.U.)
RNAi: GFP Rif1 ORC2
Mean: 6412 3006 5745
GFP Rif1 ORC2
5265 3830 4534
E
Merge
DAPI
anti-Rif1
RNAi
GFP
Rif1
ORC2

Figure 4.9. ***Depleting Rif1 reduces chromatin associated ORC2.*** (A) Horseshoe plot with DNA content (DAPI) plotted against ORC2 intensity for each depletion for one biological replicate. Black box indicates G1 or G2/M population of nuclei used for the quantification in (B). A.U.: arbitrary units. (B) Quantification of ORC2 intensity in 1500 randomly selected G1 or G2/M nuclei from three biological replicates. Shown is the median and interquartile range. Asterisk indicates $p<0.0001$ relative to the negative control determined by one-way ANOVA with post-hoc Dunnett's test. (C) Same as (A) for Rif1 intensity. (D) Quantification of (C). (E) Representative images of immunofluorescence with anti-Rif1 antibody performed in cells depleted for GFP, Rif1, or ORC2. In the merged images, blue corresponds to DAPI signal and red corresponds to Rif1 signal. Scale bar = 10 μM. Contributions: data and figure generated by Logan Richards.

Discussion

Our results show that Rif1 interacts with ORC and members of the Nup107-160 subcomplex of the nuclear pore, but only late in embryogenesis, establishing a connection between Rif1 and ORC in *Drosophila melanogaster* and providing further evidence for the connection between nucleoporins and DNA replication initiation. Furthermore, Rif1 interacts with its binding partner PP1 through the course of embryonic development. This indicates that the Rif1-PP1 interaction is not developmental regulated, which is consistent with previous published findings (Seller et al., 2018). We also do not enrich for MCM2-7 subunits of the replicative helicase, which is unexpected considering the prevailing model for Rif1 activity, but consistent with other published datasets of IP-MS of Rif1 (Alver et al., 2017; Sukackaite et al., 2017). Rif1 is highly enriched at ORC2 genomic binding sites and ORC2 is also enriched at Rif1 genomic binding sites. We find that approximately 50% of ORC2 genomic binding sites overlap with Rif1 genomic binding sites, and that Rif1 genomic binding sites have characteristics of euchromatic regions, falling within early-replicating and promoter regions of the genome. We show that depleting Rif1 is sufficient to reduce the chromatin association of ORC2 in both G1 and G2/M. We also show that depletion of ORC2 reduces the ability of Rif1 to associate with chromatin in G1 and more strongly in G2/M. Though our data is consistent with others in the field, the exception being the genomic binding profile of Rif1 we observe, the question of how Rif1 regulates replication timing is still unanswered.

The regulation of Drosophila melanogaster ORC (DmORC) activity is not well characterized, but previous work has established that ORC1 and ORC2 are phosphorylated in vivo and are targeted by CDK (Remus et al., 2005). Furthermore, CDK hyperphosphorylation of DmORC inhibits the ATP hydroylsis and DNA binding ability of DmORC (Remus et al., 2005). These effects are also reversable if phosphorylation is inhibited in vitro (Remus et al., 2005). The likely purpose of inhibiting either the activity or DNA binding is to prevent re-replication of the genome, by ensuring that each ORC binding site loads helicase only once during the cell cycle. In metazoans, how ORC is dephosphorylated after S phase is complete, to potentially reset for the next cell cycle is not well characterized. Furthermore, it is also unknown if ORC phosphorylation is opposed through S phase by phosphatases, in a similar manner that Rif1-PP1 oppose the DDK-mediated phosphorylation of MCM2-7. Rif1 could be targeted to ORC to oppose phosphorylation by CDKs early in S phase, to maintain ORC in active state, and ensure that certain genomic regions load helicases more efficiently than others. Our data has shown that Rif1 and ORC2 bind similar genomic regions across the genome in early-replicating regions and association of Rif1 with chromatin is dependent on ORC, which is consistent with the model that Rif1 is recruited to chromatin-bound ORC to promote helicase loading in early-replicating regions. Understanding the interplay between ORC phosphorylation and Rif1 will be essential in understanding the function of the Rif1-ORC interaction, which is currently beyond the scope of this work.

Previous work has shown that depleting Rif1 in human cells reduces chromatin associated levels of ORC1; however, there was little effect on ORC2 levels (Hiraga et al., 2017). The proposed model for this effect is that Rif1 maintains ORC1 in a dephosphorylated state and prevents ORC1 from being targeted for proteolytic degradation (Hiraga et al., 2017). Rif1 could have a similar role in maintaining ORC2 levels in Drosophila. The exact mechanisms that regulate ORC protein levels or ORC activity in Drosophila cells, remains unclear but there could be shared features

consistent with budding yeast as well as metazoans. From our data, we cannot distinguish between these possibilities; however, we do not observe a dramatic decrease in ORC2 protein levels in Rif1-depleted cells relative to the GFP negative control (Fig. 4.6). Therefore, we favor a model where Rif1 promotes the chromatin association of ORC; however, additional work is needed to determine if the steady-state levels of other ORC subunits depend on Rif1.

Interestingly, the chromatin assocation of ORC is also dependent on Rif1. Therefore, we argue that Rif1 and ORC work together to form a functional feedback loop to promote ORC activity in early-replicating genomic regions. In addition to promoting the activity of ORC on chromatin, Rif1 may also reverse the CDK-mediated phosphorylation of ORC off chromatin to promote the DNA binding ability of ORC. This hypothesis is also consistent with our data as we observe less ORC2 bound to chromatin in the Rif1 depletion. This model assumes that the activity of Rif1 is cell cycle regulated, which we also hypothsize. In order to intergrate our findings with the findings in the field, we propose that Rif1 has a distinct function in G1 phase where it regulates the activity of ORC and in S phase regulates the activity of helicase activation. Rather than cell cycle regulation, this could also be achieved by dividing Rif1 into two populations, Rif1 at early-replicating regions of the genome promoting ORC activity and Rif1 at late-replicating regions delaying helicase activity. Investigating the mechanisms that direct Rif1 either through the cell cycle or differentially through the genome is an exciting area of research and likely to be the focus of future work.

Limitations of Study

We have shown that Rif1 associates with ORC and that Rif1 and ORC2 have similar genomic binding profiles. We have also shown that Rif1 and ORC2 are co-dependent on each other for chromatin association; however, several outstanding questions remain. First, the function of the Rif1-ORC interaction remains elusive. While the data in the field suggests that Rif1 may protect ORC1 from degradation, we do not know if that is the function of this interaction in Drosophila. Alternatively, Rif1 could be promoting the chromatin association of ORC directly, and additional work is needed to test these possibilities. Also, our data suggests that MCM loading, a readout for ORC activity, should be reduced in a Rif1 depletion, as there is a reduction in chromatin bound ORC; however, we are unable to address this currently due to technical limitations. Furthermore, Rif1 is dependent on ORC for chromatin association, but the reason for this remains unclear. Lastly, the molecular mechanism of how Rif1 interacts with ORC is still unknown, and while we predict there to be a direct interaction between Rif1 and ORC, this interaction could be bridged by an unknown factor. Addressing these questions centered around the dynamics between Rif1 and ORC will be crucial to understanding the activity of Rif1 and replication timing.

CHAPTER V

DISCUSSION AND FUTURE DIRECTIONS

Summary of dissertation work

Failure to accurately duplicate the genome can lead to developmental disease and lead to genomic instability that drives the formation of cancer. Therefore, the study of DNA replication and its regulation is imperative to understanding how genome stability is maintained.

ORC loading is a critical step in the initiation of DNA replication and properly loading enough ORC across the genome is essential to mitigate against replication stress. Excessive ORC is loaded onto origins of replication, many of which are inactivate, or dormant, until the need arises. Dormant origins are activated in response to replication stress from internal or external sources that stalls replication forks, potentially resulting in fork collapse and double-stranded breaks in DNA. Nups appear to facilitate the loading of ORC onto chromatin, as several Nups interact with ORC2 and bind to the same the genomic regions as ORC2. Elys is a mediator of NPC assembly and also binds to chromatin to influence chromatin compaction and gene expression. We therefore hypothesized that Elys facilitates the chromatin association of ORC as Elys does with other Nups. Consistent with this hypothesis, we observe less chromatin bound ORC2 in Drosophila S2 cells if Elys is depleted. The predicted outcome of loading insufficient ORC onto chromatin is increased DNA damage caused by reduced origin usage and failure to rescue stalled forks by dormant origin activation. If Elys is depleted, thereby reducing the amount of ORC loaded onto chromatin, we do indeed observe an increase in DNA damage. Our findings indicate that Elys facilitates the loading of ORC onto chromatin (Fig. 5.1, also see Chapter III), but the molecular mechanism through which this occurs remains to be discovered.

The controlled activation of loaded helicases through S phase is also a critical aspect in the overall regulation of DNA replication initiation to avoid the rapid depletion of nucleotides and histones during DNA synthesis. Helicase activation and the initiation of DNA replication that occurs through the duration of S phase is dictated by the replication timing program. Rif1 is an active regulator of the replication timing program and is proposed to function by targeting PP1 to loaded helicases within late-replicating regions of the genome to oppose DDK-mediated phosphorylation of helicase subunits. By opposing DDK at a subpopulation of helicases, Rif1 delays the activation of those helicases and delays the initiation of DNA replication, thus regulating replication timing. The activity of Rif1 is developmentally regulated in Drosophila, therefore, we used this as a tool to interrogate the interactors of Rif1 that may influence Rif1 activity.

Surprisingly we found a robust interaction between Rif1 and all six subunits of ORC as well as all 10 subunits of the Nup107-160 subcomplex of the NPC, indicating Rif1 likely binds to these assembled complexes rather than individual subunits. Interestingly, we observed these interactions only late in Drosophila embryogenesis. Rif1 associates with multiple protein phosphatases over the course of development. This suggests that the Rif1-PP1 interaction itself is not a mode of regulating Rif1 activity and suggests the possibility that Rif1 may interacts with different protein phosphatases to perform different biological functions. We expected to observe interactions between Rif1 and MCM subunits of the helicase, given the observations in the field, but failed capture this. However, our failure to capture Rif1 interacting with MCMs is consistent with other attempts in the field, and there still remains a lack of direct evidence that supports a physical interaction between Rif1 and MCMs. We found that Rif1 and ORC2 bind similar genomic regions, with approximately 50% of ORC2 genomic binding sites also containing Rif1. Depletion of Rif1 is also sufficient to reduce the amount of chromatin bound ORC2, and inversely, depletion of ORC2 reduces the amount of chromatin bound Rif1. Given the interaction between Rif1 and

ORC, the genomic co-localization, and ORC2 being dependent on Rif1 for chromatin association (see Chapter IV), we propose that Rif1-PP1 targets ORC to promote the DNA binding of ORC (Fig. 5.1), likely regulated by phosphorylation in Drosophila.

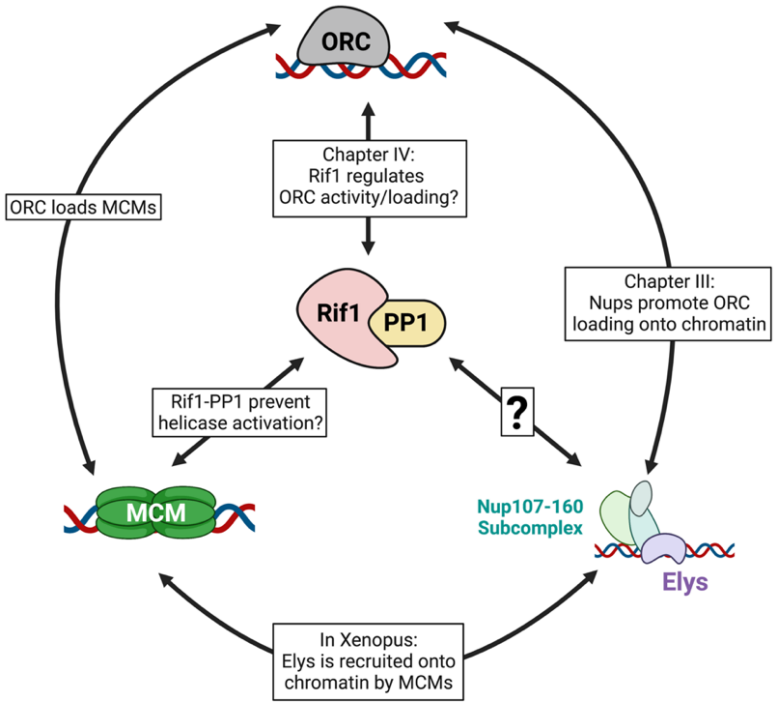

Figure. 5.1. ***Summary of dissertation work***. Shown are the interactions between Rif1, Nups, MCMs, or ORC based on previously published data or the work presented in this dissertation. Chapter III and IV discuss the interaction between Nups and ORC or Rif1 and ORC, respectively. The interaction between Elys and MCMs has been observed only in Xenopus, and the question if this interaction occurs in Drosophila remains unanswered. Rif1 also has a robust interaction with the Nup107-160 subcomplex of the NPC and the reason for this remains unknown. Figure made by Logan Richards.

Discussion

In this dissertation, I have examined the factors that influence the initiation of DNA replication and have established a link between nucleoporins and ORC. The molecular mechanism remains unknown, and I will propose a testable model to guide the direction of future work. There are also

observations in the field for Rif1 activity and genomic binding that oppose my own observations, and I will reconcile this by proposing a model where the activities of Rif1 are cell cycle regulated. For both models, I will discuss some observations that are inconsistent with my models, describe outstanding questions to be addressed, and provide my perspective on future work to be done to formally test my models.

Potential models for the Rif1-Nup-ORC interaction

As described in Chapter IV, Rif1 immunoprecipitates with all 6 subunits of ORC and all 10 subunits of the Nup107-160 subcomplex of the NPC. It is tempting to speculate that Rif1, ORC, and the Nup107-160 subcomplex assemble together to form a hub that promotes both the chromatin association and activity of ORC (Fig. 5.2C). Further evidence supporting the model that these proteins form a functional hub could be generated by investigating the ChIP-seq signal of Rif1, ORC2, and Elys. Elys appears to bind to many more genomic sites than Rif1 and ORC2, and essentially all Rif1 and ORC2 binding sites overlap with Elys (Fig. 5.2A-B). A major caveat to this result; however, is that ChIP-seq is not indicative of when different proteins bind to DNA, as these results were generated in an asynchronous population of cells. If a protein were to disassociate from a genomic site, and afterwards, a different protein was to bind to the same genomic site, this would give the impression that these proteins bind the same genomic region *together*, which may not be the case (for example, see 5.2D, right pathway). Furthermore, there is the possibility that Rif1 may interact with Nups and ORC separately in two discrete complexes (Fig. 5.2D). In the next sections, I will explore the different potential modes of Rif1, ORC, and Nup recruitment onto chromatin in greater detail and provide a possible molecular mechanism of this recruitment.

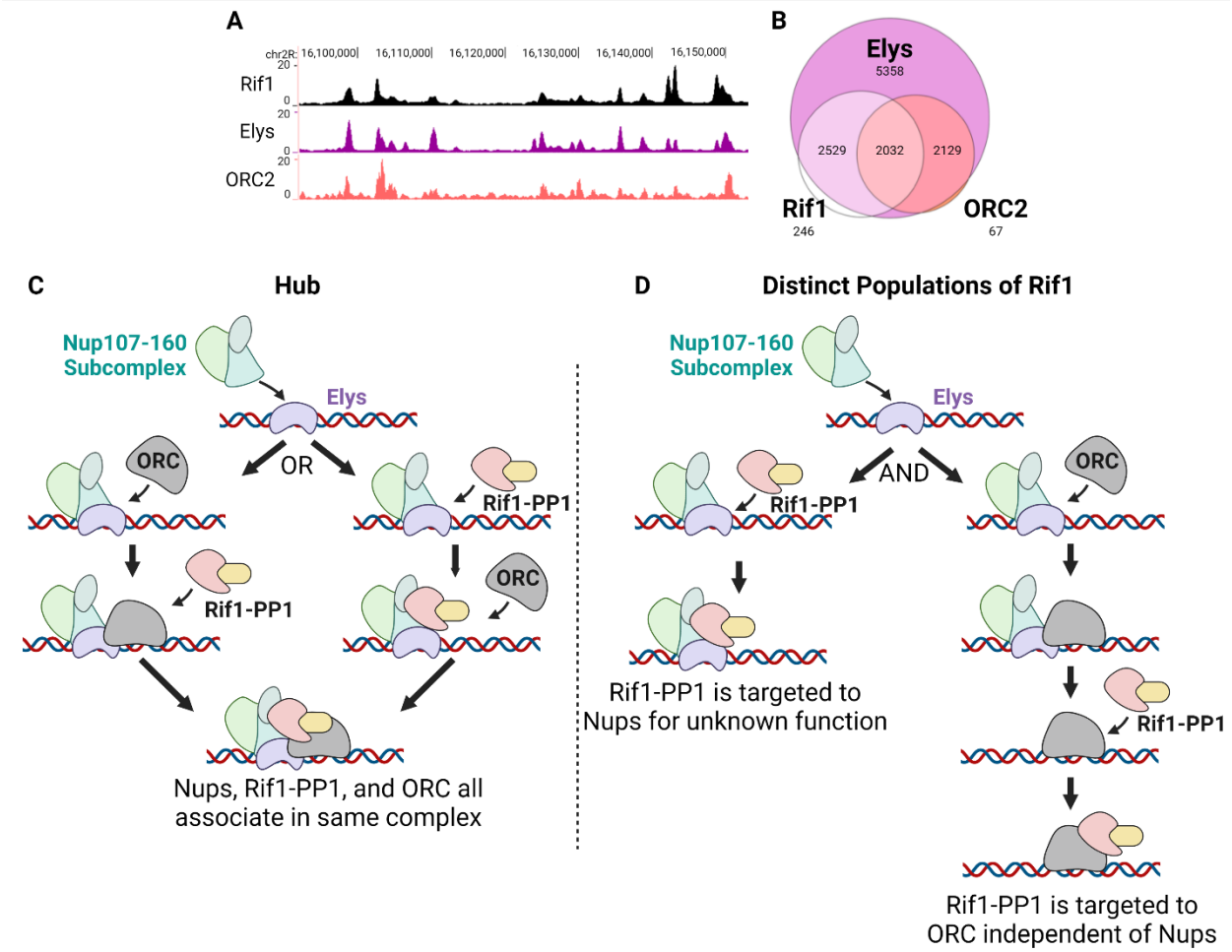

Figure 5.2. ***Models for the interactions between Rif1, ORC, and Nups.*** (A) Representative view of Rif1, Elys, or ORC2 ChIP-seq signal visualized with the UCSC genome browser. (B) Venn diagram of peak overlap between Elys, Rif1, and ORC2. Numbers indicate respective number of peaks (for example, 2529 is the number of Rif1 peaks that overlapped with Elys peaks but not ORC2 peaks). Elys and ORC2 ChIP-seq data generated by Maya Capelson and David MacAlpine, respectively. (C) A schematic of the "hub" model where Elys binds to chromatin followed by the Nup107-160 subcomplex of the NPC. The order of recruitment is unknown, where Rif1-PP1 or ORC can then bind to chromatin, facilitated directly or indirectly by Nups. (D) Alternatively, Rif1 may interact with Nups and ORC separately. Left: Rif1-PP1 are targeted to Nups independent of ORC for an unknown function. Right: Nups may dissociate from chromatin after promoting ORC loading, creating the possibility that Rif1-PP1 is targeted to ORC independently of Nups. Data analyzed and figure created by Logan Richards.

Given that Elys binds to essentially all Rif1 or ORC2 genomic binding sites and that Elys co-IPs with both Rif1 and ORC, I speculate that Elys may be a key driver of the interactions between Rif1, ORC, and the Nup107-160 subcomplex. As such, I propose that Elys is the first to bind to

chromatin in both my “hub” model (Fig. 5.2C) and the alternative model with “distinct populations of Rif1” (Fig. 5.2D), which then allows for the recruitment of the Nup107-160 subcomplex onto chromatin. After recruitment of Nups in the “hub” model, Rif1 or ORC are recruited onto chromatin either indirectly or directly by Nups to associate together at the same genomic site to potentially link NPC and replisome assembly (Fig. 5.2C). Alternatively, assembly of this hub may facilitate the initiation of DNA replication but not necessarily NPC assembly as Nups play roles in chromatin compaction independently of the NPC. Investigating if this replisome/NPC assembly hub exists could represent an exciting area of future work relevant to multiple fields. Later, I will describe potential experiments to interrogate this model.

As described earlier, Rif1, Nups, and ORC may not exist in the same complex, but rather form discrete complexes to perform different biological functions. In the “separate Rif1 populations” model (Fig. 5.2D), Rif1-PP1 could both target Nups and ORC on chromatin separately, where Rif1-PP1 regulate the phosphorylation state of both Nups and ORC. The regulation of Nups by phosphorylation has been observed, and CDK-mediated phosphorylation is thought to promote NPC disassembly, leading to breakdown of the nuclear envelope that occurs in the beginning of mitosis (Otsuka and Ellenberg, 2018). Perhaps, Rif1-PP1 reverses this phosphorylation toward the end of mitosis to then promote reassembly of the NPC. This new function of Rif1-PP1 would not be unsurprising as Rif1-PP1 have been implicated in a host of biological process including DNA damage repair, DNA replication initiation, and abscission timing (the regulation of the final stages of cytokinesis) (Bhowmick et al., 2019; Mattarocci et al., 2016).

Model for the activities of Rif1 through the cell cycle

I have established that ORC is likely regulated in some way by Rif1-PP1; however, how Rif1-PP1 achieves this while also regulating helicase activation remains unclear. I hypothesize that the

ability of ORC to bind to DNA is controlled by phosphorylation and Rif1-PP1 opposes this phosphorylation during G1 phase of the cell cycle. In this model, Rif1 promotes the chromatin association by reversing CDK-mediated phosphorylation of ORC at the end of mitosis and beginning of G1 phase. I predict that Rif1 is targeted to ORC via a direct interaction, but additional work is needed to test this. Once ORC is dephosphorylated, ORC and Rif1-PP1 are able to bind to origins of replication, where Rif1-PP1 protect ORC from phosphorylation during G1 to allow ORC to load helicases (Fig. 5.3, blue G1 arrow). ORC therefore depends on Rif1 for chromatin association and Rif1 also depends on ORC for chromatin association in this model, which is consistent with my data described in Chapter IV.

I hypothesize that Rif1-PP1 is capable of achieving this as CDK activity is low in early G1 but increases as cells approach the G1 to S phase transition (Bertoli et al., 2013). Once CDK activity has increased sufficiently, CDK activity exceeds Rif1-PP1 activity, causing ORC to be phosphorylated and deactivated at the end G1 phase. After ORC is phosphorylated, it can no longer effectively bind DNA, causing both ORC and Rif1 to dissociate from DNA. Once cells are in S phase, Rif1 activity switches, and Rif1-PP1 are recruited to late-activating helicases to implement the replication timing program (Fig. 5.3, red S arrow). As S phase progress, DDK activity increases (or alternatively Rif1-PP1 activity decreases), and helicases within late-replicating regions of the genome are phosphorylated and activated, allowing for DNA replication to occur (Fig. 5.3, red S arrow).

Presumably, Rif1-PP1 is inhibited from later stages of the S phase onward to the next cell cycle, to ensure both helicases and ORC stay phosphorylated, to maintain helicase activity and inhibit ORC activity. This regulation likely occurs through the phosphorylation of Rif1 itself, allowing for Rif1 activity to be controlled through the cell cycle. This assumption is supported by evidence the fact that a Drosophila mutant of Rif1 that is unable to be phosphorylated is overactive and highly

detrimental to cell proliferation (Seller et al., 2018). The predicted reason for this is that helicases remain dephosphorylated and unable to activate, causing failures in DNA replication. A key aspect of this model is the regulation of Rif1-PP1 activity through the cell cycle, which I have explored to integrate my observations with those in the field. Therefore, determining if Rif1 activity is regulated through the cell cycle and how this occurs will be critical questions to address in future work.

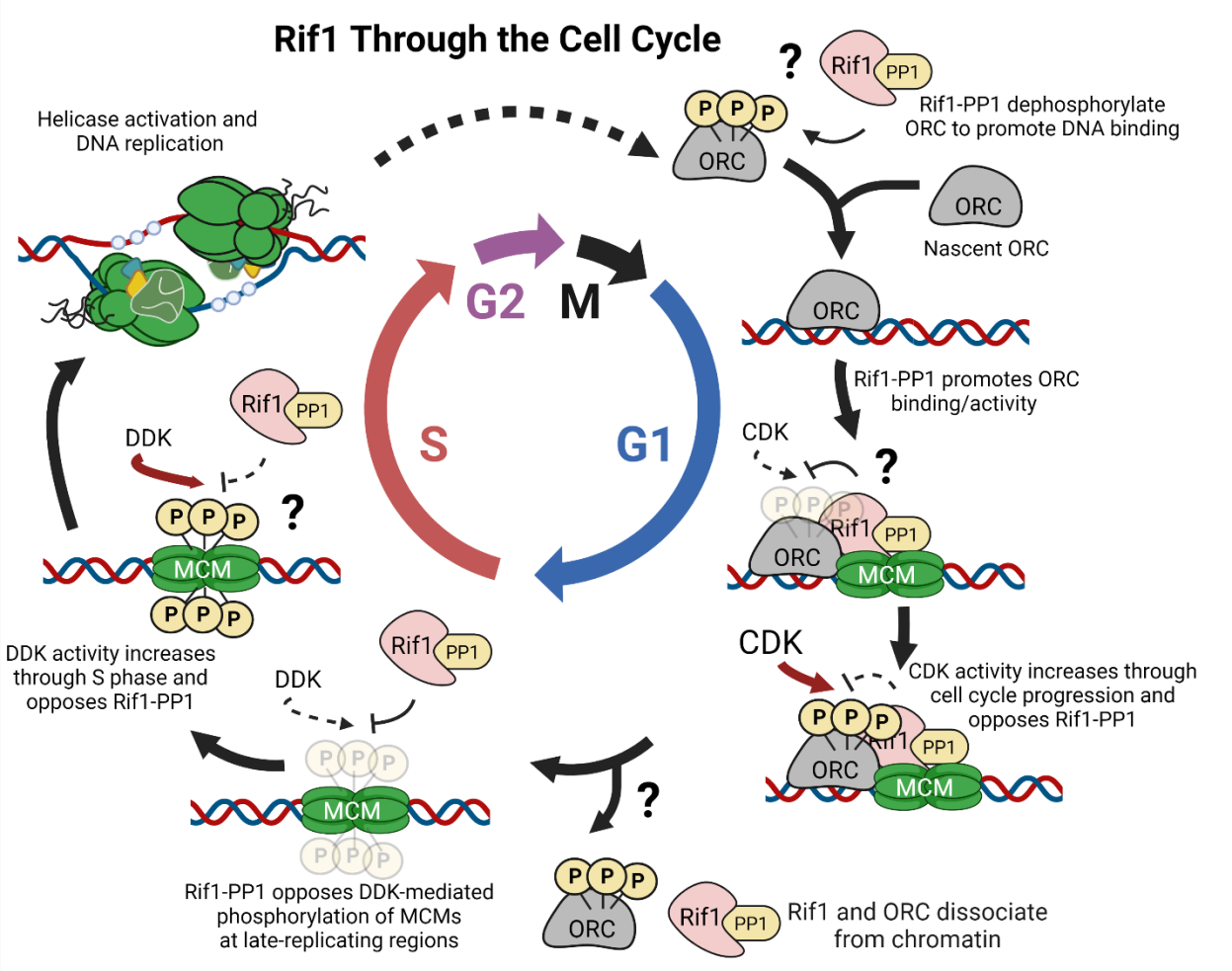

Figure 5.3. ***Model for activity of Rif1-PP1 through the cell cycle.*** In this model, the DNA binding ability of ORC is inhibited by phosphorylation. Prior to the start of the new cell cycle, ORC is phosphorylated and unable to bind to chromatin. When CDK activity is low, Rif1-PP1 promote the DNA binding and activity of ORC by reversing phosphorylation. After dephosphorylation by Rif1-PP1, ORC loading onto origins of replication occurs at the end of mitosis and early G1 phase. Rif1 continues to oppose CDK-mediated phosphorylation as ORC loads helicases through G1 phase, with Rif1-PP1 targeted origins of replication loading helicases more efficiently. CDK

activity increases during G1 phase as cells near the transition into S phase and eventually negates the activity of Rif1-PP1. Once ORC is phosphorylated, ORC and Rif1 no longer bind to chromatin. In S phase, Rif1 now opposes DDK-mediated phosphorylation specifically at late-activating origins of replication to implement the replication timing program. Later in S phase, DDK activity increases (or alternatively Rif1-PP1 activity decreases) and helicases within late-replicating regions of the genome are activated, allowing for DNA replication to occur. Presumably, ORC remains phosphorylated until the next cell cycle to prevent re-replication from occurring, which is then reversed by Rif1-PP1 in G1 phase to start the cycle anew. Figure created by Logan Richards

A possible mechanism for the recruitment of Nups, ORC, and Rif1

Now that I have established a potential order of recruitment for Rif1, ORC, Elys and the Nup107-160 subcomplex as well as explored a model for the activity of Rif1 through the cell cycle, I would like to discuss a possible mechanism for the recruitment of these proteins and complexes onto chromatin. Recent work has shown that factors involved in DNA replication machinery, specifically, ORC, Cdc6, and Cdt1, undergo liquid-liquid phase-separation (LLPS) in a DNA-dependent manner (Parker et al., 2019). LLPS is the process of forming a biomolecular condensate into a compartment that is not enclosed by a membrane, and LLPS plays roles in chromatin organization, gene expression, and protein degradation (Hyman et al., 2014; Lu et al., 2021; Rippe, 2022). LLPS appears to be a commonly occurring mechanism to create hubs of biological activity (Hyman et al., 2014; Lu et al., 2021; Rippe, 2022). Given that it has also been implicated in DNA replication initiation (Parker et al., 2019), it is possible that LLPS may also be involved in the assembly of the complexes discussed previously.

To begin to explore this, I used a software that predicts the presence of intrinsically disordered regions (IDRs) (Jones and Cozzetto, 2015), in the key proteins of my dissertation: Elys, Rif1, and ORC2. IDRs are believed to play a key role in phase-separation and proteins that contain IDRs are viewed as good candidates that can undergo LLPS (Lu et al., 2021). Excitingly, all three proteins contain an IDR with Rif1 and ORC2 having a smaller IDR, approximately 200 amino

acids long, in comparison to the long C-terminal IDR of Elys, approximately 500 amino acids long (Fig. 5.4). Given that all three possess IDRs, I hypothesize that these proteins undergo LLPS to associate into the complexes identified in Chapter III and IV, and I predict the IDRs in each protein to be necessary for their ability to associate in complex.

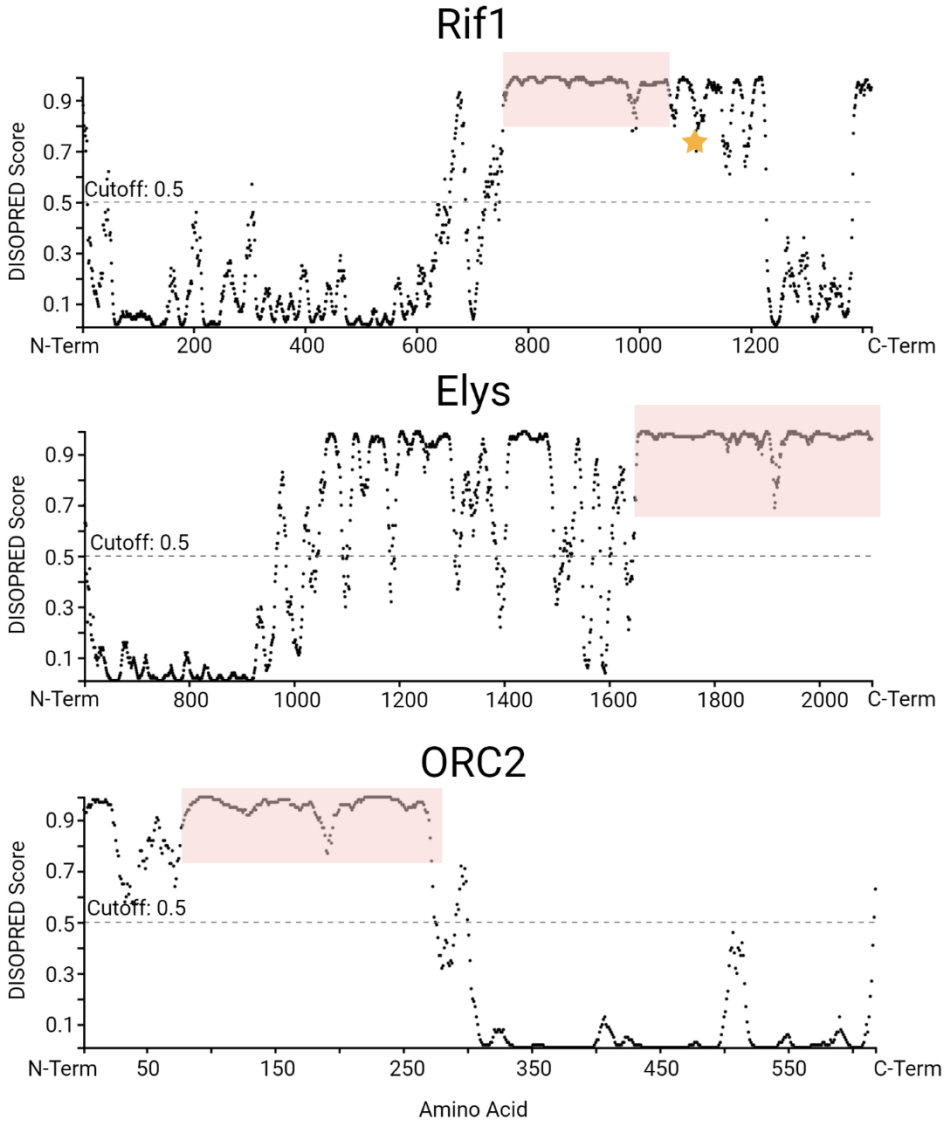

Figure 5.4. ***Rif1, Elys, and ORC2 all possess intrinsically disordered regions.*** DISOPRED plot for Rif1, Elys, and ORC2. Stretches of amino acids with a DISOPRED score greater than 0.5 are predicted to be an intrinsically disordered region (IDR) of the protein. Likely IDRs for each protein are highlighted in red box. PP1 binding domain of Rif1 is indicated with a gold star. Figure created by Logan Richards.

Elys has an AT hook domain, which proposed to allow for Elys to bind to DNA (Kimura et al., 2002). and binds to essentially all Rif1 and ORC2 genomic binding sites. Furthermore, Elys has a long C-terminal IDR and binds to thousands of other genomic sites independently of Rif1 and ORC2. Therefore, I speculate that Elys is a key driver in the formation of phase-separated condensates, and specifically, the C-terminal domain is essential for this. This speculation could be justified with the data I already have from my co-immunoprecipitation experiments. I may simply be isolating phase-separated condensates. However, this is unlikely as phase-separated condensates typically require DNA for their formation, and the embryonic extracts used for the IPs were treated with a nuclease. Perhaps protein-protein interactions themselves are sufficient to stabilize phase separated condensates, but additional work is needed to further address these possibilities.

Furthermore, I hypothesize that the function of Elys is to serve as scaffolding protein to promote the initial stages of condensate formation, mediated by self-interactions by the C-terminal IDR (Fig. 5.5), which I envision to be a long disordered “tail” at the end of the protein. After initial droplet formation, Elys serves as an effective landing platform for other proteins to be recruited into the condensate and bind to chromatin within the droplet. This is a highly speculative model requiring extensive work, but the findings from this work may provide mechanistic insight as to how phase droplet formation occurs and possibly provide further detail as to how NPC and replisome assembly are initiated.

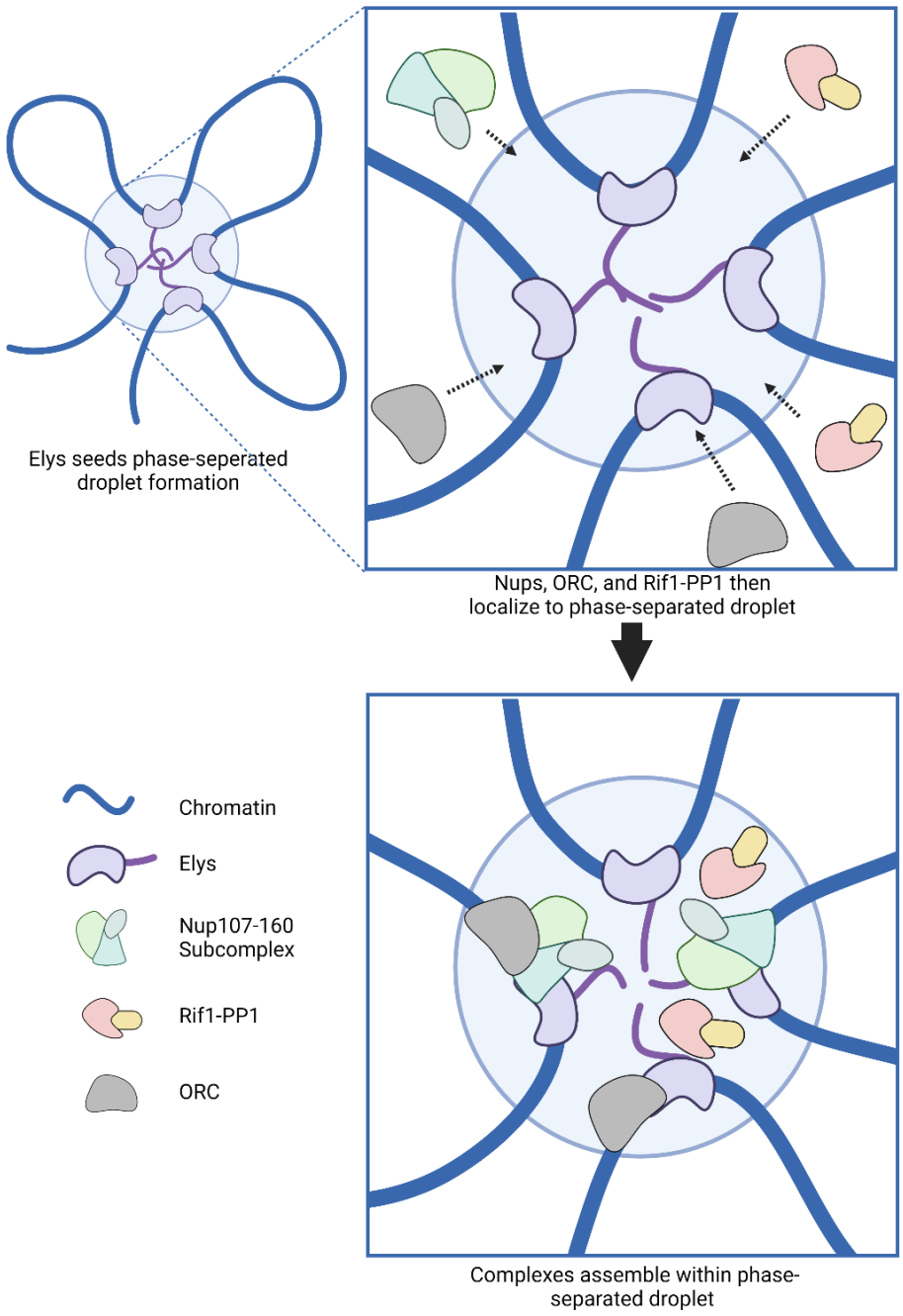

Figure 5.5. ***Model for mechanism of recruitment for Nups, ORC, and Rif1-PP1***. Elys possesses a long IDR at the C-Terminal end which may be key for the formation of phase-separated droplets, shown as a tail on Elys. In this model, Elys binds to chromatin serving as a scaffold to promote phase-separation droplet formation. After Elys recruitment, Rif1 and ORC localize to droplets, as they both also contain IDRs, leading to the assembly of the different potential complexes discussed in this dissertation. Figure created by Logan Richards.

Observations that conflict with my models or data

In this section, I will describe observations within the field that do not easily fit my models, or conflict with my own observations. I will highlight a few and provide possible explanations.

- Failure to observe Rif1 at late-replicating regions of the genome. – As described in Chapter IV, my ChIP-seq data shows that Rif1 localizes primarily to early-replicating regions of the genome. This contrasts with previously published data where the genomic distribution of Rif1 in mouse embryonic cells and human cell lines is enriched at late-replicating regions (Foti et al., 2016; Klein et al., 2021). However, in budding yeast, Rif1 associates with the coding regions of highly transcribed genes and is also enriched at origins in budding yeast and fission yeast (Hiraga et al., 2018). Rif1 CUT&RUN data in human cells is similar to that of yeast, with Rif1 being enriched at late-replicating regions and at origins of replication (Klein et al., 2021). The difference between my data and the other data could be explained by differences in the species used to perform these experiments; however, that does not seem very likely. Alternatively, the differences could be explained by differences in the methodology used to capture Rif1, as heterochromatin is historically difficult to immunoprecipitate.

- No stable interaction between Rif1 and MCMs. – In my mass spec data for Rif1, I expected to capture an interaction between Rif1 and helicase subunits but fail to do so. Given that other groups also have not captured a robust interaction between Rif1 and MCMs, this is not entirely surprising (Alver et al., 2017; Sukackaite et al., 2017). Perhaps Rif1 has a transient interaction with MCMs that is not easily captured by immunoprecipitation. To address this possibility, I have also performed an immunoprecipitation of Rif1-GFP in the presence of a crosslinker, which should stabilize transient interactions. In the presence of

a crosslinker, I can co-purify MCMs with Rif1 (Table 5.1), but interestingly, I do not co-purify ORC or Nup107-160 subcomplex subunits. As for the differences between the IPs with or without a crosslinking agent, ORC, Nups, and Rif1 could form a large complex that becomes insoluble and difficult to IP when crosslinked, which could explain these differences. Further work is needed to investigate the direct interactions of Rif1, which will be described in later sections.

	Rif1-GFP Repl. 1	Rif1-GFP Repl. 2	ORR Repl. 1	ORR Repl. 2	P-value
Rif1	387	105	0	1	< 0.00010
MCM4	42	15	4	1	< 0.00010
MCM5	44	6	2	0	< 0.00010
MCM6	41	10	1	0	< 0.00010
MCM2	41	6	2	0	< 0.00010
MCM3	30	13	1	1	< 0.00010
MCM7	35	5	2	0	< 0.00010

Table 5.1. ***Summary of peptide counts for Rif1-GFP IP-MS with crosslinker.*** IP performed in Rif1-GFP or ORR Drosophila embryos aged 18-24 hours using anti-GFP nanobody. Extracts were fixed with 2% PFA prior to the IP to stabilize transient protein-protein interactions. Shown are peptide counts from MS for Rif1 and helicase subunits for 2 biological replicates. P-value determined by Fisher's test. Contributions: IP-MS samples prepared by Logan Richards. MS performed at the Vanderbilt Mass Spectrometry Core and raw data analyzed by Hayes McDonald. Table prepared by Logan Richards.

- Elys promoting chromatin accessibility. Much work has shown that Elys and other Nups influence gene expression (Capelson et al., 2010; Kalverda et al., 2010; Kuhn et al., 2019; Panda et al., 2014; Pascual-Garcia et al., 2014, 2017; Raices and D'Angelo, 2017; Vaquerizas et al., 2010). The proposed mechanism is that Nups promote chromatin decompaction, where there is evidence that Nups recruit chromatin-remodelers to create nucleosome-free regions (Kuhn et al., 2019). If I deplete Elys, I do not see changes in chromatin accessibility as measured by ATAC-seq, which seems to be inconsistent with

previously published data. The key difference is the choice of assay where I used ATAC-seq to measure chromatin accessibility whereas others used MNase-seq. Furthermore, I used a global approach and do not see a general reduction in chromatin accessibility, whereas previous publications report reductions in nucleosome occupancy at specific genes that are targeted by Elys and used qPCR to quantify this (Kuhn et al., 2019). Perhaps these technical differences could account for the differences in my data versus previous results. Alternatively, if I were to focus on specific genes in my ATAC-seq data, I may observe a reduction in chromatin accessibility in the Elys depletion. This reduction may not be as obvious when viewed globally or perhaps the reduction in chromatin accessibility is subtle and gene-specific. Additional work is needed to determine if Elys recruits factors such as ORC or chromatin remodelers by promoting chromatin accessibility or if there is another mechanism at work.

- Elys is nonessential in Drosophila. – Elys is essential for mice, as a null mutant of *Elys* is lethal in the early stages of embryonic development (Okita et al., 2004). Unlike mice, The *C. elegans* homolog MEL-28 is nonessential for zygotic development; however, it has a maternal effect (Fernandez et al., 2014). A recent study determined that a null mutant for the *Drosophila melanogaster* homolog of Elys has a similar effect as the *C. elegans*, where homozygous mutants are viable, and males are fertile, but females are sterile (Hirai et al., 2018). However, in my experience with these same *Elys* null mutant stocks, they are very sick, and homozygous null mutant flies are rare within the stock compared to flies heterozygous for *Elys*. In contrast, when I deplete Elys, I do not observe a defect in cell proliferation relative to the negative control. In Chapter III, we argued that this is a result of loading excessive ORC, which is not needed unless replication stress occurs. With all

this in mind, perhaps Elys is confers some advantage to the organism as a whole but may be less essential in cell lines.

Given that Elys has functions in gene expression and NPC assembly (Shevelyov, 2020), the reason why Elys is nonessential is less clear. Perhaps, the role of Elys in NPC assembly is also situational, as NPC assembly can occur in interphase and mitosis (Otsuka and Ellenberg, 2018). The mechanism of NPC assembly during interphase occurs independently of Elys (Otsuka and Ellenberg, 2018), and this alternative means of assembling NPCs could compensate for the lack of Elys. In my own models, Elys plays a central role in the recruitment of ORC, Nups, and Rif1 to the genome. Considering that excessive ORC is loaded, Rif1 is also a nonessential gene in Drosophila (Munden et al., 2018, Seller et al., 2018), and there are alternative ways to build NPCs, a question that still lingers in my mind is: what truly is the reason of having Elys in Drosophila? Is there truly a competitive advantage to having Elys in flies over flies that do not express Elys? If so, what is the advantage? Why is Elys essential in mice but not flies? Interestingly, there is low protein sequence conservation between Drosophila and mouse Elys, with a sequence identity of only 25%. Additionally, the 25% that is conserved contains the Elys family of protein domains, with the remaining 75% not containing any predicted domains (determined by NCBI blast, data not shown). This creates the possibility of high sequence and functional divergence between Drosophila and mouse Elys, which could explain why Elys is essential in mice but not flies. Addressing this and other previously described questions will be critical to future work as the true importance of Elys remains to be determined.

Outstanding questions regarding the Nup-ORC interaction

- Does the depletion of Elys affect the of MCM in G1 phase?

  If there is less ORC loading as a result of depleting Elys, I expect to also observe less helicases loaded in G1 phase as a consequence of less chromatin associated ORC. I have attempted to answer this using a pan-MCM antibody that recognizes all MCM subunits. Indeed, I observe less pan-MCM signal in G1 phase Elys-depleted nuclei (Fig. 5. #); however, there should be little to no MCM signal in G2 phase nuclei, as MCMs are unloaded off chromatin at the completion of S phase. Unfortunately, I do see MCM signal in G2 phase nuclei, causing doubts that my data represents loaded helicases and not just chromatin associated MCMs (data not shown). As such, this question remains unanswered but an important one to address in future work.

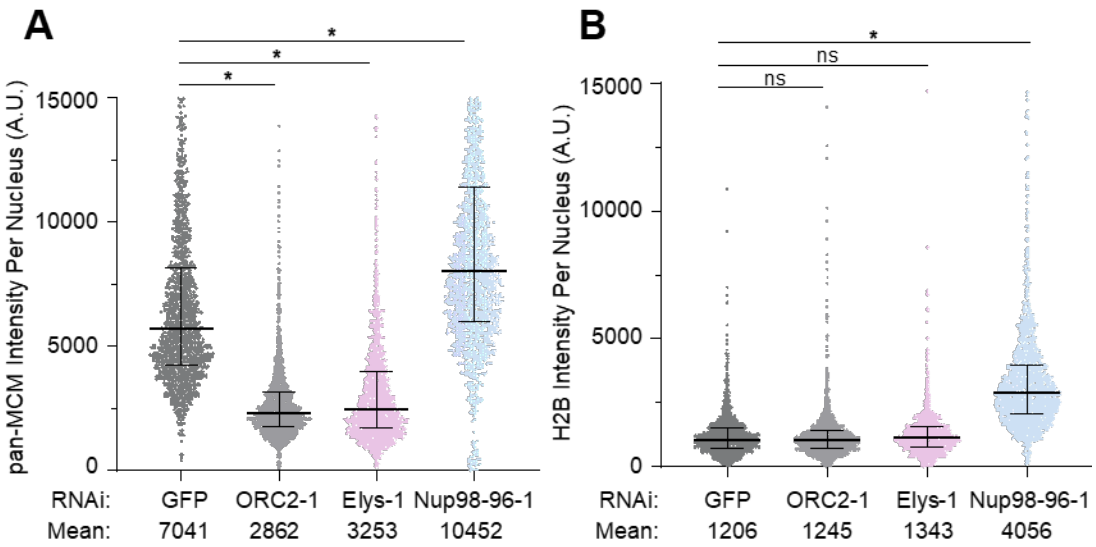

Figure 5.6. ***Elys depletion reduces MCM chromatin association.*** (A) 1500 randomly selected G1 nuclei across two biological replicates were used to quantify the pan-MCM intensity per nucleus for each depletion. Asterisk indicates p<0.0001 relative to the negative control by One-Way ANOVA with a post-hoc Dunnett's test. (B) Same as (A) for Histone H2B. Contributions: data and figure generated by Logan Richards.

- Does Elys interact with ORC directly?

Answering this will be a major challenge but is an important question to address. Elys is a large protein (approximately 235 kDa) and possesses a long IDR as previously discussed, which may make purifications challenging. Furthermore, the specific subunits of ORC that Elys interacts with remains unknown. These issues can be circumvented by attempting to purify a fragment of Elys without the IDR and performing *in vitro* IPs with individual ORC subunits; however, I anticipate the IDR of Elys to mediate the interaction with ORC. Unfortunately, this question remains unanswered but one to address in future work.

Outstanding questions regarding the Rif1 and ORC interaction

- What replication factors does Rif1 directly interact with?

  Given that Rif1 co-IPs with ORC in benzonase-treated extract but only co-IPs with MCMs in the presence of a crosslinker, I argue that Rif1 is more likely to have a direct interaction with ORC over MCMs, as there is a strong possibility the interaction between Rif1 and MCMs is bridged by chromatin. An important point to consider; however, is that interaction between Rif1 and ORC could also be bridged, but by other additional proteins rather than chromatin. Nups are a good candidate for possibly bridging the interaction between Rif1 and ORC as Rif1 IPs with both Nups and ORC. To determine the physical and direct interactions between Rif1 and ORC, future work will likely turn to *in vitro* immunoprecipitations, using purified Rif1, ORC subunits, and possibly subunits of the Nup107-160 subcomplex to address this question.

- Does Rif1 regulate helicase loading?

  If Rif1 promotes the activity of ORC, either by affecting the DNA binding or helicase loading of ORC, I hypothesize a direct consequence to be less helicase loaded across the genome if Rif1 is depleted. Using FACS to quantify the amount of chromatin-associated MCMs in

a Rif1 depletion seems the most obvious approach to addressing this question; however, as discussed previously, measuring this has been more challenging than anticipated. Using quantified proteomics, previous work has shown that depletion of Rif1 causes reduced chromatin association for all MCM subunits (Hiraga et al., 2017). Interestingly, the authors also observed slightly increased chromatin association of ORC2, ORC3, and ORC5. In contrast, the amount of chromatin-associated ORC1 is significantly reduced (Hiraga et al., 2017).

In terms of phosphorylation levels in the Rif1 depletion, MCM2, 4, and 6 show a marked increase (Hiraga et al., 2017), which is consistent with the model that Rif1-PP1 opposes DDK-mediated phosphorylation of MCMs. ORC1 also has increased phosphorylation, which is believed to target ORC1 for degradation (Hiraga et al., 2017). Therefore, the model for Rif1 activity in human cells is that Rif1-PP1 protects ORC1 from degradation while simultaneously inhibiting helicase activation. Whether or not Rif1 has a similar mechanism in Drosophila remains to be determined. An exciting experiment to investigate the possible mechanism of Rif1 activity would be to perform phosphoproteomics in a Rif1 depletion. I will discuss this in greater detail in later sections and describe additional information performing this experiment in Drosophila could provide.

- <u>When and where does Rif1 bind to chromatin during the cell cycle?</u>

  In my model, Rif1 is targeted to ORC during G1 phase, but to helicases during S phase, in euchromatic and heterochromatic regions of the genome, respectively. A critical experiment to formally test this model would be to determine the genomic sites that Rif1 binds across the cell cycle. This could be performed by performing ChIP-seq for Rif1 in populations of cells where the cells are fixed in specific stages of the cell cycle. This may

also address the previously described issue in my data of not observing Rif1 in late-replicating regions of the genome.

In the asynchronous population of cells, there may be low and broad Rif1 ChIP-seq signal in late-replicating/heterochromatic genomic regions, resembling the background signal in this assay, but high and specific Rif1 ChIP-seq signal at origins. This would give the impression that there is a lack of Rif1 in heterochromatic regions, even though it is simply being overshadowed by the signal of Rif1 at origins. Perhaps by selectively using S phase cells to perform the ChIP, the Rif1 ChIP-seq signal in heterochromatic regions could be improved. Also, if the genomic localization of Rif1 is different in G1 versus S phase cells, this would provide additional evidence to support my model of Rif1 activity through the cell cycle.

Future directions

Investigate the direct interactions of Rif1

I hypothesize that Rif1 directly interacts with ORC but not MCM2-7. This can be tested by carrying out *in vitro* immunoprecipitations by incubating Rif1 with ORC and Rif1 with MCM2-7. Rif1 can be captured using an antibody and if Rif1 co-immunoprecipitates with ORC or MCM2-7 can be determined by Western blot. The same experiment can be conducted with the addition of PP1 and again tested for co-immunoprecipitation. Additionally, an experiment can be performed *in vitro* to test for phosphorylation/de-phosphorylation with purified proteins. For example, ORC could be phosphorylated by CDK with radiolabeled ATP. Rif1-PP1 can then be added to the reaction to test if Rif1-PP1 is able to de-phosphorylate ORC *in vitro*. Performing these experiments will determine the direct interactions of Rif1, and determine if ORC is targeted by

Rif1 *in vitro*. The results of these experiments would be highly significant to the replication timing field as there is still ongoing debate as how Rif1 regulated replication timing.

Elucidate the molecular mechanism of Rif1 recruitment onto chromatin

The molecular mechanism of Rif1's recruitment to DNA and chromatin is still unknown. As described previously, Rif1 possesses an intrinsic disorder region (IDR), which may allow it to phase separate. Furthermore, ORC and other replication initiation factors have been shown to contain an IDR that enables phase separation (Parker et al., 2019). Importantly, ORC undergoes phase separation only in the presence of DNA (Parker et al., 2019). Based on this, I hypothesize that Rif1 will phase separate in the presence of DNA, similar to ORC, and that Rif1 and ORC phase separate into the same compartment.

The ability of Rif1 to form phase separated condensates in the presence or absence of DNA will be tested by a droplet forming assay (adapted from Parker et al., 2019). To achieve this, purified Rif1-GFP can be incubated with or without DNA that is labeled with Cy5 and then imaged by fluorescent microscopy. If Rif1 forms droplets that are GFP and Cy5 positive, this is strong evidence that Rif1 has bound the DNA and undergone phase separation. Rif1 may require its binding partner PP1 to bind to its targets effectively, and this assay will also be done in the presence and absence of PP1. A complication to this assay is that the C-terminal tail of Elys may be key in driving droplet formation, and this portion of Elys may also be needed for Rif1 to phase separate. To account for this, this same experiment can also be performed in the presence or absence of the C-terminal tail of Elys.

These experiments will test if Rif1 alone binds DNA or if Rif1 needs PP1 or the C-terminal tail of Elys; however, it does not test if Rif1 interacts with ORC or MCM2-7 in a phase separated

condensate. To test this, a similar assay can be performed where ORC or MCM2-7 with a fluorescent tag are expressed, purified, and incubated Rif1, PP1 and/or the IDR of Elys. This will formally test which factors are key to the formation of phase separated droplets. If droplets are formed that contain Rif1, PP1, ORC, and possibly the IDR of Elys, but not MCM2-7, this is highly suggestive that Rif1 is recruited to ORC through phase-separation. Performing this work will be critical to elucidating the mechanisms for the recruitment of Rif1 and replication initiation factors onto chromatin and will be relevant to multiple fields.

Determine when Rif1 associates with chromatin within the cell cycle

To characterize when across the cell cycle Rif1 and ORC bind the same genomic regions, the Drosophila FUCCI cell system can be utilized. In FUCCI cells, E2F is tagged with GFP and cyclin B is tagged with RFP (Zielke et al., 2014). With these markers, cells in G1 phase express only E2F-GFP, cells in S phase express only cyclin B-RFP and cells in G2 phase express both (Zielke et al., 2014). With this system, which phase of the cell cycle the cells are in can be easily distinguished and the desired population of cells can by collected by flow sorting. Chromatin immunoprecipitations can then be done for ORC2 and Rif1 in sorted G1, S, and G2 phase populations. This will elucidate the localization pattern of these proteins and determine if the localization pattern changes through the cell cycle. Specifically, this can be achieved by chemically fixing the FUCCI S2 cells after sorting them and sonicating the genomic DNA obtained from the cells into small enough fragments, after which ChIP-seq with anti-Rif1 or anti-ORC2 antibodies can be performed. Alternatively, cells can be synchronized and released with hydroxyurea, which arrests cells at the G1 to S transition. Using flow cytometry and DAPI staining, cells can also be staged using this method, but may not be as precise as FUCCI cells. By

investigating when Rif1 associates with chromatin during the cell cycle and where Rif1 localizes across the genome, this will further test my model for Rif1 activity.

Determine if the phosphorylation of ORC is regulated by Rif1

A major advantage of the Drosophila system is the effect Rif1 has on ORC or MCM phosphorylation can be investigated through embryogenesis. To achieve this, chromatin extracts from staged Drosophila embryos can be prepared in wild type and *Rif1* null genetic backgrounds. Using these chromatin extracts, quantitative mass spectrometry (MS) can be performed. To ensure the data is quantitative, the samples will need to be labeled the samples with TMT mass tags. This will allow for both the amount chromatin associated ORC and MCM and the level of phosphorylation on each subunit to be quantified. This experiment will reveal if there is a Rif1-dependent increase or decrease in either the relative amount of chromatin association or phosphorylation for each individual subunit. If differences in phosphorylation are observed as I hypothesize, this would strongly suggest that Rif1 influences ORC phosphorylation. MCM phosphorylation is also expected to increase based on previously published work and could serve as an internal control for this experiment. A caveat to these results is that this experiment does not test if the effects seen are directly caused by an absence of Rif1 or are attributed to indirect effects. This experiment should therefore be coupled to the proposed *in vitro* IPs for Rif1 previously described.

Determine if Rif1, Nups, and ORC exist in the same or separate complexes

The previously described experiments; however, do not answer the question if Rif1, ORC, and Nups bind to the same genomic regions at the same time. The possibility still exists that Rif1, ORC, or Nups bind to the same regions transiently without interacting with each other, or if Rif1,

ORC, and Nup binding is mutually exclusive. Alternatively, Rif1 and ORC could associate in one discrete complex, Rif1 and Nups could associate in another, and Nups and ORC could associate in yet another. To address these possibilities, ChIP-reChIP should be performed to test if Rif1, ORC, and Nups bind the same genomic regions at the same time. To accomplish this, asynchronous S2 cells can be fixed and a chromatin extract can be prepared. After this, Rif1 containing complexes can be captured using an antibody against Rif1. After Rif1 complexes are isolated and eluted, an antibody against ORC2 can be used to subsequently enrich for ORC containing complexes. By doing this, complexes that contain both Rif1 and ORC are isolated. The presence of Rif1, ORC, and Nups in these different complexes can be determined by performing a Western blot for either Rif1, ORC, or Elys (serving as a proxy for the Nup107-160 subcomplex). This experiment can be done in a multitude of ways to determine which proteins are associating in each potential complex. Additionally, the DNA bound in these different complexes can be sequenced to specifically characterize where across the genome both Rif1, ORC and/or Nups are found.

Concluding remarks

In conclusion, I have investigated the factors that promote the activity of ORC, either by promoting the association of ORC onto origins of replication or by promoting the helicase loading activity of ORC. In Chapter III, I identified an interaction between ORC and the Nup107-160 subcomplex of the NPC in Drosophila, and further characterized this interaction by showing that Nups promote sufficient loading of ORC onto chromatin. Importantly, depleting Nups sensitizes cells to replication fork stalling, suggesting that Nups facilitate dormant origin firing. In Chapter IV, I interrogated the potential factors that regulate the activity of Rif1 during Drosophila and identified robust interactions between Rif1, ORC, the Nup107-160 subcomplex. I chose to focus on the interaction between Rif1 and ORC and found that depleting Rif1 reduces chromatin bound ORC2

and inversely depleting ORC2 also reduces chromatin bound Rif1. Interestingly, Rif1 and ORC2 bind a similar set of genomic regions and the key nucleoporin Elys binds to effectively all Rif1 and ORC2 genomic binding sites. Overall, my thesis project has shed new light on factors that regulate ORC and links nucleoporins to both DNA replication initiation and replication timing.

REFERENCES

Afgan, E., Baker, D., van den Beek, M., Blankenberg, D., Bouvier, D., Čech, M., Chilton, J., Clements, D., Coraor, N., Eberhard, C., et al. (2016). The Galaxy platform for accessible, reproducible and collaborative biomedical analyses: 2016 update. Nucleic Acids Res. *44*, W3.

Aggarwal, B.D., and Calvi, B.R. (2004). Chromatin regulates origin activity in Drosophila follicle cells. Nat. 2004 4306997 *430*, 372–376.

Ahmad, K., and Spens, A.E. (2019). Separate Polycomb Response Elements control chromatin state and activation of the vestigial gene. PLOS Genet. *15*, e1007877.

Allis, C.D., and Jenuwein, T. (2016). The molecular hallmarks of epigenetic control. Nat. Rev. Genet. 2016 178 *17*, 487–500.

Almouzni, G., and Cedar, H. (2016). Maintenance of Epigenetic Information. Cold Spring Harb. Perspect. Biol. *8*, 19372–19373.

Altman, A.L., and Fanning, E. (2001). The Chinese Hamster Dihydrofolate Reductase Replication Origin Beta Is Active at Multiple Ectopic Chromosomal Locations and Requires Specific DNA Sequence Elements for Activity. Mol. Cell. Biol. *21*, 1098–1110.

Alver, R.C., Chadha, G.S., and Blow, J.J. (2014). The contribution of dormant origins to genome stability: From cell biology to human genetics. DNA Repair (Amst). *19*, 182.

Alver, R.C., Chadha, G.S., Gillespie, P.J., and Blow, J.J. (2017). Reversal of DDK-Mediated MCM Phosphorylation by Rif1-PP1 Regulates Replication Initiation and Replisome Stability Independently of ATR/Chk1. Cell Rep. *18*, 2508–2520.

Araki, M., Wharton, R.P., Tang, Z., Yu, H., and Asano, M. (2003). Degradation of origin recognition complex large subunit by the anaphase-promoting complex in Drosophila. EMBO J. *22*, 6115.

Armstrong, R.L., Das, S., Hill, C.A., Duronio, R.J., and Nordman, J.T. (2020). Rif1 Functions in a Tissue-Specific Manner to Control Replication Timing through Its PP1-Binding Motif. Genetics *215*, 75–87.

Asano, M., and Wharton, R.P. (1999). E2F mediates developmental and cell cycle regulation of ORC1 in Drosophila. EMBO J. *18*, 2435.

Austin, R.J., Orr-Weaver, T.L., and Bell, S.P. (1999). Drosophila ORC specifically binds to ACE3, an origin of DNA replication control element. Genes Dev. *13*, 2639.

Beall, E.L., Manak, J.R., Zhou, S., Bell, M., Lipsick, J.S., and Botchan, M.R. (2002). Role for a Drosophila Myb-containing protein complex in site-specific DNA replication. Nat. *420*, 833–837.

Beck, M., and Hurt, E. (2017). The nuclear pore complex: Understanding its function through structural insight. Nat. Rev. Mol. Cell Biol. *18*, 73–89.

Bell, S.P. (2002). The origin recognition complex: from simple origins to complex functions. Genes Dev. *16*, 659–672.

Bell, S.P., and Dutta, A. (2003). DNA Replication in Eukaryotic Cells. Annu. Rev. Biochem. *71*, 333–374.

Bell, S.P., and Labib, K. (2016). Chromosome Duplication in Saccharomyces cerevisiae. Genetics *203*, 1027–1067.

Bell, S.P., and Stillman, B. (1992). ATP-dependent recognition of eukaryotic origins of DNA replication by a multiprotein complex. Nat. *357*, 128–134.

Bertoli, C., Skotheim, J.M., and De Bruin, R.A.M. (2013). Control of cell cycle transcription during G1 and S phases. Nat. Rev. Mol. Cell Biol. *14*, 518.

Bester, A.C., Roniger, M., Oren, Y.S., Im, M.M., Sarni, D., Chaoat, M., Bensimon, A., Zamir, G., Shewach, D.S., and Kerem, B. (2011). Nucleotide Deficiency Promotes Genomic Instability in Early Stages of Cancer Development. Cell *145*, 435.

Bhowmick, R., Singh Thakur, R., Es, A., Venegas, B., Liu, Y., Nilsson, J., Barisic, M., and Hickson Correspondence, I.D. (2019). The RIF1-PP1 Axis Controls Abscission Timing in Human Cells. Curr. Biol. *29*, 1232-1242.e5.

Bicknell, L.S., Bongers, E.M.H.F., Leitch, A., Brown, S., Schoots, J., Harley, M.E., Aftimos, S., Al-Aama, J.Y., Bober, M., Brown, P.A.J., et al. (2011). Mutations in the pre-replication complex cause Meier-Gorlin syndrome. Nat. Genet. 434 *43*, 356–359.

Blobel, G. (1985). Gene gating: a hypothesis. Proc. Natl. Acad. Sci. *82*, 8527–8529.

Blumenthal, A.B., Kriegstein, H.J., and Hogness, D.S. (1974). The units of DNA replication in Drosophila melanogaster chromosomes. Cold Spring Harb. Symp. Quant. Biol. *38*, 205–223.

Bosco, G., Du, W., and Orr-Weaver, T.L. (2001). DNA replication control through interaction of E2F–RB and the origin recognition complex. Nat. Cell Biol. *3*, 289–295.

Boyer, A.S., Walter, D., and Sørensen, C.S. (2016). DNA replication and cancer: From dysfunctional replication origin activities to therapeutic opportunities. Semin. Cancer Biol. *37–38*, 16–25.

Brewer, B.J. (1994). Intergenic DNA and the sequence requirements for replication initiation in eukaryotes. Curr. Opin. Genet. Dev. *4*, 196–202.

Brewer, B.J., and Fangman, W.L. (1987). The localization of replication origins on ARS plasmids in S. cerevisiae. Cell *51*, 463–471.

Brickner, J.H., and Walter, P. (2004). Gene Recruitment of the Activated INO1 Locus to the Nuclear Membrane. PLoS Biol. *2*, e342

Buenrostro, J.D., Wu, B., Chang, H.Y., and Greenleaf, W.J. (2015). ATAC-seq: A Method for Assaying Chromatin Accessibility Genome-Wide. Curr. Protoc. Mol. Biol. *109*, 21.29.1-21.29.9.

Buonomo, S.B.C., Wu, Y., Ferguson, D., and de Lange, T. (2009). Mammalian Rif1 contributes to replication stress survival and homology-directed repair. J. Cell Biol. *187*, 385–398.

Cairns, B.R. (2009). The logic of chromatin architecture and remodelling at promoters. Nat. 2009 4617261 *461*, 193–198.

Capelson, M., Liang, Y., Schulte, R., Mair, W., Wagner, U., and Hetzer, M.W. (2010). Chromatin-Bound Nuclear Pore Components Regulate Gene Expression in Higher Eukaryotes. Cell *140*, 372–383.

Castaño, I., Pan, S.J., Zupancic, M., Hennequin, C., Dujon, B., and Cormack, B.P. (2005). Telomere length control and transcriptional regulation of subtelomeric adhesins in Candida glabrata. Mol. Microbiol. *55*, 1246–1258.

Cayrou, C., Coulombe, P., Vigneron, A., Stanojcic, S., Ganier, O., Peiffer, I., Rivals, E., Puy, A., Laurent-Chabalier, S., Desprat, R., et al. (2011). Genome-scale analysis of metazoan replication origins reveals their organization in specific but flexible sites defined by conserved features. Genome Res. *21*, 1438–1449.

Celniker, S.E., Dillon, L.A.L., Gerstein, M.B., Gunsalus, K.C., Henikoff, S., Karpen, G.H., Kellis, M., Lai, E.C., Lieb, J.D., MacAlpine, D.M., et al. (2009). Unlocking the secrets of the genome. Nat. *459*, 927.

Cha, R.S., and Kleckner, N. (2002). ATR homolog Mec1 promotes fork progression, thus averting breaks in replication slow zones. Science *297*, 602–606.

Chapman, J.R.R., Barral, P., Vannier, J.-B.B., Borel, V., Steger, M., Tomas-Loba, A., Sartori, A.A.A., Adams, I.R.R., Batista, F.D.D., and Boulton, S.J.J. (2013). RIF1 Is Essential for 53BP1-Dependent Nonhomologous End Joining and Suppression of DNA Double-Strand Break Resection. Mol. Cell *49*, 858–871.

Chesnokov, I.N. (2007). Multiple Functions of the Origin Recognition Complex. Int. Rev. Cytol. *256*, 69–109.

Chesnokov, I., Remus, D., and Botchan, M. (2001). Functional analysis of mutant and wild-type Drosophila origin recognition complex. Proc. Natl. Acad. Sci. *98*, 11997–12002.

Chesnokov, I.N., Chesnokova, O.N., and Botchan, M. (2003). A cytokinetic function of Drosophila ORC6 protein resides in a domain distinct from its replication activity. Proc. Natl. Acad. Sci. *100*, 9150–9155.

Ciardo, D., Haccard, O., Narassimprakash, H., Cornu, D., Chiara Guerrera, I., Goldar, A., and Marheineke, K. (2021). Polo-like kinase 1 (Plk1) regulates DNA replication origin firing and interacts with Rif1 in Xenopus. Nucleic Acids Res. *49*.

Collart, C., Allen, G.E., Bradshaw, C.R., Smith, J.C., and Zegerman, P. (2013). Titration of four replication factors is essential for the Xenopus laevis midblastula transition. Science *341*, 893–896.

Contrino, S., Smith, R.N., Butano, D., Carr, A., Hu, F., Lyne, R., Rutherford, K., Kalderimis, A., Sullivan, J., Carbon, S., et al. (2012). modMine: flexible access to modENCODE data. Nucleic Acids Res. *40*, D1082–D1088.

Cornacchia, D., Dileep, V., Quivy, J.-P., Foti, R., Tili, F., Santarella-Mellwig, R., Antony, C., Ve Almouzni, G., Gilbert, D.M., and Bc Buonomo, S. (2012). Mouse Rif1 is a key regulator of the replication-timing programme in mammalian cells. EMBO J. *31214*, 3678–3690.

Cortez, D., Glick, G., and Elledge, S.J. (2004). Minichromosome maintenance proteins are direct targets of the ATM and ATR checkpoint kinases. Proc. Natl. Acad. Sci. *101*, 10078.

Coverley, D., and Laskey, R.A. (1994). Regulation of eukaryotic DNA replication. Annu. Rev. Biochem. *63*, 745–776.

Danis, E., Brodolin, K., Menut, S., Maiorano, D., Girard-Reydet, C., and Méchali, M. (2004). Specification of a DNA replication origin by a transcription complex. Nat. Cell Biol. *6*, 721–730.

Das, S., Caballero, M., Kolesnikova, T., Zhimulev, I., Koren, A., and Nordman, J. (2021). Replication timing analysis in polyploid cells reveals rif1 uses multiple mechanisms to promote underreplication in drosophila. Genetics *219*, 3.

Davé, A., Cooley, C., Garg, M., and Bianchi, A. (2014). Protein Phosphatase 1 Recruitment by Rif1 Regulates DNA Replication Origin Firing by Counteracting DDK Activity. Cell Rep. *7*, 53–61.

Davis, L.I., and Blobel, G. (1986). Identification and characterization of a nuclear pore complex protein. Cell *45*, 699–709.

Deegan, T.D., Yeeles, J.T., and Diffley, J.F. (2016). Phosphopeptide binding by Sld3 links Dbf4-dependent kinase to MCM replicative helicase activation. EMBO J. *35*, 961–973.

Demczuk, A., Gauthier, M.G., Veras, I., Kosiyatrakul, S., Schildkraut, C.L., Busslinger, M., Bechhoefer, J., and Norio, P. (2012). Regulation of DNA Replication within the Immunoglobulin Heavy-Chain Locus During B Cell Commitment. PLOS Biol. *10*, e1001360.

DePamphilis, M.L. (2005). Cell Cycle Dependent Regulation of the Origin Recognition Complex. Cell Cycle *4*, 70–79.

Diffley, J.F.X. (2004). Regulation of Early Events in Chromosome Replication. Curr. Biol. *14*, R778–R786.

Dijkwel, P.A., Wang, S., and Hamlin, J.L. (2002). Initiation Sites Are Distributed at Frequent Intervals in the Chinese Hamster Dihydrofolate Reductase Origin of Replication but Are Used with Very Different Efficiencies. Mol. Cell. Biol. *22*, 3053–3065.

Dileep, V., and Gilbert, D.M. (2018). Single-cell replication profiling to measure stochastic variation in mammalian replication timing. Nat. Commun. *9*, 1–8.

Dixon, J.R., Selvaraj, S., Yue, F., Kim, A., Li, Y., Shen, Y., Hu, M., Liu, J.S., and Ren, B. (2012). Topological domains in mammalian genomes identified by analysis of chromatin interactions. Nat. *485*, 376–380.

Doksani, Y., Bermejo, R., Fiorani, S., Haber, J.E., and Foiani, M. (2009). Replicon Dynamics, Dormant Origin Firing, and Terminal Fork Integrity after Double-Strand Break Formation. Cell *137*, 247–258.

Dominguez-Sola, D., Ying, C.Y., Grandori, C., Ruggiero, L., Chen, B., Li, M., Galloway, D.A., Gu, W., Gautier, J., and Dalla-Favera, R. (2007). Non-transcriptional control of DNA replication by c-Myc. Nat. *448*, 445–451.

Douglas, M.E., Ali, F.A., Costa, A., and Diffley, J.F.X. (2018). The mechanism of eukaryotic CMG helicase activation. Nat. *555*, 265–268.

Eaton, M.L., Galani, K., Kang, S., Bell, S.P., and MacAlpine, D.M. (2010). Conserved nucleosome positioning defines replication origins. Genes Dev. *24*, 748–753.

Eaton, M.L., Prinz, J.A., MacAlpine, H.K., Tretyakov, G., Kharchenko, P. V., and MacAlpine, D.M. (2011). Chromatin signatures of the Drosophila replication program. Genome Res. *21*, 164–174.

Ehrenhofer-Murray, A.E., Gossen, M., Pak, D.T.S., Botchan, M.R., and Rine, J. (1995). Separation of Origin Recognition Complex Functions by Cross-Species Complementation. Science *270*, 1671–1674.

Escribano-Díaz, C., Orthwein, A., Fradet-Turcotte, A., Xing, M., Young, J.T.F., Tkáč, J., Cook, M.A., Rosebrock, A.P., Munro, M., Canny, M.D., et al. (2013). A Cell Cycle-Dependent Regulatory Circuit Composed of 53BP1-RIF1 and BRCA1-CtIP Controls DNA Repair Pathway Choice. Mol. Cell *49*, 872–883.

Farrell, J.A., and O'Farrell, P.H. (2014). From egg to gastrula: how the cell cycle is remodeled during the Drosophila mid-blastula transition. Annu. Rev. Genet. *48*, 269–294.

Feng, J., Liu, T., Qin, B., Zhang, Y., and Liu, X.S. (2012). Identifying ChIP-seq enrichment using MACS. Nat. Protoc. *7*, 1728–1740.

Fernandez, A.G., Mis, E.K., Lai, A., Mauro, M., Quental, A., Bock, C., and Piano, F. (2014). Uncovering buffered pleiotropy: A genome-scale screen for mel-28 genetic interactors in caenorhabditis elegans. G3 (Bethesda) *4*, 185–196.

Fontoura, B.M.A., Blobel, G., and Matunis, M.J. (1999). A Conserved Biogenesis Pathway for Nucleoporins: Proteolytic Processing of a 186-Kilodalton Precursor Generates Nup98 and the Novel Nucleoporin, Nup96. J. Cell Biol. *144*, 1097.

Foss, M., McNally, F.J., Laurenson, P., and Rine, J. (1993). Origin Recognition Complex (ORC) in Transcriptional Silencing and DNA Replication in S. cerevisiae. Science *262*, 1838–1844.

Foti, R., Gnan, S., Cornacchia, D., Dileep, V., Bulut-Karslioglu, A., Diehl, S., Buness, A., Klein, F.A.A., Huber, W., Johnstone, E., et al. (2016). Nuclear Architecture Organized by Rif1 Underpins the Replication-Timing Program. Mol. Cell *61*, 260–273.

Fragkos, M., Ganier, O., Coulombe, P., and Méchali, M. (2015). DNA replication origin activation in space and time. Nat. Rev. Mol. Cell Biol. *16,* 360–274.

Franz, C., Walczak, R., Yavuz, S., Santarella, R., Gentzel, M., Askjaer, P., Galy, V., Hetzer, M., Mattaj, I.W., and Antonin, W. (2007). MEL-28/ELYS is required for the recruitment of nucleoporins to chromatin and postmitotic nuclear pore complex assembly. EMBO Rep. *8*, 165–172.

Galy, V., Askjaer, P., Franz, C., López-Iglesias, C., and Mattaj, I.W. (2006). MEL-28, a Novel Nuclear-Envelope and Kinetochore Protein Essential for Zygotic Nuclear-Envelope Assembly in C. elegans. Curr. Biol. *16*, 1748–1756.

Ge, X.Q., Jackson, D.A., and Blow, J.J. (2007). Dormant origins licensed by excess Mcm2–7 are required for human cells to survive replicative stress. Genes Dev. *21*, 3331–3341.

Gilbert, D.M. (2001). Making Sense of Eukaryotic DNA Replication Origins. Science *294*, 96.

Gilbert, D.M. (2002). Replication timing and transcriptional control: beyond cause and effect. Curr. Opin. Cell Biol. *14*, 377–383.

Gillespie, P.J., Khoudoli, G.A., Stewart, G., Swedlow, J.R., and Blow, J.J. (2007). ELYS/MEL-28 chromatin association coordinates nuclear pore complex assembly and replication licensing. Curr. Biol. *17*, 1657–1662.

Gindin, Y., Valenzuela, M.S., Aladjem, M.I., Meltzer, P.S., and Bilke, S. (2014). A chromatin structure-based model accurately predicts DNA replication timing in human cells. Mol. Syst. Biol. *10*, 722.

Gineau, L., Cognet, C., Kara, N., Lach, F.P., Dunne, J., Veturi, U., Picard, C., Trouillet, C., Eidenschenk, C., Aoufouchi, S., et al. (2012). Partial MCM4 deficiency in patients with growth retardation, adrenal insufficiency, and natural killer cell deficiency. J. Clin. Invest. *122*, 821.

Gnan, S., Flyamer, I.M., Klein, K.N., Castelli, E., Rapp, A., Maiser, A., Chen, N., Weber, P., Enervald, E., Cardoso, M.C., et al. (2021). Nuclear organisation and replication timing are coupled through RIF1–PP1 interaction. Nat. Commun. *12*, 1–10.

Gozalo, A., Duke, A., Lan, Y., Pascual-Garcia, P., Talamas, J.A., Nguyen, S.C., Shah, P.P., Jain, R., Joyce, E.F., and Capelson, M. (2020). Core Components of the Nuclear Pore Bind Distinct States of Chromatin and Contribute to Polycomb Repression. Mol. Cell *77*, 67-81.e7.

Green, E.M., Jiang, Y., Joyner, R., and Weis, K. (2012). A negative feedback loop at the nuclear periphery regulates GAL gene expression. Mol. Biol. Cell *23*, 1367–1375.

Hardy, C.F.J., Sussel, L., and Shore, D. (1992). A RAP1-interacting protein involved in transcriptional silencing and telomere length regulation. Genes Dev. *6*, 801–814.

Hayano, M., Kanoh, Y., Matsumoto, S., Renard-Guillet, C., Shirahige, K., and Masai, H. (2012). Rif1 is a global regulator of timing of replication origin firing in fission yeast. Genes Dev. *26*, 137–150.

Hengeveld, R.C.C., de Boer, H.R., Schoonen, P.M., de Vries, E.G.E., Lens, S.M.A., and van Vugt, M.A. (2015). Rif1 Is Required for Resolution of Ultrafine DNA Bridges in Anaphase to Ensure Genomic Stability. Dev. Cell *34*, 466–474.

Hershberg, E.A., Camplisson, C.K., Close, J.L., Attar, S., Chern, R., Liu, Y., Akilesh, S., Nicovich, P.R., and Beliveau, B.J. (2021). PaintSHOP enables the interactive design of transcriptome- and genome-scale oligonucleotide FISH experiments. Nat. Methods *18*, 937–944.

Hiraga, S., Ly, T., Garzón, J., Hořejší, Z., Ohkubo, Y., Endo, A., Obuse, C., Boulton, S.J., Lamond, A.I., and Donaldson, A.D. (2017). Human RIF1 and protein phosphatase 1 stimulate DNA replication origin licensing but suppress origin activation. EMBO Rep. *18*, 403–419.

Hiraga, S., Monerawela, C., Katou, Y., Shaw, S., Clark, K.R., Shirahige, K., and Donaldson, A.D. (2018). Budding yeast Rif1 binds to replication origins and protects DNA at blocked replication forks. EMBO Rep. *19*, e46222.

Hiraga, S.I., Alvino, G.M., Chang, F., Lian, H.Y., Sridhar, A., Kubota, T., Brewer, B.J., Weinreich, M., Raghuraman, M.K., and Donaldson, A.D. (2014). Rif1 controls DNA replication by directing Protein Phosphatase 1 to reverse Cdc7-mediated phosphorylation of the MCM complex. Genes Dev. *28*, 372–383.

Hirai, K., Wang, Z., Miura, K., Hayashi, T., Awasaki, T., Wada, M., Keira, Y., Ishikawa, H.O., and Sawamura, K. (2018). Genetic Analyses of Elys Mutations in Drosophila Show Maternal-Effect Lethality and Interactions with Nucleoporin Genes. G3 (Bethesda) *8*, 2421.

Hiratani, I., and Takahashi, S. (2019). DNA Replication Timing Enters the Single-Cell Era. Genes (Basel). *10*.

Hiratani, I., Takebayashi, S., Lu, J., and Gilbert, D.M. (2009). Replication timing and transcriptional control: beyond cause and effect--part II. Curr. Opin. Genet. Dev. *19*, 142–149.

Hook, S.S., Lin, J.J., and Dutta, A. (2007). Mechanisms to Control Rereplication and Implications for Cancer. Curr. Opin. Cell Biol. *19*, 663.

Hoshina, S., Yura, K., Teranishi, H., Kiyasu, N., Tominaga, A., Kadoma, H., Nakatsuka, A., Kunichika, T., Obuse, C., and Waga, S. (2013). Human Origin Recognition Complex Binds Preferentially to G-quadruplex-preferable RNA and Single-stranded DNA. J. Biol. Chem. *288*, 30161.

Hua, B.L., Bell, G.W., Kashevsky, H., Von Stetina, J.R., and Orr-Weaver, T.L. (2018). Dynamic changes in ORC localization and replication fork progression during tissue differentiation. BMC Genomics *19*, 623.

Huberman, J.A., Spotila, L.D., Nawotka, K.A., El-Assouli, S.M., and Davis, L.R. (1987). The in vivo replication origin of the yeast 2 microns plasmid. Cell *51*, 473–481.

Hughes, C.R., Guasti, L., Meimaridou, E., Chuang, C.H., Schimenti, J.C., King, P.J., Costigan, C., Clark, A.J.L., and Metherell, L.A. (2012). MCM4 mutation causes adrenal failure, short stature, and natural killer cell deficiency in humans. J. Clin. Invest. *122*, 814.

Hyman, A.A., Weber, C.A., and Jülicher, F. (2014). Liquid-Liquid Phase Separation in Biology. Annu. Rev. Cell Dev. Biol. *30*, 39–58.

Hyrien, O., Maric, C., and Méchali, M. (1995). Transition in Specification of Embryonic Metazoan DNA Replication Origins. Science *270*, 994–997.

Ibarra, A., and Hetzer, M.W. (2015). Nuclear pore proteins and the control of genome functions. Genes Dev. *29*, 337–349.

Ibarra, A., Schwob, E., and Méndez, J. (2008). Excess MCM proteins protect human cells from replicative stress by licensing backup origins of replication. Proc. Natl. Acad. Sci. *105*, 8956–8961.

Jackson, A.P., Laskey, R.A., and Coleman, N. (2014). Replication proteins and human disease. Cold Spring Harb. Perspect. Biol. *6*, a013060.

Jares, P., Donaldson, A., and Blow, J.J. (2000). The Cdc7/Dbf4 protein kinase: target of the S phase checkpoint? EMBO Rep. *1*, 319.

Jenkinson, F., Tan, K.W., Schöpf, B., Santos, M.M., and Zegerman, P. (2023). Dephosphorylation of the pre-initiation complex is critical for origin firing. Mol. Cell *83*, 12-25.e10.

De Jesús-Kim, L., Friedman, L.J., Lõoke, M., Ramsoomair, C.K., Gelles, J., and Bell, S.P. (2021). Ddk regulates replication initiation by controlling the multiplicity of Cdc45-GINS binding to Mcm2-7. Elife *10*, 1–83.

Jia, P., Jin, H., Meador, C.B., Xia, J., Ohashi, K., Liu, L., Pirazzoli, V., Dahlman, K.B., Politi, K., Michor, F., et al. (2013). Next-generation sequencing of paired tyrosine kinase inhibitor-sensitive and -resistant EGFR mutant lung cancer cell lines identifies spectrum of DNA changes associated with drug resistance. Genome Res. *23*, 1434–1445.

Jones, D.T., and Cozzetto, D. (2015). DISOPRED3: precise disordered region predictions with annotated protein-binding activity. Bioinformatics *31*, 857.

Kadota, S., Ou, J., Shi, Y., Lee, J.T., Sun, J., and Yildirim, E. (2020). Nucleoporin 153 links nuclear pore complex to chromatin architecture by mediating CTCF and cohesin binding. Nat. Commun. 2020 *11*, 1–17.

Kalverda, B., Pickersgill, H., Shloma, V. V., and Fornerod, M. (2010). Nucleoporins Directly Stimulate Expression of Developmental and Cell-Cycle Genes Inside the Nucleoplasm. Cell *140*, 360–371.

Kanoh, J., and Ishikawa, F. (2001). spRap1 and spRif1, recruited to telomeres by Taz1, are essential for telomere function in fission yeast. Curr. Biol. *11*, 1624–1630.

Kanoh, Y., Matsumoto, S., Fukatsu, R., Kakusho, N., Kono, N., Renard-Guillet, C., Masuda, K., Iida, K., Nagasawa, K., Shirahige, K., et al. (2015). Rif1 binds to G quadruplexes and suppresses replication over long distances. Nat. Struct. Mol. Biol. *22*, 889–897.

Kawabata, T., Luebben, S.W., Yamaguchi, S., Ilves, I., Matise, I., Buske, T., Botchan, M.R., and Shima, N. (2011). Stalled fork rescue via dormant replication origins in unchallenged S phase promotes proper chromosome segregation and tumor suppression. Mol. Cell *41*, 543.

Kent, W.J., Sugnet, C.W., Furey, T.S., Roskin, K.M., Pringle, T.H., Zahler, A.M., and Haussler, and D. (2002). The Human Genome Browser at UCSC. Genome Res. *12*, 996.

Kimura, N., Takizawa, M., Okita, K., Natori, O., Igarashi, K., Ueno, M., Nakashima, K., Nobuhisa, I., and Taga, T. (2002). Identification of a novel transcription factor, ELYS, expressed predominantly in mouse foetal haematopoietic tissues. Genes to Cells *7*, 435–446.

Klein, K.N., Zhao, P.A., Lyu, X., Sasaki, T., Bartlett, D.A., Singh, A.M., Tasan, I., Zhang, M., Watts, L.P., Hiraga, S.I., et al. (2021). Replication timing maintains the global epigenetic state in human cells. Science *372*, 371–378.

Kopytova, D., Popova, V., Kurshakova, M., Shidlovskii, Y., Nabirochkina, E., Brechalov, A., Georgiev, G., and Georgieva, S. (2016). ORC interacts with THSC/TREX-2 and its subunits promote Nxf1 association with mRNP and mRNA export in Drosophila. Nucleic Acids Res. *44*, 4920–4933.

Koren, A., Massey, D.J., and Bracci, A.N. (2021). TIGER: inferring DNA replication timing from whole-genome sequence data. Bioinformatics.

Kosar, M., Giannattasio, M., Piccini, D., Maya-Mendoza, A., García-Benítez, F., Bartkova, J., Barroso, S.I., Gaillard, H., Martini, E., Restuccia, U., et al. (2021). The human nucleoporin Tpr protects cells from RNA-mediated replication stress. Nat. Commun. *12*, 1–18.

Kuhn, T.M., and Capelson, M. (2019). Nuclear Pore Proteins in Regulation of Chromatin State. Cells *8*, 1414.

Kuhn, T.M., Pascual-Garcia, P., Gozalo, A., Little, S.C., and Capelson, M. (2019). Chromatin targeting of nuclear pore proteins induces chromatin decondensation. J. Cell Biol. *218*, 2945–2961.

Langmead, B., and Salzberg, S.L. (2012). Fast gapped-read alignment with Bowtie 2. Nat. Methods *9*, 357–359.

Lee, K.Y., Bang, S.W., Yoon, S.W., Lee, S.H., Yoon, J.B., and Hwang, D.S. (2012). Phosphorylation of ORC2 Protein Dissociates Origin Recognition Complex from Chromatin and Replication Origins. J. Biol. Chem. *287*, 11891.

Leonard, A.C., and Méchali, M. (2013). DNA replication origins. Cold Spring Harb. Perspect. Biol. *5*, a010116.

Letessier, A., Millot, G.A., Koundrioukoff, S., Lachagès, A.M., Vogt, N., Hansen, R.S., Malfoy, B., Brison, O., and Debatisse, M. (2011). Cell-type-specific replication initiation programs set fragility of the FRA3B fragile site. Nat. *470*, 120–123.

Levy, D.L., and Blackburn, E.H. (2004). Counting of Rif1p and Rif2p on Saccharomyces cerevisiae Telomeres Regulates Telomere Length. Mol. Cell. Biol. *24*, 10857–10867.

Li, C.J., and DePamphilis, M.L. (2002). Mammalian Orc1 Protein Is Selectively Released from Chromatin and Ubiquitinated during the S-to-M Transition in the Cell Division Cycle. Mol. Cell. Biol. *22*, 105.

Li, H., and Stillman, B. (2012). The origin recognition complex: a biochemical and structural view. Subcell. Biochem. *62*, 37.

Li, C., Vassilev, A., and DePamphilis, M.L. (2004). Role for Cdk1 (Cdc2)/Cyclin A in Preventing the Mammalian Origin Recognition Complex's Largest Subunit (Orc1) from Binding to Chromatin during Mitosis. Mol. Cell. Biol. *24*, 5875.

Lian, H.Y., Robertson, E.D., Hiraga, S., Alvino, G.M., Collingwood, D., McCune, H.J., Sridhar, A., Brewer, B.J., Raghuraman, M.K., and Donaldson, A.D. (2011). The effect of Ku on telomere replication time is mediated by telomere length but is independent of histone tail acetylation. Mol. Biol. Cell *22*, 1753–1765.

Liang, C., and Stillman, B. (1997). Persistent initiation of DNA replication and chromatin-bound MCM proteins during the cell cycle in cdc6 mutants. Genes Dev. *11*, 3375.

Lieberman-Aiden, E., Van Berkum, N.L., Williams, L., Imakaev, M., Ragoczy, T., Telling, A., Amit, I., Lajoie, B.R., Sabo, P.J., Dorschner, M.O., et al. (2009). Comprehensive mapping of long-range interactions reveals folding principles of the human genome. Science *326,* 289-293.

Liontos, M., Koutsami, M., Sideridou, M., Evangelou, K., Kletsas, D., Levy, B., Kotsinas, A., Nahum, O., Zoumpourlis, V., Kouloukoussa, M., et al. (2007). Deregulated Overexpression of hCdt1 and hCdc6 Promotes Malignant Behavior. Cancer Res. *67*, 10899–10909.

Loupart, M.L., Krause, S.A., and Heck, M.M.S. (2000). Aberrant replication timing induces defective chromosome condensation in Drosophila ORC2 mutants. Curr. Biol. *10*, 1547–1556.

Lu, J., Qian, J., Xu, Z., Yin, S., Zhou, L., Zheng, S., and Zhang, W. (2021). Emerging Roles of Liquid–Liquid Phase Separation in Cancer: From Protein Aggregation to Immune-Associated Signaling. Front. Cell Dev. Biol. *9*, 1465.

Lu, L., Zhang, H., and Tower, J. (2001). Functionally distinct, sequence-specific replicator and origin elements are required for Drosophila chorion gene amplification. Genes Dev. *15*, 134–146.

MacAlpine, D.M., Rodríguez, H.K., and Bell, S.P. (2004). Coordination of replication and transcription along a Drosophila chromosome. Genes Dev. *18*, 3094.

MacAlpine, H.K., Gordân, R., Powell, S.K., Hartemink, A.J., and MacAlpine, D.M. (2010). Drosophila ORC localizes to open chromatin and marks sites of cohesin complex loading. Genome Res. *20*, 201–211.

Mantiero, D., Mackenzie, A., Donaldson, A., and Zegerman, P. (2011). Limiting replication initiation factors execute the temporal programme of origin firing in budding yeast. EMBO J. *30*, 4805–4814.

Marchal, C., Sasaki, T., Vera, D., Wilson, K., Sima, J., Rivera-Mulia, J.C., Trevilla-García, C., Nogues, C., Nafie, E., and Gilbert, D.M. (2018). Genome-wide analysis of replication timing by next-generation sequencing with E/L Repli-seq. Nat. Protoc. *13*, 819–839.

Matson, J.P., Dumitru, R., Coryell, P., Baxley, R.M., Chen, W., Twaroski, K., Webber, B.R., Tolar, J., Bielinsky, A.K., Purvis, J.E., et al. (2017). Rapid DNA replication origin licensing protects stem cell pluripotency. Elife *6*, e30473

Mattarocci, S., Shyian, M., Lemmens, L., Damay, P., Altintas, D.M.M., Shi, T., Bartholomew, C.R.R., Thomä, N.H., Hardy, C.F.J.F.J., and Shore, D. (2014). Rif1 Controls DNA Replication Timing in Yeast through the PP1 Phosphatase Glc7. Cell Rep. *7*, 62-69.

Mattarocci, S., Hafner, L., Lezaja, A., Shyian, M., and Shore, D. (2016). Rif1: A Conserved Regulator of DNA Replication and Repair Hijacked by Telomeres in Yeasts. Front. Genet. *30*, 45

Méndez, J., Zou-Yang, X.H., Kim, S.Y., Hidaka, M., Tansey, W.P., and Stillman, B. (2002). Human Origin Recognition Complex Large Subunit Is Degraded by Ubiquitin-Mediated Proteolysis after Initiation of DNA Replication. Mol. Cell *9*, 481–491.

Micklem, G., Rowley, A., Harwood, J., Nasmyth, K., and Diffley, J.F.X. (1993). Yeast origin recognition complex is involved in DNA replication and transcriptional silencing. Nat. *366*, 87–89.

Miotto, B., Ji, Z., and Struhl, K. (2016). Selectivity of ORC binding sites and the relation to replication timing, fragile sites, and deletions in cancers. Proc. Natl. Acad. Sci. *113*, E4810–E4819.

Mirman, Z., Lottersberger, F., Takai, H., Kibe, T., Gong, Y., Takai, K., Bianchi, A., Zimmermann, M., Durocher, D., and de Lange, T. (2018). 53BP1/Rif1/Shieldin counteract DSB resection through CST/Polα-dependent fill-in. Nat. *560*, 112.

Moiseeva, T.N., Qian, C., Sugitani, N., Osmanbeyoglu, H.U., and Bakkenist, C.J. (2019). WEE1 kinase inhibitor AZD1775 induces CDK1 kinase-dependent origin firing in unperturbed G1- and S-phase cells. Proc. Natl. Acad. Sci. *116*, 23891–23893.

Moyer, S.E., Lewis, P.W., and Botchan, M.R. (2006). Isolation of the Cdc45/Mcm2-7/GINS (CMG) complex, a candidate for the eukaryotic DNA replication fork helicase. Proc. Natl. Acad. Sci. *103*, 10236–10241.

Mukherjee, C., Tripathi, V., Manolika, E.M., Margriet Heijink, A., Ricci, G., Merzouk, S., Rudolf De Boer, H., Demmers, J., Van Vugt, M.A.T.M., and Chaudhuri, A.R. RIF1 promotes replication fork protection and efficient restart to maintain genome stability. Nat. Commun. *10,* 3287.

Munden, A., Wright, M.T., Han, D., Tirgar, R., Plate, L., and Nordman, J.T. (2022). Identification of replication fork-associated proteins in Drosophila embryos and cultured cells using iPOND coupled to quantitative mass spectrometry. Sci. Reports 121 *12*, 1–11.

Newman, T.J., Mamun, M.A., Nieduszynski, C.A., and Blow, J.J. (2013). Replisome stall events have shaped the distribution of replication origins in the genomes of yeasts. Nucleic Acids Res. *41*, 9705–9718.

Nguyen, S.C., and Joyce, E.F. (2019). Programmable Chromosome Painting with Oligopaints. Methods Mol. Biol. *2038*, 167–180.

Nguyen, V.Q., Co, C., and Li, J.J. (2001). Cyclin-dependent kinases prevent DNA re-replication through multiple mechanisms. Nat. *411*, 1068–1073.

Noordermeer, S.M., Adam, S., Setiaputra, D., Barazas, M., Pettitt, S.J., Ling, A.K., Olivieri, M., Álvarez-Quilón, A., Moatti, N., Zimmermann, M., et al. (2018). The Shieldin complex mediates 53BP1-dependent DNA repair. Nat. *560*, 117.

Nora, E.P., Lajoie, B.R., Schulz, E.G., Giorgetti, L., Okamoto, I., Servant, N., Piolot, T., Van Berkum, N.L., Meisig, J., Sedat, J., et al. (2012). Spatial partitioning of the regulatory landscape of the X-inactivation center. Nat. *485*, 381.

Ohtani, K., Degregori, J., Leone, G., Herendeen, D.R., Kelly, T.J., and Nevins, J.R. (1996). Expression of the HsOrc1 gene, a human ORC1 homolog, is regulated by cell proliferation via the E2F transcription factor. Mol. Cell. Biol. *16*, 6977–6984.

Okita, K., Kiyonari, H., Nobuhisa, I., Kimura, N., Aizawa, S., and Taga, T. (2004). Targeted disruption of the mouse ELYS gene results in embryonic death at peri-implantation development. Genes Cells *9*, 1083–1091.

Otsuka, S., and Ellenberg, J. (2018). Mechanisms of nuclear pore complex assembly - two different ways of building one molecular machine. FEBS Lett. *592*, 475–488.

Pak, D.T.S., Pflumm, M., Chesnokov, I., Huang, D.W., Kellum, R., Marr, J., Romanowski, P., and Botchan, M.R. (1997). Association of the origin recognition complex with heterochromatin and HP1 in higher eukaryotes. Cell *91*, 311–323.

Panda, D., Pascual-Garcia, P., Dunagin, M., Tudor, M., Hopkins, K.C., Xu, J., Gold, B., Raj, A., Capelson, M., and Cherry, S. (2014). Nup98 promotes antiviral gene expression to restrict RNA viral infection in Drosophila. Proc. Natl. Acad. Sci. *111*, E3890–E3899.

Parker, M.W., Bell, M., Mir, M., Kao, J.A., Darzacq, X., Botchan, M.R., and Berger, J.M. (2019). A new class of disordered elements controls DNA replication through initiator self-assembly. Elife *8*, e48562.

Pascual-Garcia, P., Jeong, J., and Capelson, M. (2014). Nucleoporin Nup98 associates with Trx/MLL and NSL histone-modifying complexes and regulates Hox gene expression. Cell Rep. *9*, 433–442.

Pascual-Garcia, P., Debo, B., Aleman, J.R., Talamas, J.A., Lan, Y., Nguyen, N.H., Won, K.J., and Capelson, M. (2017). Metazoan Nuclear Pores Provide a Scaffold for Poised Genes and Mediate Induced Enhancer-Promoter Contacts. Mol. Cell *66*, 63-76.e6.

Peace, J.M., Ter-Zakarian, A., and Aparicio, O.M. (2014). Rif1 Regulates Initiation Timing of Late Replication Origins throughout the S. cerevisiae Genome. PLoS One *9*, e98501.

Pinto, S., Quintana, D.G., Smith, P., Mihalek, R.M., Zhi-Hui, H., Boynton, S., Jones, C.J., Hendricks, M., Velinzon, K., Wohlschlegel, J.A., et al. (1999). latheo Encodes a Subunit of the Origin Recognition Complex and Disrupts Neuronal Proliferation and Adult Olfactory Memory When Mutant. Neuron *23*, 45–54.

Pope, B.D., Ryba, T., Dileep, V., Yue, F., Wu, W., Denas, O., Vera, D.L., Wang, Y., Hansen, R.S., Canfield, T.K., et al. (2014). Topologically associating domains are stable units of replication-timing regulation. Nat. *515*, 402–405.

Prasanth, S.G., Prasanth, K. V., and Stillman, B. (2002). Orc6 involved in DNA replication, chromosome segregation, and cytokinesis. Science *297*, 1026–1031.

Rabut, G., Doye, V., and Ellenberg, J. (2004). Mapping the dynamic organization of the nuclear pore complex inside single living cells. Nat. Cell Biol. *6*, 1114–1121.

Raices, M., and D'Angelo, M.A. (2017). Nuclear pore complexes and regulation of gene expression. Curr. Opin. Cell Biol. *46*, 26–32.

Ramírez, F., Ryan, D.P., Grüning, B., Bhardwaj, V., Kilpert, F., Richter, A.S., Heyne, S., Dündar, F., and Manke, T. (2016). deepTools2: a next generation web server for deep-sequencing data analysis. Nucleic Acids Res. *44*, W160–W165.

Rasala, B.A., Orjalo, A. V., Shen, Z., Briggs, S., and Forbes, D.J. (2006). ELYS is a dual nucleoporin/kinetochore protein required for nuclear pore assembly and proper cell division. Proc. Natl. Acad. Sci. *103*, 17801–17806.

Remus, D., and Diffley, J.F. (2009). Eukaryotic DNA replication control: Lock and load, then fire. Curr. Opin. Cell Biol. *21*, 771–777.

Remus, D., Beall, E.L., and Botchan, M.R. (2004). DNA topology, not DNA sequence, is a critical determinant for Drosophila ORC–DNA binding. EMBO J. *23*, 897–907.

Remus, D., Blanchette, M., Rio, D.C., and Botchan, M.R. (2005). CDK phosphorylation inhibits the DNA-binding and ATP-hydrolysis activities of the Drosophila origin recognition complex. J. Biol. Chem. *280*, 39740–39751.

Rhind, N., and Gilbert, D.M. (2013). DNA replication timing. Cold Spring Harb. Perspect. Biol. *5*, a010132.

Rhind, N., Yang, S.C.H., and Bechhoefer, J. (2010). Reconciling stochastic origin firing with defined replication timing. Chromosom. Res. *18*, 35–43.

Richards, L., Das, S., and Nordman, J.T. (2022a). Rif1-Dependent Control of Replication Timing. Genes (Basel). *13*, 550.

Richards, L., Lord, C.L., Benton, M.L., Capra, J.A., and Nordman, J.T. (2022b). Nucleoporins facilitate ORC loading onto chromatin. Cell Rep. *41*, 111590.

Rippe, K. (2022). Liquid-Liquid Phase Separation in Chromatin. Cold Spring Harb. Perspect. Biol. *14*, a040683

Roh, T.Y., Cuddapah, S., and Zhao, K. (2005). Active chromatin domains are defined by acetylation islands revealed by genome-wide mapping. Genes Dev. *19*, 542.

Rohrbough, J., Pinto, S., Mihalek, R.M., Tully, T., and Broadie, K. (1999). latheo, a Drosophila gene involved in learning, regulates functional synaptic plasticity. Neuron *23*, 55–70.

Royzman, I., Austin, R.J., Bosco, G., Bell, S.P., and Orr-Weaver, T.L. (1999). ORC localization in Drosophila follicle cells and the effects of mutations in dE2F and dDP. Genes Dev. *13*, 827.

Sasaki, T., Sawado, T., Yamaguchi, M., and Shinomiya, T. (1999). Specification of Regions of DNA Replication Initiation during Embryogenesis in the 65-Kilobase DNApolα-dE2F Locus of Drosophila melanogaster. Mol. Cell. Biol. *19*, 547.

Schwaiger, M., and Schübeler, D. (2006). A question of timing: Emerging links between transcription and replication. Curr. Opin. Genet. Dev. *16*, 177–183.

Seller, C.A., O'Farrell, P.H., and O'Farrell, P.H. (2018). Rif1 prolongs the embryonic S phase at the Drosophila mid-blastula transition. PLOS Biol. *16*, e2005687.

Shareef, M.M., King, C., Damaj, M., Badagu, R., Da Wei Huang, and Kellum, R. (2001). Drosophila Heterochromatin Protein 1 (HP1)/OriginRecognition Complex (ORC) Protein Is Associated with HP1 and ORC and Functions in Heterochromatin-induced Silencing. Mol. Biol. Cell *12*, 1671.

Shen, Z., Sathyan, K.M., Geng, Y., Zheng, R., Chakraborty, A., Freeman, B., Wang, F., Prasanth, K. V., and Prasanth, S.G. (2010). A WD-Repeat Protein Stabilizes ORC Binding to Chromatin. Mol. Cell *40*, 99–111.

Sher, N., Bell, G.W., Li, S., Nordman, J., Eng, T., Eaton, M.L., MacAlpine, D.M., and Orr-Weaver, T.L. (2012). Developmental control of gene copy number by repression of replication initiation and fork progression. Genome Res. *22*, 64.

Shermoen, A.W., McCleland, M.L., and O'Farrell, P.H. (2010). Developmental Control of Late Replication and S Phase Length. Curr. Biol. *20*, 2067–2077.

Sheu, Y.J., and Stillman, B. (2006). Cdc7-Dbf4 phosphorylates MCM proteins via a docking site-mediated mechanism to promote S phase progression. Mol. Cell *24*, 101–113.

Shevelyov, Y.Y. (2020). The role of nucleoporin elys in nuclear pore complex assembly and regulation of genome architecture. Int. J. Mol. Sci. *21*, 1–13.

Shima, N., Buske, T.R., and Schimenti, J.C. (2007). Genetic Screen for Chromosome Instability in Mice: Mcm4 and Breast Cancer. Cell Cycle *6*, 1135–1140.

Shore, D. (2001). Transcriptional silencing: Replication redux. Curr. Biol. *11*, R816–R819.

Siddiqui, K., On, K.F., and Diffley, J.F.X. (2013). Regulating DNA replication in eukarya. Cold Spring Harb. Perspect. Biol. *5*, a012930.

Silverman, J., Takai, H., Buonomo, S.B.C., Eisenhaber, F., and de Lange, T. (2004). Human Rif1, ortholog of a yeast telomeric protein, is regulated by ATM and 53BP1 and functions in the S-phase checkpoint. Genes Dev. *18*, 2108–2119.

Sima, J., and Gilbert, D.M. (2014). Complex correlations: replication timing and mutational landscapes during cancer and genome evolution. Curr. Opin. Genet. Dev. *25*, 93–100.

Skene, P.J., and Henikoff, S. (2017). An efficient targeted nuclease strategy for high-resolution mapping of DNA binding sites. Elife *6*. e21856

Skene, P.J., Henikoff, J.G., and Henikoff, S. (2018). Targeted in situ genome-wide profiling with high efficiency for low cell numbers. Nat. Protoc. *13*, 1006–1019.

Smith, O.K., and Aladjem, M.I. (2014). Chromatin Structure and Replication Origins: Determinants Of Chromosome Replication And Nuclear Organization. J. Mol. Biol. *426*, 3330.

Smith, C.D., Smith, D.L., DeRisi, J.L., and Blackburn, E.H. (2003). Telomeric Protein Distributions and Remodeling Through the Cell Cycle in Saccharomyces cerevisiae. Mol. Biol. Cell *14*, 556.

Sreesankar, E., Senthilkumar, R., Bharathi, V., Mishra, R.K., and Mishra, K. (2012). Functional diversification of yeast telomere associated protein, Rif1, in higher eukaryotes. BMC Genomics *13*, 1–13.

Stamatoyannopoulos, J.A., Adzhubei, I., Thurman, R.E., Kryukov, G. V, Mirkin, S.M., and Sunyaev, S.R. (2009). Human mutation rate associated with DNA replication timing. Nat. Genet. *41*, 393–395.

Stiff, T., Alagoz, M., Alcantara, D., Outwin, E., Brunner, H.G., Bongers, E.M.H.F., O'Driscoll, M., and Jeggo, P.A. (2013). Deficiency in Origin Licensing Proteins Impairs Cilia Formation: Implications for the Aetiology of Meier-Gorlin Syndrome. PLOS Genet. *9*, e1003360.

Strambio-De-Castillia, C., Niepel, M., and Rout, M.P. (2010). The nuclear pore complex: bridging nuclear transport and gene regulation. Nat. Rev. Mol. Cell Biol. *11*, 490–501.

Sukackaite, R., Cornacchia, D., Jensen, M.R., Mas, P.J., Blackledge, M., Enervald, E., Duan, G., Auchynnikava, T., Köhn, M., Hart, D.J., et al. (2017). Mouse Rif1 is a regulatory subunit of protein phosphatase 1 (PP1). Sci. Rep. *7*, 2119.

Takeda, T., Ogino, K., Tatebayashi, K., Ikeda, H., Arai, K.I., and Masai, H. (2001). Regulation of Initiation of S Phase, Replication Checkpoint Signaling, and Maintenance of Mitotic Chromosome Structures during S Phase by Hsk1 Kinase in the Fission Yeast. Mol. Biol. Cell *12*, 1257.

Tanaka, S., Nakato, R., Katou, Y., Shirahige, K., and Araki, H. (2011). Origin Association of Sld3, Sld7, and Cdc45 Proteins Is a Key Step for Determination of Origin-Firing Timing. Curr. Biol. *21*, 2055–2063.

Truong, L.N., and Wu, X. (2011). Prevention of DNA re-replication in eukaryotic cells. J. Mol. Cell Biol. *3*, 13.

Vaquerizas, J.M., Suyama, R., Kind, J., Miura, K., Luscombe, N.M., and Akhtar, A. (2010). Nuclear Pore Proteins Nup153 and Megator Define Transcriptionally Active Regions in the Drosophila Genome. PLOS Genet. *6*, e1000846.

Vashee, S., Cvetic, C., Lu, W., Simancek, P., Kelly, T.J., and Walter, J.C. (2003). Sequence-independent DNA binding and replication initiation by the human origin recognition complex. Genes Dev. *17*, 1894.

Vaziri, C., Saxena, S., Jeon, Y., Lee, C., Murata, K., Machida, Y., Wagle, N., Hwang, D.S., and Dutta, A. (2003). A p53-Dependent Checkpoint Pathway Prevents Rereplication. Mol. Cell *11*, 997–1008.

Di Virgilio M., Callen E., Yamane A., Zhang W., Jankovic M., Gitlin A.D., Feldhahn N., Resch W., Oliveira T.Y., Chait B.T., Nussenzweig A., Casellas R., Robbiani D.F., Nussenzweig M.C. (2013). Rif1 prevents resection of DNA breaks and promotes immunoglobulin class switching. Science *339*, 711–715.

Wang, W., Klein, K.N., Proesmans, K., Yang, H., Marchal, C., Zhu, X., Borrman, T., Hastie, A., Weng, Z., Bechhoefer, J., et al. (2021). Genome-wide mapping of human DNA replication by optical replication mapping supports a stochastic model of eukaryotic replication. Mol. Cell *81*, 2975-2988.e6.

Wente, S.R., and Rout, M.P. (2010). The Nuclear Pore Complex and Nuclear Transport. Cold Spring Harb. Perspect. Biol. *2*, a000562

Wyrick, J.J., Aparicio, J.G., Chen, T., Barnett, J.D., Jennings, E.G., Young, R.A., Bell, S.P., and Aparicio, O.M. (2001). Genome-wide distribution of ORC and MCM proteins in S. cerevisae: High-resolution mapping of replication origins. Science *294*, 2357–2360.

Xu, L., and Blackburn, E.H. (2004). Human Rif1 protein binds aberrant telomeres and aligns along anaphase midzone microtubules. J. Cell Biol. *167*, 819–830.

Xu, W., Aparicio, J.G., Aparicio, O.M., and Tavaré, S. (2006). Genome-wide mapping of ORC and Mcm2p binding sites on tiling arrays and identification of essential ARS consensus sequences in S. cerevisiae. BMC Genomics *7*, 1–16.

Yamazaki, S., Ishii, A., Kanoh, Y., Oda, M., Nishito, Y., and Masai, H. (2012). Rif1 regulates the replication timing domains on the human genome. EMBO J. *31*, 3667–3677.

Yates, J.R., Eng, J.K., McCormack, A.L., and Schieltz, D. (1995). Method to correlate tandem mass spectra of modified peptides to amino acid sequences in the protein database. Anal. Chem. *67*, 1426–1436.

Zegerman, P., and Diffley, J.F.X. (2006). Phosphorylation of Sld2 and Sld3 by cyclin-dependent kinases promotes DNA replication in budding yeast. Nat. *445*, 281–285.

Zeman, M.K., and Cimprich, K.A. (2013). Causes and consequences of replication stress. Nat. Cell Biol. *16*, 2–9.

Zeng, W., Ball, A.R., and Yokomori, K. (2010). HP1: Heterochromatin binding proteins working the genome. Epigenetics *5*, 287.

Zhang, J., Xu, F., Hashimshony, T., Keshet, I., and Cedar, H. (2002). Establishment of transcriptional competence in early and late S phase. Nat. *420*, 198–202.

Zielke, N., Korzelius, J., vanStraaten, M., Bender, K., Schuhknecht, G.F.P., Dutta, D., Xiang, J., and Edgar, B.A. (2014). Fly-FUCCI: A Versatile Tool for Studying Cell Proliferation in Complex Tissues. Cell Rep. *7*, 588–598.

Zimmermann, M., Lottersberger, F., and Buonomo, S.B. (2013). 53BP1 regulates DSB repair using Rif1 to control 5' end resection. Science *339*, 700–704.